

**IDENTIFICATION AND CHARACTERIZATION  
OF PEPTIDES BINDING TO *PESTE DES PETITS*  
RUMINANTS (PPR) VIRUS USING PHAGE  
DISPLAY**

**Thesis**

Submitted to the  
**DEEMED UNIVERSITY**  
Indian Veterinary Research Institute  
Izatnagar - 243 122 (U.P.), India



**Dr. Deepika Bisht**  
Roll No. 5289

**IN PARTIAL FULFILMENT OF THE REQUIREMENTS FOR  
THE DEGREE OF**

**Master of Veterinary Science  
(Animal Biotechnology)**

**2015**



*Dedicated to....*

*Almighty God  
&  
My Beloved Family*



भारतीय पशु चिकित्सा अनुसंधान संस्थान  
(सम विश्वविद्यालय)  
इज्जतनगर -243122, (उ.प्र.), भारत



**DIVISION OF VETERINARY BIOTECHNOLOGY**  
**ICAR-INDIAN VETERINARY RESEARCH INSTITUTE**  
(Deemed University)  
IZATNAGAR - 243 122, U.P., INDIA

**Dr. Satish Kumar**

Ph.D.

Principal Scientist & Head

Dated: 2015

## *Certificate*

*This is to be certified that the research work embodied in this thesis entitled "Identification and characterization of peptides binding to Peste des Petits Ruminants (PPR) virus using phage display" submitted by Dr. Deepika Bisht, Roll No. 5289, for the award of Master of Veterinary Science Degree in Animal Biotechnology at Indian Veterinary Research Institute, Izatnagar, is the original work carried out by the candidate herself under my supervision and guidance.*

*It is further certified that Dr. Deepika Bisht, Roll No. 5289, has worked for more than 21 months in the Institute and has put in more than 150 days attendance under me from the date of registration for the Master of Veterinary Science Degree in this Deemed University, as required under the relevant ordinance.*

  
**DR. SATISH KUMAR**  
**(SATISH KUMAR)** CHAIRMAN  
STUDENT ADVISORY COMMITTEE (SAC)  
Chairman  
Advisory Committee

# Certificate

We the undersigned members of Advisory Committee of Dr. Deepika Bisht, Roll No. 5289 a candidate for the degree of **Master of Veterinary Science** with the major discipline **Animal Biotechnology**, agree that the thesis entitled "**Identification and characterization of peptides bindings to Peste des Petits Ruminants (PPR) virus using phage display**" may be submitted in partial fulfillment of the requirement for the degree.

We have gone through the contents of the thesis and are fully satisfied with the work carried out by the candidate, which is being presented for the award of **Master of Veterinary Science Degree** of this Institute.

It is further certified that the candidate has completed all the prescribed requirements governing the award of **Master of Veterinary Science Degree** of the Deemed University, Indian Veterinary Research Institute, Izatnagar.



Signature  
Name **Dr. K.P. Singh**  
External Examiner

Date : 16-7-15

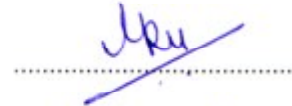


(**Satish Kumar**)  
**Chairman**  
STUDENT ADVISORY COMMITTEE (SAC)

Date : 20-6-15

## MEMBERS OF STUDENT'S ADVISORY COMMITTEE

**Dr. G.V.P.S. Ravikumar**, Senior Scientist  
Division of Veterinary Biotechnology, ICAR-IVRI, Izatnagar



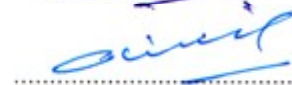
**Dr. Praveen Singh**, Principal Scientist  
Division of Animal Biochemistry, ICAR-IVRI, Izatnagar



**Dr. Y.P.S. Malik**, ICAR National Fellow  
Division of Biological Standardization, ICAR-IVRI, Izatnagar



**Dr. Mithilesh Kumar Singh**, Scientist  
Immunology Section, ICAR-IVRI, Izatnagar



# ACKNOWLEDGEMENTS

---

*Though only my name appears on the cover of this Thesis, a great many people have contributed to its production. I owe my gratitude to all those people who have made this study possible and because of whom my post-graduate experience has been one that I will cherish forever.*

*My deepest gratitude is to my advisor, **Dr. Satish Kumar**, Principal Scientist & Head, Division of Animal Biotechnology. I am thankful to the **Almighty** for giving me a mentor like him, who gave me the freedom to explore on my own and at the same time the guidance to recover when my steps faltered. He taught me how to question thoughts and express ideas. His patience and support helped me overcome many crisis situations and complete this thesis.*

*Besides my advisor, I would like to express my warm regards and sincere thanks to other members of my advisory committee: **Dr. Praveen Singh**, Principal Scientist, Division of Animal Biochemistry; **Dr. Y.P.S. Malik**, ICAR National Fellow, Division of Biological Standardization, **Dr. G.V.P.S. Ravi Kumar**, Senior Scientist, Division of Veterinary Biotechnology; **Dr. Mithilesh Kumar Singh**, Scientist, Immunology Section, for their encouragement and insightful comments during the hours of need.*

*I thank **Director (IVRI)**, **Joint Directors (Academic and Research)** and ICAR for providing me the facility to carry out the research work.*

*I feel immense pleasure to express a note of thanks to all scientists of Division of Veterinary Biotechnology **Dr. P.P Goswami**, **Dr. P.K. Gupta**, **Dr. A.K.Tiwai**, **Dr. C. Madan Mohan**, **Dr. (Mrs) Sohini Dey**, **Dr. Sonal**, **Dr. Sameer Shrivastav**, **Dr. A.P. Sahoo** & **Dr. Deepak Kumar** for their kind support and timely help.*

*I sincerely thank, **Dr. Vikas Dighe**, who not only taught me elementary of experiments on Phage display but also the preliminary lab skills and was always there for me whenever required.*

*I could'nt have made it through this research without the help of **Dr. B.K. Sajjanar**. I am indebted to him for his continuous encouragement and guidance. I am also thankful to him for reading my thesis work, commenting on my views and helping me understand and enrich my ideas.*

*I would express my special deep sense of gratitude to **Shikha Mam** for being always ready to help and making the atmosphere of our lab as friendly as possible. I feel indebted to **Arvind Sir** for his valuable advice and also being constant support during this period.*

*I have been amazingly fortunate to have a long list of beloved friends to thank. **Nitish, Anna, Mintu, Ruby, Anjali, Meesam, Munazah, Yasmeen, Sandeep & Vinay** gave me lot of strength by their ever ready helping hands. They often created lighter moments, which I am going to treasure forever.*

*I extend my thanks to all my Seniors specially **Dr. Aman Kamboj, Dr. Hina Malik, Dr. Swati Sachan, Dr. Sonam, Dr. Chetan, Dr. Kalpana, Dr. Jyotilaxmi, Dr. Lekshmi** to help and support me whenever needed.*

*I feel extremely grateful to my juniors **Geeta, Shumaila, Shushobhit, Ashutosh, Jugal, Richa, Reshma, Neha & Chandan** for their kindness and belongingness.*

*I would express my gratitude to the staff of CIF, **Surendranath Sir** for his valuable advice and help. **Subhash ji, Hariji and Bablaji** were always there to help and assist. Their helping hands made me comfortable throughout this journey.*

*I thank all the members of **Pantnagar mess**, not only to provide meals but also to keep memories of Pantnagar live in my heart.*

*Mere words cannot match the quantum of love & affection that I have received from my family. This present endeavor could have not possible without the blessings of **my parents** and encouragement of my younger sister **Geetanjali**, and brother **Rahul**. Their sacrifices and constant motivation helped me to come this far. I dedicate this work to them.*

*Last but not the least: I thank **Chachu** and his team for their skilful typing and printing.*

Date: 27/6/15  
Place: IVRI, Izatnagar

  
(Deepika Bisht)

## ABBREVIATIONS

---

%	: Per cent
AuNPs	: Gold nanoparticles
BSA	: Bovine serum albumin
CD	: Circular Dichroism
DCM	: Dichloromethane
DIPC	: N,N-diisopropyl carbodiimide
DMAP	: Dimethylamino pyridine
DMEM	: Dulbecco's Modified Eagles medium
DMF	: Dimethylformamide
DNA	: Deoxyribonucleic acid
EDT	: 1,2-ethanedithiol
ELISA	: Enzyme linked immunosorbant assay
<i>et al.</i>	: <i>et alia</i> (and others)
eq.	: Equivalent
HBTU	: 2-(1H-benzotriazolyl-1-yl)-1,1,3,3-tetramethyluroniumhexafluoro phosphate
HoBT	: 1-hydroxy benztriazole
IPTG	: Iso-propyl-thiogalactopyranoside
MAP	: Multiple antigenic peptide
MALDI	: Matrix Associated Laser Desorption Ionisation
NFW	: Nuclease free water
OD	: Optical Density
PBS	: Phosphate buffer saline
PDL	: Phage display library
PEG	: Poly ethylene glycol
PFU	: Plaque forming unit
PhD-12	: Phage display library-12 mer
PPR	: <i>Peste des petits ruminants</i>
PPRV	: <i>Peste des petits ruminants virus</i>
RNA	: Ribonucleic acids
RP	: Rinderpest
RP-HPLC	: Reversed phase high performance liquid chromatography

SPPS	:	Solid Phase Peptide Synthesis
ssDNA	:	Single stranded DNA
Tet	:	Tetracycline
TFA	:	Trifluoroacetic acid
TFE	:	Trifluoroethanol
TVG	:	Trypsin-Versene-Glucose
v/v	:	Volume/volume
XGal	:	5 Bomo-4-chloro-3 Indolyl $\beta$ -D- galactopyranoside

# LIST OF TABLES

Table No.	Title	After Page No.
Table 3.1	Reagents used for PCR amplification of phage DNA	33
Table 3.2	PCR cycling temperature and time conditions	33
Table 3.3	Solvent gradient in Semi-preparative RP-HPLC	42
Table 4.1	Determination of concentration with Bradford assay	47
Table 4.2	PPRV binding phage titer before and after panning and after phage amplification	49
Table 4.3	Retrieved sequences of Phage DNA and translated peptide sequences	49
Table 4.4	List of peptide synthesised and their attributes	49
Table 4.5	List of MAP synthesised	50
Table 4.6	Retention time and % ACN on which peptide eluted	50
Table 4.7	Calculated mass and observed mass using MALDI	52
Table 4.8	Elucidation of Secondary Structure of PPR binding peptides (P1, P2 & P3) using CD spectroscopy	54
Table 4.9	Elucidation of Secondary Structure of PPR binding peptides (P4, P5 & P6) using CD spectroscopy	55
Table 4.10	Elucidation of Secondary Structure of PPR binding peptides (P7, P8 & P9) using CD spectroscopy	56
Table 4.11	Elucidation of Secondary Structure of PPR binding peptides (P10, P11 & P12) using CD spectroscopy	57
Table 4.12	Elucidation of Secondary Structure of PPR binding peptides (MAP-4, 8, 9 & 12) using CD spectroscopy	58

## LIST OF FIGURES

Fig. No.	Title	After Page No.
Fig. 2.1	Basic steps involved in <i>in vitro</i> biopanning (direct target coating)	8
Fig. 2.2	Steps involved in PPRV replication	19
Fig. 3.1	Solid phase Peptide synthesis scheme	34
Fig. 3.2	Schematic diagram of MAP core	41
Fig. 4.1	Propagation of PPRV in Vero cells	47
Fig. 4.2	Standard curve plotted in Bradford Assay	47
Fig. 4.3	LB/Tet/Xgal/IPTG plates showing blue colonies (plaques) of phage grown on $\alpha$ -Complementing host ER2738.	49
Fig. 4.4	Agarose gel electrophoresis of amplified ss-DNA of phage	49
Fig. 4.5	Schematics of sequence map of peptide displayed on minor coat protein of M13 phage	49
Fig. 4.6	Histogram representing affinity of all the 12 phage clones through Phage ELISA	49
Fig. 4.7	Histogram representing ratio of O.D. at 450nm of all the 12 phage clones	49
Fig. 4.8	Histogram representing comparison of P/N ratio of Optical densities of antibody with that of phage clones	49
Fig. 4.9	RP-HPLC chromatogram of PPRV binding peptides (P1, P2, P3, P4, P5 and P6) on semi-preparatory coulumn	51
Fig. 4.10	RP-HPLC chromatogram of PPRV binding peptides (P7, P8, P9, P10, P11 and P12) on semi-preparatory coulumn	51
Fig. 4.11	RP-HPLC chromatogram of PPRV binding peptides (P1, P2, P3, P4, P5 and P6) on analytical coulumn	51
Fig. 4.12	RP-HPLC chromatogram of PPRV binding peptides (P7, P8, P9, P10, P11 and P12) on analytical coulumn	51

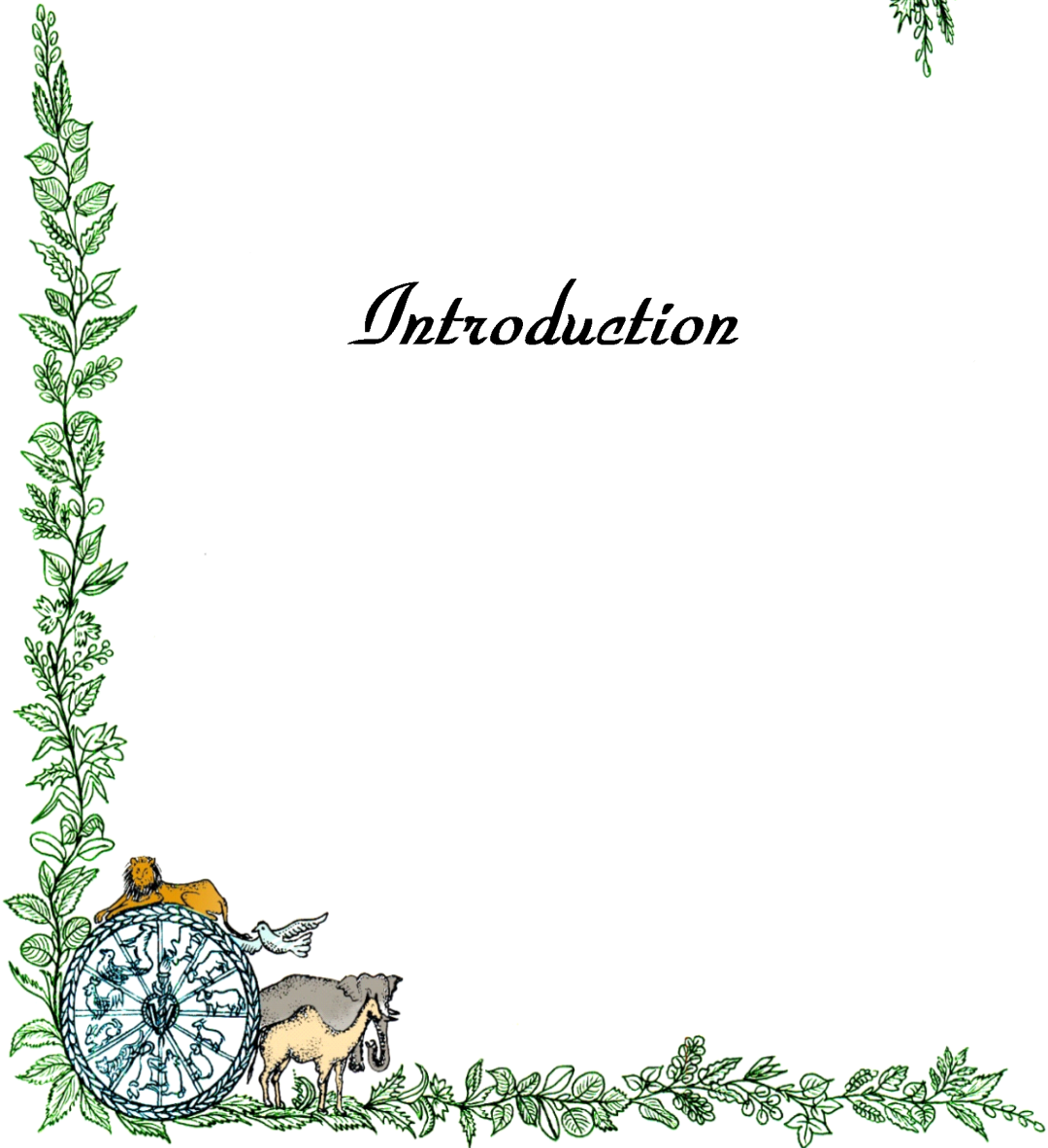
<b>Fig. No.</b>	<b>Title</b>	<b>After Page No.</b>
Fig. 4.13	RP-HPLC chromatogram of MAP (MAP-4, 8, 9 & 12) on semi-preparatory coulmm	51
Fig. 4.14	RP-HPLC chromatogram of MAP (MAP-4, 8, 9 & 12) on analytical coulmm	51
Fig. 4.15	MALDI-TOF of peptides (P4, P8, P9 & P12)	53
Fig. 4.16	Histogram representing virus capture ELISA using MAP	53
Fig. 4.17	CD spectra of PPRV binding peptides (P1, P2 & P3) in different polar and apolar solutions	58
Fig. 4.18	CD spectra of PPRV binding peptides (P4, P5 & P6) in different polar and apolar solutions	58
Fig. 4.19	CD spectra of PPRV binding peptides (P7, P8 & P9) in different polar and apolar solutions	58
Fig. 4.20	CD spectra of PPRV binding peptides (P10, P11 & P12) in different polar and apolar solutions	58
Fig. 4.21	CD spectra of PPRV binding MAPs (MAP-4, MAP-8, MAP-9 & MAP-12) in different polar and apolar solutions	58
Fig. 4.22	Conjugation of MAP cysteine to AuNP	58
Fig. 4.23	Visual colour change (red to blue) in MAP conjugated gold nanoparticles on addition of PPRV.	58

# CONTENTS

<b>Sl. No.</b>	<b>CHAPTER</b>	<b>PAGE NO.</b>
1.	INTRODUCTION	01-03
2.	REVIEW OF LITERATURE	04-22
3.	MATERIALS AND METHODS	23-45
4.	RESULTS	46-58
5.	DISCUSSION	59-62
6.	SUMMARY AND CONCLUSIONS	63-65
7.	MINI ABSTRACT	66
8.	HINDI ABSTRACT	67
9.	REFERENCES	68-79
10.	APPENDIX	



# *Introduction*



In 1985, George Smith showed that the linkage between phenotype and genotype could be established in filamentous bacteriophage (Smith, 1985) and gave rise to a new technology known as phage-display. Subsequently in 1990, Scott and Smith, Dower and Devlin independently cloned libraries of peptides and showed that peptides of specific activity could be retrieved from the libraries by panning. Since then, the technique has evolved and is being widely used to study molecular biology mechanisms involving protein-protein (Sidhu *et al.*, 2003) or protein- non protein interactions (Yu *et al.*, 2009). Phage display is a powerful tool for selecting novel peptides and antibodies that have tendency to bind a wide range of targets involving whole cells, protein as well as lipid targets.

Phage random library contains a pool of billions of phage clones expressing heterologous peptides. It is produced by the fusion of random nucleic acid sequences to the N-terminus of one of the capsid protein genes of a filamentous bacteriophage. The phage selection procedure is highly flexible and dynamic step in phage display and is known as Biopanning. The characteristic aspect of the phage display technology is affinity selection that selects for ligands against any target. By permitting control over selection and screening conditions, display technologies allow the identification of peptides binding to defined antigen conformations or epitopes. Advantage of in vitro methods is that they overcome immunological tolerance, allowing the selection of affinity reagents that recognize highly conserved targets (Bradbury, 2010).

Using this technology many small peptide ligands and antibodies have been identified, which have tendency to inhibit the function of targeted receptors for a wide range of applications (Huang *et al.*, 2012). This technology has been applied successfully in numerous aspects, including antibody engineering, peptide/protein drug discovery and manufacture, diagnostic

analysis and vaccine development. Whole viruses like Newcastle disease virus (Ozawa *et al.*, 2005), hantavirus (Hall *et al.*, 2008), Andes virus (Hall *et al.*, 2009), influenza virus (Wu Dan *et al.*, 2011), porcine reproductive and respiratory syndrome virus (Ke Liu *et al.*, 2012) etc. have also been employed for phage display screening in order to identify peptides which were capable of being used either as diagnostic reagents or as antiviral peptides.

In the proposed study, using phage display technology we tried to identify and characterise the peptides that can bind to PPR virus. We have taken PPR virus as model of our study as this disease is widely prevalent in India and small ruminant rearing practice faces a very serious hurdle due to challenges posed by frequent incidences of PPR. In the wake of WTO stringent regulations, concerning international trade of livestock, frequent outbreak of this disease is of major concern and most serious obstacle in the export of germplasm and livestock products, adding huge losses to country's economy.

PPR is a highly contagious and economically important viral disease of sheep and goats characterized by pyrexia, mucopurulent nasal and ocular discharges, necrotizing and erosive stomatitis, enteritis and pneumonia with morbidity and mortality as high as 90% and 100%, respectively (Abu-Elzein *et al.*, 1990). It is caused by RNA virus that belongs to genus Morbillivirus, order Mononegavirales and family Paramyxoviridae (Tober *et al.*, 1998). This disease was first reported in sheep and goats in the Ivory Coast of Africa (Gargadennec and Lalanne, 1942). In India for the first time it was reported from Arasur village in the Villapuram district of Tamil Nadu in 1987 (Shaila *et al.*, 1989). It remained localised in south India for some time and then became endemic throughout the country (Shaila *et al.*, 1996).

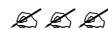
Effective control of any infectious disease is facilitated by early and accurate identification of causative agent as well as timely treatment of infected animal. In case of PPR, earlier laboratory confirmation was done by virus isolation and characterization, detection of viral antigen in pathological samples by agar gel immunodiffusion (AGID) and detection of serological response by virus neutralisation test. However, all these tests are either time consuming or less sensitive. The progress in molecular biology and immunology has lead to the development of more specific, rapid and sensitive techniques like Enzyme linked immunosorbent assay (ELISA), nucleic acid hybridisation using DNA probes, RT-PCR using specific primers. All these techniques require extensive infrastructure & skilled man-power.

Phage display technology can be used to select for and produce novel peptides that bind to the target molecules of interest. It allows rapid identification and amplification of the peptide ligands for a certain target molecule by the affinity of their specific- binding. This technique is superior to the methods with antibodies, which have been often used to detect such binding peptides, since a peptide displayed on the surface of filamentous bacteriophage is able to bind to the regions in a molecule that the immune system cannot recognize. In other words such a peptide can target a very small epitope. It searches for a binding site with a small amino acid loop while the large antibodies find an epitope of a molecule with two binding sites, a heavy chain and light chain. In addition, the phage display system is better than the methods with antibodies because it is inexpensive, easy to handle, and does not require much laboratory equipment (Ozawa *et al.*, 2005). In 2011, Wu and co-workers used phage display to identify the peptides binding to influenza virus strain H5N1 and they showed that in terms of the minimum quantity of viruses, the phage-based ELISA was as good as antiserum-based ELISA and a manual, semi-quantitative endpoint RT-PCR for detecting H5N1 viruses. More importantly, the selected phages bearing the specific peptides to H5N1 viruses were capable of differentiating this virus from other avian viruses in enzyme-linked immunosorbent assays (Wu Dan *et al.*, 2011).

In the proposed study, we plan to identify the peptides binding to PPR virus using phage display library. Those peptides are supposed to mimic the paratopes of PPR virus. Identification of such peptides may help in development of novel diagnostic reagents. Those peptides will be of synthetic origin thus they may be used as much more stable and clean diagnostic reagents eliminating the need of sophisticated laboratory infrastructure. Another possibility is that those peptides may cause neutralisation of the virus and thus may be used as antiviral peptides against PPR virus.

For this purpose, the present study was undertaken with following objectives:

- 1. To identify the peptides binding to PPR virus using phage display technology**
- 2. To characterize PPRV specific peptides and testing their binding efficacy**





*Review  
of  
Literature*



Phage display technology is based on the construction of a polypeptide library fused to a bacteriophage coat protein. Although T4, T7, and  $\lambda$  phage have been used for phage display (Efimov *et al.*, 1995; Sternberg N and Hoess RH., 1995), the most commonly used phages are filamentous phage because they do not lyse the infected bacteria during their life cycle but rather induces a state in which the infected bacteria produce and secrete phage particles into the growing medium. The filamentous phage particles mostly used for display purposes are known as Ff and include strains M13, f1, Fd and ft.

### **M13 Phage**

M13 Filamentous bacteriophage consists of a genome of circular single- stranded DNA and a flexible rod shaped cylinder composed of 5 coat proteins (pIII, pVI, pVII, pVIII & pIX). It is approximately 1  $\mu$ m long and 6nm in diameter. All the coat proteins can be used for display, but pVIII and pIII are the most commonly applied. Each M13 virion contains 2,700 copies of pVIII protein which together compose 87% of the total virion mass. The pVIII protein is largely  $\alpha$ - helical and rod shaped, with approximately 50% of its 50 amino acids being surface exposed, making it suitable for display. However, pVIII is limited to displaying short peptide sequences as larger sequence may cause difficulty in virion packaging. pIII is an ideal option for displaying large insertions, yet the infectivity of phage may be reduced. Most of the currently used phage display vectors use the N-terminus of pIII protein or pVIII protein to display the foreign peptide or protein (Smith and Scott, 1993). The pIII libraries are able to display maximum 5 copies of each individual peptide (Scott and Smith, 1990), whereas pVIII

libraries can display up to 2700 copies of small (up to six amino acids) peptides (Greenwood *et al.*, 1991). The pIII protein appears to have two functional domains: an exposed N-terminal domain that binds the F pilus, but is not required for phage particle assembly, and a C-terminal domain that is buried in the particle and is an integral part of the capsid structure. The C-terminal portion of pVIII is inside the phage particle, close to the DNA, while the N-terminal part is exposed to the surroundings. The circular single-stranded DNA enters the bacteria where it is converted by the host DNA replication machinery into double-stranded plasmid replicative form. By rolling circle replication, the replicative form makes single-stranded DNA and the templates for expression of proteins pIII and pVIII are formed. Phage descendants are assembled by packaging of the single-stranded DNA into protein coats and extruded through the bacterial membrane (Russel, 1991).

### **Phage display**

Phage display describes a selection technique in which a library of peptide or protein variants is expressed on the surface of a phage virion, while the genetic material encoding each variant resides on the inside (Sidhu *et al.*, 2000). It leads to the selection of peptides and proteins, including antibodies, with high affinity and specificity to almost any target. The technology involves the insertion of exogenous peptide coding sequences into the genome of the phage capsid proteins. The encoded peptides are expressed or “displayed” on the phage surface as a fusion product with the phage coat proteins. This way, instead of having to genetically engineer different proteins or peptides one at a time and then express, purify, and analyze each variant, phage display libraries containing up to  $10^{10}$  variants can be constructed simultaneously. Phage particles withstand very harsh conditions, such as low pH and low temperatures, without losing their capability to infect bacteria. The strength of phage technology is its ability to identify interactive regions of proteins and other molecules without pre-existing notions about the nature of the interaction.

### **Biopanning**

The most common screening method is based on enriching the phage clones with binding affinity for the target by a process called biopanning. Biopanning is of two types; in-vitro biopanning and in-vivo biopanning.

## **In-vivo Biopanning**

In this technique phage libraries are injected intravenously into animals and then organs or tissues are collected and examined for phage bound to tissue-specific endothelial cell markers. In vivo phage display is a high-throughput method for identifying target ligands specific for different vascular beds. Targeting is possible due to the heterogeneous expression of receptors and other antigens in a particular vascular bed. Such expression is additionally influenced by the physiological or pathological status of the vasculature. In vivo phage display represents a technique that is usable in both, vascular mapping and targeted drug development (Janka *et al.*, 2013). First in vivo biopanning was done by Pasqualini who isolated peptides that home to renal and cerebral vascular endothelium (Pasqualini and Ruoslahti, 1996). In vivo panning has several advantages: (i) the isolated phage-displayed peptides home selectively to “intact” targets of interest; (ii) an inherent blocking step is included where most of the phage-displayed peptides that recognize ubiquitous plasma and cell surface proteins are eliminated; (iii) these peptides may be useful for the functional analysis of new receptors and potential identification of novel drug target candidates because some of the isolated peptides have been found to bind to endothelial receptors expressed in the vasculature of specific tissues. Since Pasqualini’s study, identification of receptor-ligand pairs has been described for several organs such as lung, kidney, pancreas, adrenal gland, muscles, intestines and uterus.

In vivo phage display has also led to identification of many receptor-ligand pairs in malignant (Koivunen *et al.*, 1999) and benign diseases (Kolonin *et al.*, 2002). Kolonin and colleagues published a study in which a fat-targeting peptide was used to cure high-calorie related obesity in living animals (Kolonin *et al.*, 2004).

It also revealed a prostate homing peptide that specifically binds to the prostate vasculature and parenchyma. After coupling this peptide to a pro-apoptotic peptide and injecting the chimera intravenously in mice, Arap and colleagues were able not only to obtain selective tissue destruction, but also in delaying development of tumors in prostate cancer-prone transgenic mice (Arap *et al.*, 2002). This may mean a reduction in prostate cancer risk, as well as alternatives to surgical prostate ablation. Recently, many novel brain and testis-homing peptides

were selected from a phage library (Dighe V., 2014). Both organs are privileged with blood brain barrier and blood testis barrier respectively. Finding homing peptide/ ligand which can recognize such vascular addresses for brain and testis may help in making drugs more selective, thus providing higher therapeutic efficiency while simultaneously decreasing systemic toxicity while treating the CNS disorders, testicular infections and cancer.

These findings not only mean hope for the treatment of several high-incidence diseases, but also demonstrate the versatility of phage display technology.

**In vitro biopanning-** The major step involved are:

- 1) Target immobilization: The target molecules can be immobilized by passive adsorption to a modified 96-well polystyrene microtiter plates. The unbound target is washed off and the remaining sites in the well are blocked with unrelated proteins or non-ionic detergents.
- 2) Phage binding: The phage display random peptide library is added to the target coated well in a solution that allows stability of the target and minimal non-specific binding of the phage. It is important to start the first round with a large and highly diverse library for a better chance of isolating peptides of interest.
- 3) Removing unbound phage: The first round of biopanning requires higher yield of the fittest phage clones over the background and hence the washes are less stringent. The stringency of selection can be increased by more extensive washes in subsequent rounds to isolate phage with higher affinity.
- 4) Phage elution: The specific elution of the target bound phage can be carried out in a solution containing either free target or a competing ligand.

Due to stability of the filamentous phage, extremes of pH, denaturants, ionic strength, limited proteolysis or sonication can be used for non-specific elution of the target bound phage. The eluted phage is amplified and the biopanning process is repeated three to six times following which the phage clones are analyzed by DNA sequencing to identify the target binding peptides. Selectivity test can evaluate the affinity and specificity of the phage clones selected after

biopanning and save the cost of synthesis of peptides which may have been enriched due to artifacts in the screening process.

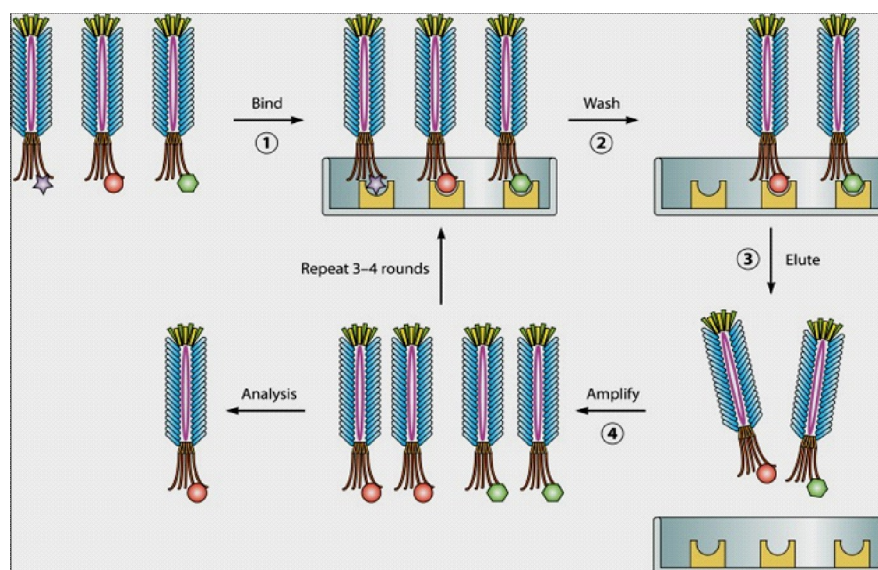


Figure 2.1: Basic steps involved in *in vitro* biopanning (Adopted from Huang *et al.*, 2012)

### Applications of phage display

#### **Protein-protein interactions:**

In recent years, phage display has evolved into a powerful tool providing opportunities to define natural protein-protein interactions and to mold novel ligand receptors. Over 80% of cellular proteins may work in complexes with other proteins and their protein-protein interactions are regulated by several mechanisms (Berggard *et al.*, 2007). Its use with combinatorial mutagenesis provides a rapid method to identify residues contributing energetically to binding at protein-protein interfaces. For example, phage display experiments predicted interaction between bacterial membrane transport proteins TonB and BtuF, identifying the potential binding residues on each protein. Phage displayed peptides were affinity selected in complementary biopanning using either TonB or BtuF as targets. Identified three consensus regions in TonB as potential BtuF binding sites and three regions in BtuF where TonB may bind (James *et al.*, 2009). Phage display has also been used to map intracellular interactions of distinct protein domains like SH3 and PDZ (Fuh *et al.*, 2000). The peptide modules affinity selected from a

phage display library can be mapped back to the whole genome sequences to identify the potential binding partners of the target proteins.

### **Enzyme specificity and inhibitors**

Phage display has been used in enzymology to determine the substrate specificity and to develop modulators of both the active and allosteric sites of the enzyme (Diamond, 2007; Kehoe and Kay, 2005; Benhar, 2001). The method can be used to display mutants of enzymes to study their mechanisms of action (Verhaert *et al.*, 2002). Since filamentous phage is resistant to broad range of proteases, it has been used in identification of substrates of various proteases (Matthews and Wells, 1993). Phage display can be used to gain insight into enzyme-substrate interactions that may be responsible for enzyme specificity. Botulinum type B and tetanus endopeptidases are neurotoxins that may interact with a region of the substrate (recognition motif) which is different from the cleavage site. Phage display library of vesicle associated membrane protein with mutated recognition motif was screened for cleavage by botulinum type B toxin to identify the alternative substrates and the role of recognition motifs in endopeptidase specificity (Evans *et al.*, 2005). In another example, phage display has been used to develop peptide inhibitors that bind either anthrax toxin or its cell surface receptors (Basha *et al.*, 2006; Gujraty *et al.*, 2005). Studies with inhibitors have been useful in providing information on the mechanism of cytotoxicity of anthrax toxin (Basha *et al.*, 2006).

### **Antibodies**

Phage display of antibody fragments has been used successfully in generating target specific antibodies which can be useful in multiple applications including proteomics, specific drug delivery and in analysis of intracellular processes. There are numerous examples of success described in recent reviews on this subject (Bratkovic, 2010; Benhar, 2001; Hoogenboom, 2005; Smith and Petrenko, 1997). Phage display has also been used for the isolation of intrabodies which are antibodies directed against intracellular target molecules. Intrabodies in the form of scFvs face the difficulty of folding properly under the reducing environment of cell cytosol and nucleus. However, phage libraries of highly diverse scFv's or engineered scFv's optimized for cellular expression, have been screened to select intrabodies (Cardinale and

Biocca, 2008; Philibert *et al.*, 2007). Intrabodies are useful in visualizing and modifying the function of intracellular targets. The target-selected phage can be stored and used on demand to generate antibodies for therapeutic or diagnostic applications. Phage display has been widely used to search for antibodies with anti-tumour or anti-pathogen activities. One of the approaches involves screening phage libraries for binding to molecular targets that are up regulated on the tumor surface or that are unique to the pathogen. The tumor specific antibody can be used in target directed delivery of imaging agents and cell toxic conjugates including toxins, cytokines or radioisotopes to eliminate cells in a disease specific manner (Zhou and Marks, 2009). The affinity selected antibodies against the pathogen specific targets can be used to therapeutically neutralize the pathogens (Molinkova *et al.*, 2008). Some viruses may mutate rapidly and hence escape immune detection. Broadly cross reactive antibodies can be developed by sequentially changing antigens in subsequent rounds of panning to select phage clones that recognize epitopes conserved in various mutants or bind to more than one epitope. This process has led to selection of HIV antibody with high affinity and broad-spectrum neutralizing activity (Zhang and Dimitrov, 2009). Antibody phage display libraries can be used to reproduce antigenic epitopes by selecting anti-idiotypic antibodies (Zhikui *et al.*, 2010). The antigen mimicry by anti-idiotypic antibodies can then be used in development of vaccines. Filamentous phage can itself be used as a carrier for antigens either fused to the coat protein or cross linked to its surface for eliciting antibody response (Van Houten *et al.*, 2006).

### **Receptors and G-proteins**

Phage display has been used to identify agonists and antagonists to probe the receptor structure and function. The peptide libraries can be screened for binding to functionally folded extracellular domains of receptors that contain the site for natural ligand. Selected peptides that recognize the binding interface of the receptor can antagonize its interaction with the natural ligand. The structural and functional properties of individual members of a large receptor family that bind the same natural ligands can be characterized with affinity selected peptides specific for each member (Koolpe *et al.*, 2005). Phage encoded peptide ligands have also been selected for targets like G protein coupled receptors, in which it is difficult to purify the functionally folded extracellular receptor domains. Antibodies specific for the known receptor

ligand can be used as a target to affinity select mimotopes of the ligand from phage display library. The selected mimotopes can be used to study the mechanism of interaction of ligand with its receptor and allow the development of potent agonist and antagonists (Bonetto *et al.*, 2005). Phage display approach has also been used to determine biologically relevant proteins that bind to pharmacologically active compounds such as SB-236057, Taxol and FK506. The identification of these proteins helped in resolving the mechanism of action of these compounds (Augustine-Rauch *et al.*, 2004).

### **Epitopes and mimotopes**

Phage display is a cheap and rapid method to map epitope of the antigen that is involved in specific interaction with the antibody. The identification of epitopes is essential in diagnostics, immunotherapy and vaccine development. Phage display peptide libraries can help identify critical residues within a continuous epitope that are involved in antibody binding. Since linear continuous epitopes are often six amino acids in length, the screening of libraries may affinity select peptides that exactly match the primary structure of the epitope (Fack *et al.*, 1997). The phage display peptide library can be screened to affinity select mimotopes, which are peptides that mimic discontinuous epitope structures. Mimotopes may not have similarity to any linear sequence of the antigen and may represent conformational dependent interaction of the epitope with the antibody. Several analytical tools are available to map the native epitope based on sequences of the selected mimotopes and the three dimensional structure of the antigen (Mayrose *et al.*, 2007). The phage display peptide library can also identify epitope mimics of carbohydrate and lipid antigens that have a low immunogenic profile (Förster-Waldl *et al.*, 2005). Mimotopes coupled with carrier proteins or presented as polymers have been developed for cancer, anti-allergic and contraceptive vaccines (Naz, 2009; Knittelfelder *et al.*, 2009).

### **Pathogen-targeted phage display**

Phage display has been used extensively to identify specific peptides and antibodies against pathogen targets including molecular targets, such as replication/cell division enzymes (Huang *et al.*, 2000) and host-pathogen virulence factors, whole bacterial cells (Carnazza S.

*et al.*, 2008), bacterial spores (Turnbough CL., 2003.) and viruses ((Ozawa *et al.*, 2005; Hall *et al.*, 2008; Hall *et al.*, 2009; Wu Dan *et al.*, 2011; Ke Liu *et al.*, 2012) etc. These strategies have been widely applied for developing novel diagnostic tools and therapeutic treatments for infectious diseases. (Huang, J.X. *et al.*, 2012). In 2011, Wu and co-workers used phage display in order to develop novel diagnostic test for H5N1 strain of avian influenza A virus. After panning they got three phage clones expressing peptides HAWDPIPARDPF, AAWHLIVALAPN or ATSHLHVRLPSK. These peptide bearing phages had a specific binding activity to H5N1 viruses. There results indicated that the phage-based ELISA was as good as if not better than antiserum-based ELISA and RT-PCR for detecting H5N1 viruses and the selected phages bearing specific peptides to H5N1 virus were also able to differentiate this virus with other poultry disease causing viruses in ELISA (Wu Dan *et al.*, 2011).

### ***Peste des petits Ruminants virus***

*Peste des petits ruminants* (PPR) is a highly contagious, fatal and economically important disease of both domestic and wild small ruminants, and camels. Owing to high morbidity (100%) and mortality (90%), PPR was included in the OIE (Office International des Epizooties) list of notifiable terrestrial animal diseases. The disease is currently spreading rapidly in most countries of the sub-Saharan and North Africa, the Middle East and Indian sub-continent and as far as into Tibet, China.

Officially, PPR was first described in the Republic of Cote d'Ivoire in West Africa in 1942 (Gargadenec and Lalanne, 1942), however, there are indications that the disease existed much earlier. Since PPR and RP are clinically related diseases and the viruses are antigenically similar, it is believed that PPR remained undiagnosed due to the high prevalence of RP and the inability of the available diagnostic tests to differentiate PPR from RP (Baron *et al.*, 2011). Furthermore, it is likely that, owing to cross-neutralization between PPRV and RPV, small ruminants infected with RPV would have developed protective antibodies suppressing the clinical outcome of PPRV infection (Taylor, 1979). Nevertheless, the disease gained attention when a severe rinderpest-like disease was observed in sheep and goats, which was unable to transmit to the cattle reared in the same herd or in the close vicinity.

**Geographical distribution-** After first identification, PPRV spread to sub-Saharan Africa, the Middle East, Turkey and the Indian subcontinent. During the last decade, the disease has been reported for the first time in China, Kenya, Uganda, Tanzania, Morocco and Tunisia (Banyard *et al.*, 2010; Munir *et al.*, 2013). This demonstrates that the virus is highly infectious, and is of emerging transboundary nature. Initially, PPRV was characterized and phylogenetically analysed based on the fusion gene (F), which classified all the strains of PPRV into four distinct lineages (Shaila *et al.*, 1996; Dhar *et al.*, 2002). Later, it appeared that phylogenetic analysis based on the nucleoprotein gene (N) presented a better molecular epidemiological pattern (Kwiatek *et al.*, 2007) and is currently preferred over F gene-based phylogenetic analysis. However, all the PPRV strains remained in the same group regardless of what gene was used as basis for classification, except that the F gene-based lineage I (i.e. Nig/75) became lineage II on the N gene-based tree. Recently, Balamurugan *et al.* (2010) suggested that the use of the haemagglutinin neuraminidase (HN) gene, in addition to the F and N genes, could give better resolution and permit tracing of virus transmission within outbreaks. Nevertheless, it is still unclear whether differences between lineages merely reflect geographical speciation or if they are also correlated with variability in pathogenicity between isolates (Banyard *et al.*, 2010). PPRV belonging to lineages I and II have exclusively been isolated from the countries in West Africa, where PPRV once originated. Lineage III is restricted to the Middle East and East Africa. Though lineage IV was strictly considered an Asian lineage, it is now overwhelming the other lineages in African countries, while still being predominant in Asia (Kwiatek *et al.*, 2011; Munir *et al.*, 2013).

**Economic impact of PPR-** PPR is generally considered a major constraint for small ruminant production; however, the economic impact of the disease has not been fully evaluated (Ezeokoli *et al.*, 1986; Nanda *et al.*, 1996). The economic importance of PPR is primarily due to its highly contagious nature, with a case fatality rate as high as 100%. This is of particular concern for the economics of small rural farms, where sheep and goats are reared as the sole source of income. PPR is one of the diseases in sheep and goats that are having a high impact on the poor rural small ruminant farmers. According to some studies, it was estimated that PPR causes a loss of US\$1.5 million annually in Nigeria (Hamdy *et al.*, 1976), US\$39 million

in India (Bandyopadhyay, 2002) and at least US\$1.5 million in Iran (Bazarghani *et al.*, 2006) and US\$15 million in Kenya (Thombare and Sinha, 2009).

**Morphology of PPR virus-** Like other paramyxoviruses, PPR virions are enveloped, pleomorphic particles and are comprised of single-stranded RNA genome with negative polarity. The length of the entire genome of PPRV is 15,948 nucleotides, which is the second longest among all morbilliviruses after a recently characterized feline morbillivirus (Bailey *et al.*, 2005; Woo *et al.*, 2012). The diameter of PPR virions ranges from 400 to 500 nm. The phosphoprotein (P) acts as a co-factor of large protein (L), which is the viral RNA dependent RNA polymerase (RdRp). There are three proteins associated with the host cell membrane-derived viral envelope. The matrix (M) protein acts as a link, which associates with the nucleocapsid and the two external viral proteins, the fusion (F) protein and the HN protein. The thickness of the PPRV envelope varies from 8 to 15 nm and the length of the surface glycoproteins ranges from 8.5 to 14.5 nm (Durojaiye *et al.*, 1985).

**Viral ribonucleoprotein-** The N protein surrounds the genomic RNA along with two other viral proteins, the L protein and the P protein to form the ribonucleoprotein (RNP). This RNP core encloses the entire genome of PPRV and protects from endonuclease digestion. The RNP strands appear as a herring bone with a thickness of ~14–23 nm (Durojaiye *et al.*, 1985).

**Genome organization, replication and transcription-** The PPRV genome carries six transcriptional units; each encodes for a contiguous and non-overlapping protein except the P gene, which also expresses C and V nonstructural proteins by an alternative open reading frame and RNA editing, respectively (Mahapatra *et al.*, 2003). All the genes in PPRV are arranged in an order of 3' -N-P/C/V-M-F-H-L-5' (Bailey *et al.*, 2005). An intergenic region of variable lengths separates one gene from the other (Barrett *et al.*, 2006). Notably, owing to variable lengths of the intergenic region between the M and F genes (without having an effect on the protein lengths), the genome varies among morbilliviruses. So far, no obvious role for this variable and high GC content intergenic region has been observed in the replication of the morbilliviruses. The sequence between two consecutive genes is AAAACTTAGGA

and is highly conserved throughout the morbilliviruses, including PPRV, indicating that this stretch of sequence is important for viral replications.

### **Structural Proteins:**

**Nucleocapsid Protein-**The gene that encodes for the N protein is the most transcribed among all genes for both structural and non-structural proteins of PPRV. The length of the N protein of PPRV is 525 amino acids. the N protein of PPRV is likely to interact with other N proteins (N–N interaction), with the P protein (N–P interaction) and with polymerase units (P–L interaction) to take part in the replication complex. The N protein plays an essential role in the replication of PPRV (Servan de Almeida *et al.*, 2007). It is the most accumulated protein in infected cells and is antigenically most conserved among morbilliviruses (Libeau *et al.*, 1995). Being most abundant, N is a highly immunogenic protein. However, the immune responses generated against the N protein are non-protective due to intra-viral location of the protein. Given its abundance and antigenic stability, the N protein has extensively been targeted for diagnostic assays (Munir *et al.*, 2013). Apart from its diagnostic application, the genetic diversity of the N gene has been the basis for the classification of PPRV into four lineages. This classification better represents the geographical origin than the classification based on the variation of the external glycoprotein, the F protein (Diallo *et al.*, 2007; Kwiatek *et al.*, 2007).

**Phosphoprotein (P)-** The phosphoprotein of PPRV, as other morbilliviruses, is acidic in nature and undergoes intensive post-translational phosphorylation (hence the acronym phosphoprotein), owing to richness in serine and threonine (Diallo *et al.*, 1987). The length of P proteins varies from 506 to 509 amino acids between different morbillivirus members and the P protein of the PPRV is the longest among all. Despite the essential role of the P protein in viral replication and transcription, it is one of the least conserved proteins, which is demonstrated by the fact that the P proteins from PPRV and RPV share only 51.4% amino acid identity (Mahapatra *et al.*, 2003). Moreover, the region from 21<sup>st</sup> amino acid to 306<sup>th</sup> amino acid contains the majority of unconserved residues. Given the fact that the C-terminus of the P protein is involved in the N–P interaction, this terminus is more conserved compared with the N-terminus of the P protein. In morbilliviruses, the P protein plays crucial roles at multiple

levels in both viral replication and immune regulation. For instance, the N–P interaction is required for key biological processes such as cell cycle control, transcription and translation regulation (Johansson *et al.*, 2003). The motifs required for the interaction of RPV P protein with N protein (N–P interaction) are conserved in the P protein of PPRV. Moreover, the P protein is the vital element of the viral L–polymerase complex, and it is assumed to be a key determinant of cross-species morbillivirus pathogenicity (Yoneda *et al.*, 2004). Despite these crucial roles of the P protein in the replication of morbilliviruses, its function in PPRV replication and pathogenicity remains elusive, which warrants future investigations.

**Matrix (M) Protein-** The ORF for the M protein of PPRV is located at nucleotide position 3438–4442, which is translated to a protein of 335 amino acids with a predicted molecular weight of 37.8 kDa. It is therefore considered one of the smallest proteins among all the structural proteins of morbilliviruses. The protein is highly conserved and a 92.5% and 85.0% similarity and identity have been calculated between PPRV and RPV, respectively. This high degree of conservation may reflect the essential role of the M protein in the formation of progeny viruses and interaction with the surface glycoprotein in the cell membrane (Muthuchelvan *et al.*, 2005). It constitutes the inner coat of the viral envelope and acts as a bridge to connect the surface glycoprotein (F and HN) with that of ribonucleoprotein core (genome, N, P and L).

**Fusion (F) Protein-** The F protein (59.137 kDA) is one of the highly conserved proteins not only between PPRV and RPV but also among all the morbilliviruses. This conservation probably reflects the cross-protection between PPRV and RPV (Taylor and Abegunde, 1979). In all paramyxoviruses, the F protein is embedded in the viral lipid bilayer envelope and protrudes as spikes on the viral surface (Bundza *et al.*, 1988). The cleavage of the F protein is a key mechanism of paramyxovirus virulence. The naive form of the F protein (F<sub>0</sub>) undergoes post-translational proteolytic cleavage and results in two active subunits, F<sub>1</sub> and F<sub>2</sub>. This mechanism is not well understood for PPRV.

In all morbilliviruses, the membrane associated proteins are glycosylated and hence are known as glycoproteins. This post-transcriptional modification is critical for the transport of the protein to the cell surface, and to maintain its fusogenic ability and integrity. All members

of the morbillivirus genus contain a conserved NXS/T (X indicates any amino acid) glycosylation site in the F2 subunit of the mature protein (Meyer and Diallo, 1995). In PPRV, the three N-linked glycosylation sites include <sup>25</sup>NLS<sup>27</sup>, <sup>57</sup>NIT<sup>59</sup> and <sup>63</sup>NCT<sup>65</sup>; however, their specific functions still need to be revealed.

**Haemagglutinin- neuraminidase (HN) Protein-** The HN protein is the least conserved. While both PPRV and RPV have 609 amino acid residues in their respective HN proteins, the proteins share only 50% amino acid identity. This variation probably reflects the viral specificity for cell tropism and therefore determines the host range. Most of the viral neutralizing antibodies are mainly directed against the HN protein (Renukaradhya *et al.*, 2002). The fundamental roles of the HN proteins in progression of viral infection and specific binding to host cell membrane are not defined in PPRV. However, the findings that the H protein is a major determinant of cell tropism in MV and is the main cause of cross-species pathogenesis in lapinized RPV (Yoneda *et al.*, 2002) indicate that H is the vital antigenic determinant of the morbilliviruses. However, it has been determined that the HN protein of PPRV required a homologous F protein for proper functioning in virus replication (Das *et al.*, 2000). In some paramyxoviruses, surface proteins can cause haemagglutination and can carry neuraminidase activities. Interestingly, among morbilliviruses it is only MV and PPRV that have haemagglutination capabilities (Varsanyi *et al.*, 1984; Seth and Shaila, 2001). In addition to haemagglutination (viral attachment to cell surfaces and agglutination of erythrocytes), PPRV is unique for its neuraminidase activity (cleaves sialic acid residues from the carbohydrate moieties of glycoproteins). Therefore, it is the only member of the morbilliviruses that has HN protein (Seth and Shaila, 2001), which was previously thought to be absent.

**Large (L) Protein-** The L protein of PPRV is 2183 amino acids long and is regarded as the largest protein in PPR virions. However, due to natural attenuation at each gene-junction in all mononegaviruses, the mRNA encoding for the L protein is the least abundant (Flanagan *et al.*, 2000; Yunus and Shaila, 2012). Notably, the L protein is conserved among morbilliviruses: PPRV has an identity with RPV and CDV of 70.7% and 57.0%, respectively (Bailey *et al.*, 2005). The protein is rich in leucine and isoleucine, which can be as high as 18.4% (Muthuchelvan *et al.*, 2005). The L protein of PPRV carries a length (2183 amino acids) and molecular

weight (247.3 kDa) identical to that of RPV, MV and DMV; however, the protein charge +14.5 is different from those of RPV (+22.0) and PDV (+28.0) (Munir *et al.*, 2013). In all morbilliviruses, the L protein acts as RNA-dependent RNA polymerase and performs transcription and replication of the viral genomic RNA. Additionally, the L protein is also responsible for capping, methylation and polyadenylation of viral mRNA. All these steps are crucial for efficient replication of the viruses (Munir *et al.*, 2013).

### **Accessory Proteins-**

It is only the P gene among all the genes of PPRV that encodes for more than one protein, known as C and V proteins, through alternative open reading frame and RNA editing, respectively (Mahapatra *et al.*, 2003; Barrett *et al.*, 2006).

**C-Protein-**The C protein has role in viral replication. In case of Rinderpest virus, another biological function of C-protein has been seen in inhibition of interferon  $\beta$  production (Boxer *et al.*, 2009). But in case of PPR virus any other function of this protein is not known and needs to be examined.

**V-Protein-** By virtue of having the same initial gene frame, the V protein shares the N-terminus to the P protein, but due to RNA editing, the cysteine-rich C-terminus is different (Mahapatra *et al.*, 2003). Studies are required to investigate the functions of the V protein of PPRV, and its relation to other morbilliviruses.

**Virus replication-** The basic steps involve in the replication of PPRV are depicted in the fig 2.2.

**In vitro Cultures and Animal Model-** Gilbert and Monnier (1962) were first to be able to isolate PPRV on primary lamb kidney cells. However, later, because of the problematic quality and considerable variations in primary cultures, an African green monkey kidney (Vero) cell line was used for PPRV isolation (Lefevre and Diallo, 1990).

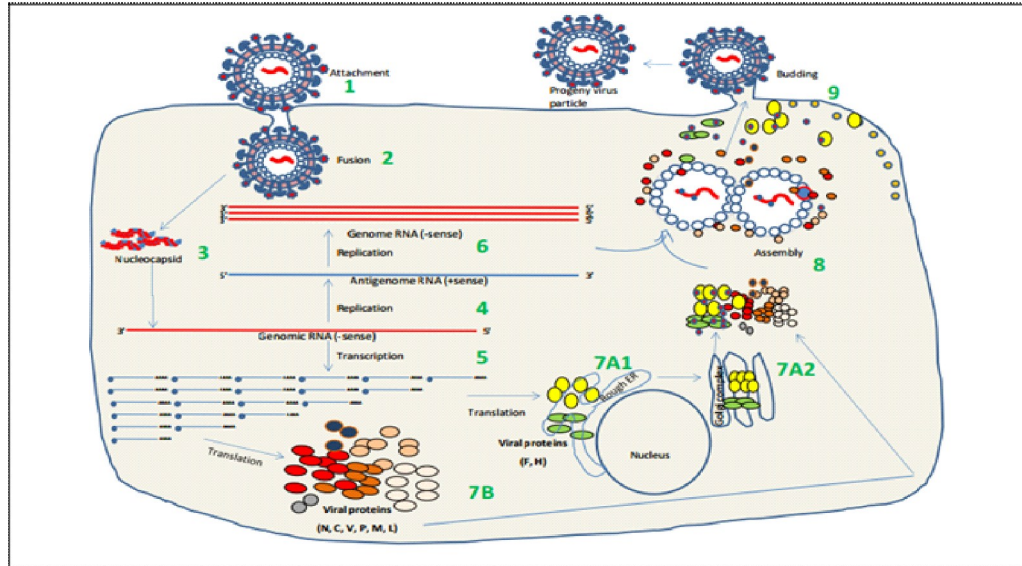


**Fig 2.2: Steps involved in PPRV replication (Adopted from Kumar N. *et al.*, 2014)**

### **Cytopathic effects in vero cell line:**

With Sungri vaccine virus strain visible CPE is observed on fourth day post infection and is characterized by cell rounding and aggregation of cells. On day six post infection, generalization of CPE and formation of syncytia takes place (Lefevre and Diallo., 1990). Whereas Arasur strain of PPR vaccine virus strain shows CPE 36-48 hr post infection and is characterized by cell rounding and formation of syncytia. However by 96 hr post infection there occurs generalization of CPE and complete detachment of cell monolayer is observed by 120 hr. (Hegde *et al.*, 2009)

### **Diagnosis**

Earliest as well as accurate diagnosis of PPR is crucial in implementing control measures, in order to contain outbreaks and minimize economic losses. Initially, the majority of PPR outbreaks were diagnosed based on typical clinical signs. However, the signs of PPR are often difficult to distinguish from those caused by a number of other diseases, such as foot-and-mouth disease and bluetongue disease (Munir *et al.*, 2013). The situation becomes even more complicated when outbreak of these diseases occurs in PPR endemic areas. In such conditions,

it becomes necessary to confirm the clinical diagnosis through laboratory testing (Munir *et al.*, 2013). Currently, the diagnosis of PPRV is made based on demonstration of antibodies, which is a good indication because an animal infected with PPRV carries antibodies for life, with the development of a sustained antibody response.

### **Serological detection**

Most of the available diagnostic assays have been developed based on the N protein. Owing to the presence at the 32 end of the genome of PPRV, the N protein produced in quantities higher than any other structural proteins because attenuation occurs at each intergenic region between two genes (Lefevre *et al.*, 1991; Yunus and Shaila, 2012). The antibodies produced against the N protein don't protect the animals from the disease. Due to abundance of the N protein it remains the most acceptable target for the design of PPRV diagnostic tools (Diallo *et al.*, 1994). Moreover, because the HN protein is the most diverse among all the members of morbilliviruses, RPV and PPRV share only 50% similarity in their HN proteins. The HN protein determines cell tropism; most of the protective host immune response is raised against HN protein. Therefore, serological assays have also been developed targeting HN protein (Munir *et al.*, 2012, 2013). Commercial ELISAs are available which are based either on the HN (Saliki *et al.*, 1993; Anderson and McKay, 1994; Singh *et al.*, 2004) or N proteins (Libeau *et al.*, 1995) for specific detection of antibodies against PPRV, in any susceptible host. The sensitivity and specificity of these assays can be as high as 90% and 99%, respectively.

### **Antigen detection**

Immunocapture (Libeau *et al.*, 1994) and sandwich ELISAs (Saliki *et al.*, 1994) are available to efficiently detect antigens in the tissues and secretions of PPRV-infected animals. Both these assays utilize monoclonal antibodies (MAbs) directed against the N protein of PPRV. Both assays are rapid, sensitive and specific with a detection limit of 100.6 TCID<sub>50</sub>/well. Since the MAbs used in these assays are raised against the non-overlapping domains of the N protein of PPR and RP viruses, this assay can be used to differentiate PPRV- from

RPV-infected animals (Libeau *et al.*, 1994).

### **Genome detection**

To overcome several shortcomings of the serological and antigen detections, such as the requirement of sera in well-preserved format, several PCRs have been developed for PPRV with wide range of sensitivities, specificities and detection limits (Munir *et al.*, 2013). Despite the high sensitivity and specificity of these assays, and their validity to detect both vaccine and field viruses, none of the assays is a formally approved OIE method. For this they need further extensive validation. None of the assays is field applicable since they require thermocycler and electrophoresis apparatus for RT-PCR, and real-time PCR for probe or SYBR-Green-based assays.

### **Control and Challenges**

After successful eradication of RP, efforts are now being made to control and eradicate PPR, which appeared to be the most appropriate target owing to identical features of the virus, disease mechanisms and epidemiological patterns. Having this aim in mind, there are factors that can favour control and eradication of PPRV. Efficient vaccines are available for immunization and sensitive assays are available to detect the virus in all possible clinical samples. Significant efforts are now being made to improve thermostability of the vaccines and field applicability of the assays. Although there appear to be four lineages, there is only one serotype for PPRV. The host spectrum of PPRV is relatively narrow with small ruminants as the dominant host, compared with several other infectious diseases. However, this range is now extended to most wild small ruminants and camels. The requirement of close contact for disease transmission, short incubation period (2–6 days) and life-long seropositivity further favour the control and eradication of the disease. With the availability of a reverse genetic system, novel recombinant, multivalent and also DIVA vaccines, the global eradication of PPR is feasible and achievable.

On the other hand, there are factors that constrain global eradication. PPR eradication cannot be completely realized without evoking its spearhead role in animal health. The full economic consequences of the disease have not been determined. Vaccines need to be cost-

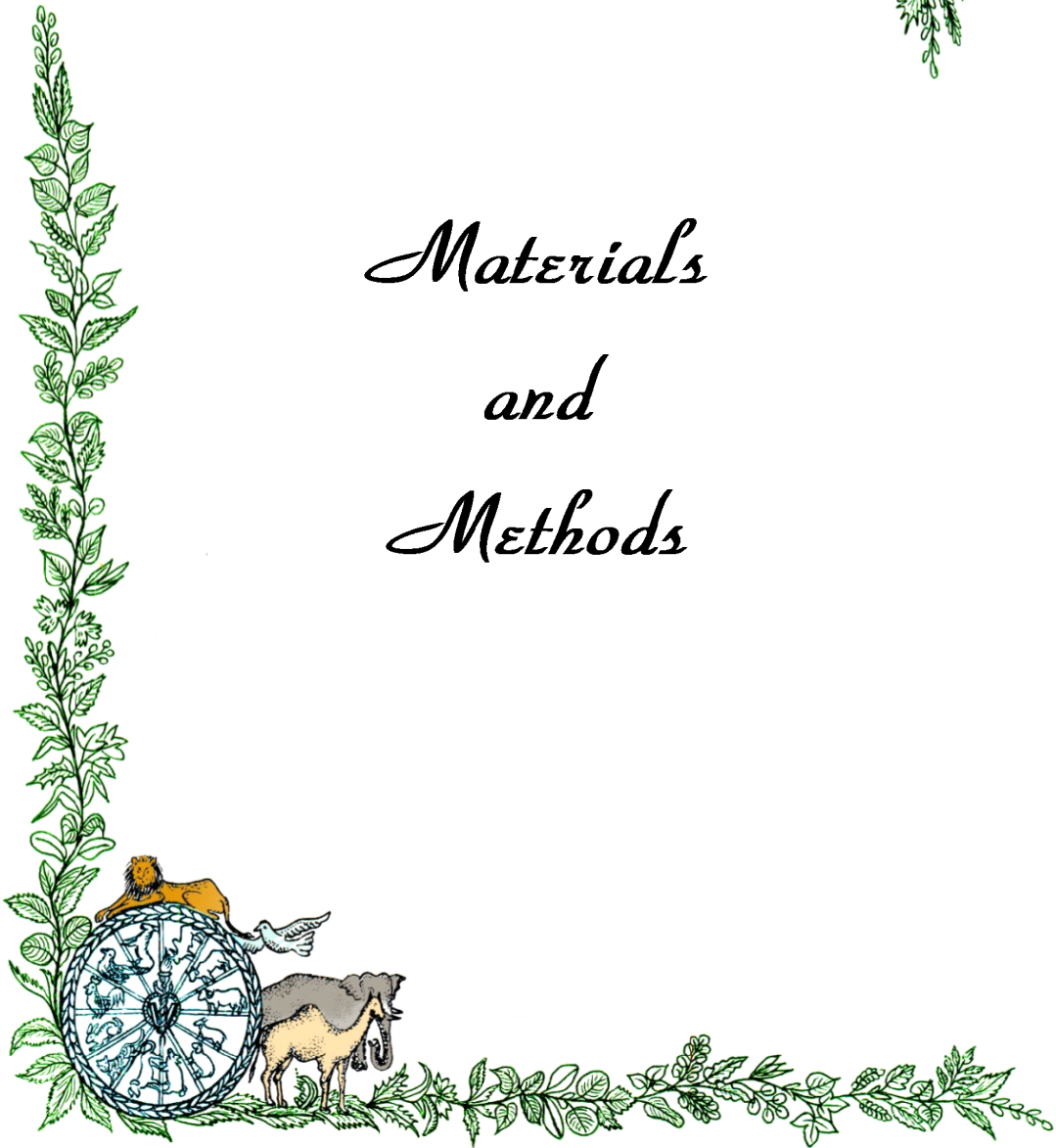
effective and available in developing and PPRV-endemic countries. The overall prevalence of PPR, especially in unusual hosts such as wild small ruminants and camels, and their role in disease epizootiology, need to be investigated before promising any effort for control and eradication of the disease. Recent identification of PPRV in Asiatic lion (*Panthera leo persica*) added another dimension in the host spectrum of PPRV (Balamurugan *et al.*, 2012). Therefore, monitoring of several wildlife species for presence of the PPRV needs to be considered.

On the other hand, due to the fact that small ruminants have a lower value compared with cattle, it is a matter of relevance when comparing the success of the RP campaign with a future PPR eradication. Collectively, the evaluation of its economic impact, improvement and commercialization of diagnostic tests and vaccines, and coordination and integration for planning eradication are key elements to be considered in the global eradication of PPR.





*Materials  
and  
Methods*



**3.1: Buffers and reagents**

The details of the media, buffers and other solutions used in this study are given in the appendix. The molecular biology grade reagents/chemicals were used for the preparation of various buffers and reagents.

**3.1.1: Glassware, plastic ware and chemicals**

The glassware used in the present study was obtained from Borosil (India) and ASGI (India). The chemicals and enzymes used were obtained from Sigma (USA), Life Technologies. Inc.(USA), New England Biolabs, Beverly, MBI Fermentas, QIAGEN (Germany), Bangalore Genei (India) and Merck (India). The plasticware like microfuge tubes, microtips, culture plates etc. were procured from Axygen (USA) and Tarsons (India).

**3.1.2: Equipments**

Thermal cycler (Biometra, UK), refrigerated microcentrifuge (REMI, India), Sorvall MC12V microcentrifuge, Spectropolarimeter (Jasco J-810), HPLC (Shimadzu, UFLC), Laminar flow, Electrophoresis apparatus (BIORAD, USA), Inverted bright field microscope (Olympus, Japan), Inverted fluorescence microscope (Nikon Eclipse Ti, Japan), Electronic microbalance (Sartorius BL 210S), Spectramax M5 (Molecular Devices), Speed Vac concentrator (Eppendorf concentrator plus), CO<sub>2</sub> incubator (New Brunswick, Galaxy 170R), Orbital shaker (GallenKamp) etc.

### 3.2: Phage Display Technique for identification of peptides binding to PPRV

Phage-display technology can be used for identification of pathogen specific peptide. In vitro phage display has become a useful tool to isolate ligands that bind to specific microbe in order to develop theranostics. The standardized protocols were applied in *in vitro* phage display for identification of PPRV binding peptides. Ph.D.-12™ Peptide Library Kit (E8100S) was purchased from New England Biolabs for this study.

Initially, the titer of the phage library (stored at -20°C) obtained from its commercial source was checked to ensure that it has not been lowered during shipment. The bacteriophage host strain *Escherichia coli*, ER2738 was supplied with the New England Biolabs Ph.D. Phage Display Library Peptide Kit ([www.neb.com](http://www.neb.com)). ER2738 maintains the F2 pilus, which is essential to allow M13 phage infection into the bacterium. Phage in this library carry the *lacZα* gene and when they infect a complementing bacterial strain (e.g., ER2738), the resulting phage plaques appear blue on plates containing X-gal/IPTG. Due to the importance of the infection step, the bacteria were grown on selective media containing tetracycline to ensure the F2 episome is retained in all progeny. To maintain optimal infectivity, fresh plate was streaked every 2 weeks from glycerol stocks of ER2738.

#### 3.2.1: Phage Titration

1. LB-tetracycline plate (12.5 µg tetracycline/mL LB agar) was streaked with *E. coli* ER2738. Plate was incubated in dark (tetracycline is inactivated by light) at 37°C overnight until single colonies appear in inverted position.
2. Next day, a single colony of ER2738 was transferred into a sterile flask containing 10 mL aliquots of LB broth (with tetracycline).
3. Next day, 50 µl ER2738 culture was inoculated in 10 ml of LB containing 10 µl tetracycline and incubated for 3-4hr i.e. to mid-log phase ( $OD_{600} \sim 0.4-0.6$ ) in a shaker incubator.
4. While incubation 0.8% top Agar was melted in microwave and dispensed 3 ml into sterile culture tubes, one per expected phage dilution. The culture tubes were maintained at 45°C.

5. LB/IPTG/Xgal plate one per dilution was pre-warmed, for at least one hour in dark at 37°C until use.
6. Ten fold serial dilutions of phage were prepared in TBS buffer (10<sup>-1</sup> to 10<sup>-16</sup> dilution).
7. When the culture in Step 3 reaches mid-log phase 200 µl of culture was dispensed into sterile microfuge tubes, one for each phage dilution
8. To carry out infection 10 µl of each phage dilution was added to each tube, vortexed quickly, and incubated at room temperature for 5 minutes
9. The infected cells were transferred one infection at a time to culture tubes containing 45°C Top Agar, vortexed briefly and poured immediately onto a pre-warmed LB/IPTG/Xgal plate to spread top agar evenly.
10. The plates were allowed to cool for 5 minutes. Once solidified plates were inverted and incubated overnight at 37°C in dark.
11. Numbers of plaques were counted on plates that have approximately 50-250 plaques.  
$$\text{Pfu/ml} = \text{no. of plaques} \times \text{dilution factor} \times 100$$

### **3.3.1: Culture of Vero cells:**

Vero cells procured from National Centre for Cell Sciences (NCCS), Pune. The cells were grown in Dulbecco's modified Eagle's medium (DMEM) with 5% fetal calf serum (FCS), incubated at 37°C with 5% CO<sub>2</sub>. The cells were passaged every 2 days after reaching the confluency. Briefly, the confluent monolayer of Vero cells in 25cm<sup>2</sup> flask was washed with sterile PBS. 1ml of Trypsin versin glucose (TVG) was added and incubated for 10 min at 37°C to detach the cells from the surface. The cells were gently pipetted and growth medium (DMEM added with 10% FBS) was added to stop the action of trypsin. Later the cells suspension was made in appropriate volume of medium and seeded to the new flask.

### **3.3.2: Propagation of PPRV in Vero cells:**

The PPRV which was adapted to grow in Vero cells was revived and propagated by passaging the virus in Vero cells. For this, the Vero cells at passage-33 were grown in 25-cm<sup>2</sup>

tissue culture flask. As the growth reached 60- 70 % confluency, cells were washed twice with maintenance medium containing 1% FBS and infected with Vero adapted Sungri strain of PPRV at 0.05MOI and incubated at 37°C temperature and 5% CO<sub>2</sub>. After allowing 1 h for virus adsorption with intermittent shaking in every 10 min, virus inoculum was replaced with 5 ml maintenance medium containing 1% FBS. It took 4 days to observe cytopathic effects of PPRV. From 6<sup>th</sup> day onwards the CPE became generalised. The characteristic cytopathic changes included cell rounding, syncytia formation and finally detachment from surface of the flask. The presence of virus in Vero cells was confirmed by ELISA using polyclonal sera against PPRV and also by PCR using primers for N-gene of the virus. Scaling up of the virus was done by infecting Vero cells in 75 cm<sup>2</sup> flasks.

### **3.3.3: Concentration of PPRV:**

1. The Vero cell culture supernatant was collected from all the PPRV infected 75cm<sup>2</sup> flasks on 6<sup>th</sup> day.
2. This cell supernatant was centrifuged at 2000g for 30 minutes at 4°C to remove cells. The clear supernatant was then ultra-centrifuged at 1,00,000Xg for 1hour at 4°C to pellet the VLPs.
3. The resultant VLPs pellet was re-suspended in 2ml PBS (pH 7.2) and further purified through sucrose gradient (20-30-60%) in PBS and sedimented by ultracentrifugation at 1,00,000X g and 4°C for 3 hours.
4. The visible opalescent band in the sucrose gradient was collected and diluted in PBS. This was pelleted again by centrifugation at 1,00,000x g for 2 hours to remove sucrose.
5. The sedimented particles were resuspended in PBS and stored at 4°C.
6. The concentration of VLPs was determined by Bradford assay.

(Above protocol has been taken from Li *et al.*, 2014)

### **3.3.4: Bradford Assay:**

Bradford's assay is a rapid and accurate method for estimation of protein concentration. When compared to Lowry's Method, it is subjected to less interference by common reagents and non-protein components of biological sample. The assay relies on the binding of the dye

Coomassie blue G250 to protein. The quantity of protein can be estimated by determining the amount of dye in the blue ionic form. This is usually achieved by measuring the absorbance of the solution at 595 nm or 625 nm.

### **Protocol**

1. Standard BSA (1mg/ml) solution was prepared in PBS and for making standard curve, different dilutions of BSA were made using this standard BSA solution.
2. Volume in all dilutions was adjusted to 60 $\mu$ l with PBS.
3. 900 $\mu$ l of Bradford's reagent was mixed thoroughly into each of these dilutions and incubation was done for 10 minutes at room temperature.
4. Optical densities were recorded on spectrophotometer at 595nm.
5. A standard curve was constructed by plotting optical density reading on 'Y' axis against standard protein concentration (in  $\mu$ g) on 'X' axis.
6. The value 'x' was recorded from the graph corresponding to the optical density reading for the test sample.
7. The concentration of protein in the test sample was calculated using the following formula:

$$\text{Protein concentration in test sample} = x/v \text{ mg/ml.}$$

Where x - Value from graph in  $\mu$ g

v - Volume of sample in  $\mu$ l.

From the standard curve, we determined and report concentration of viral protein in the test sample.

#### **3.5.1: *in vitro* panning with PhD-12 phage display library**

The most straightforward method of affinity partitioning (panning) involves directly coating a plastic surface with the target of interest (by non specific hydrophobic and electrostatic interaction), washing away the excess, and passing the pool of phage over the target-coated surface. In present study, surface panning was done in 96-well microtiter plate using concentrated PPRV as target.

### **3.5.2: First-Round Biopanning-**

1. Four different dilutions of PPR virus suspension were made (viz. 5µg/ml, 10µg/ml, 20 µg/ml, 30 µg/ml) in 0.1 M NaHCO<sub>3</sub>.
2. 150µl of these solutions were added in four different wells respectively and repeated swirling was done until the surface of well was completely wet.
3. For coating the plate with target, it was kept at 4°C for overnight incubation in a humidified container.
4. Next day, 10 ml of LB+Tet medium was inoculated with ER2738. This culture was incubated at 37°C with vigorous shaking until it reaches an O.D.<sub>600</sub> of 0.4-0.6. This culture was used in step 11 for titration.
5. The coating solution was pour off from the plate and firmly slapping down was done in order to remove residual solution. Now each well was filled with blocking buffer. It was incubated for 1½ hour at 4°C.
6. Blocking solution was discarded as in step 5. Each well was washed rapidly with TBST (TBS+0.1%Tween-20).
7. A 100 fold representation of phage library with TBST was made. 100µl of this was added in each well and gentle rocking was done for 10-60 minutes at room temperature.
8. Nonbinding phage were discarded by pouring off and slapping plate face down onto a clean paper towel.
9. Each well of the microtiter plate was washed 10 times with TBST.
10. Bound phages were eluted using 0.2 M Glycine-HCl (pH2.2), 1 mg/ml BSA. 100µl elution buffer was added in each well. Gentle rocking was done for 20 minutes. Eluate was pipetted out into a microcentrifuge tube, and neutralised with 60µl of Tris-HCl (@15µl per 100µl Glycine-HCl).
11. 2µl of the eluate was used for titration as described in earlier section.
12. Rest of the eluate was kept for phage amplification.
13. After amplification 2<sup>nd</sup> and 3<sup>rd</sup> round of panning were done similar to above mentioned protocol using amplified phage eluate of proceeding round of panning. Only difference made was increased concentration of Tween 20 (0.5 % V/V in TBST) in order to increase stringency.

14. In 4<sup>th</sup> round negative selection was done in order to remove plastic and Vero cell component binding phage clones from the phage eluate.

### **3.5.3: Negative selection of phage clones:**

1. This was performed at 4<sup>th</sup> round of panning using the unamplified phage eluate of 3<sup>rd</sup> round of panning.
2. 4 wells were coated with non-infected Vero cell supernatant and 4 wells were without any coating (to remove phages having tendency to bind with material of microtiter plate).
3. In 1<sup>st</sup> 4 wells, Blocking was done in same manner with 1% BSA in TBS as that mentioned in protocol of earlier round of panning but later 4 wells were kept unblocked with any blocking agent plastic of well surface remained exposed.
4. Unamplified Phage eluate from the 3<sup>rd</sup> round of panning was directly added into the Vero cell supernatant coated wells. Gentle rocking of the plate was done for 45 minutes at room temperature.
5. Now the unbound phage clones were collected in the form of superficial solution of phage and leaving the bound phages into the Vero cell supernatant coated wells.
6. The collected superficial phage suspension was added into the uncoated wells (to remove plastic binding phage clones) and gentle rocking was done for 45 minutes at room temperature.
7. Again the non-binding phage clones were pipetted out from the wells and collected in microfuge tube this proportion of phage solution will be devoid of phage clones having tendency to bind with material of microtiter plate as well as Vero cell components.
8. These collected phage clones were amplified to be utilised in 5<sup>th</sup> round of panning.

### **3.5.4: Phage amplification:**

Amplification of the eluted phage is essential to obtain enough phage for subsequent rounds of *in vitro* panning, as only a small proportion of the library input will bind with the chosen target. A major problem in any phage display experiment is contamination with wild-type phage in the amplification step. Wild-type phage can replicate faster than modified phage because they do not face the additional burden of expressing the peptide on the coat

protein. Using a phage library, in which the peptides are expressed linearly, has a major advantage at the amplification step over a constrained library as linear libraries are at less of a growth disadvantage than constrained libraries compared to wild-type phage. As a result, phage amplification from these two types of library is performed differently. We have used the Linear Library Amplification protocol. For constrained libraries one has to use the serial dilution of eluate and well defined selected number of phage plaques need to be picked up for next round of panning.

#### **3.5.4.1: Linear Library Amplification**

1. 10 ml of LB+Tet medium was inoculated with ER2738 and kept in shaker incubator for overnight incubation at 37°C with 180rpm speed.
2. In 49 mL LB in Erlenmayer flasks, 650µL of overnight ER2738 culture was added and 350 µL of phage eluate was added, gently mixed and kept in an orbital shaker at 37°C for 4.5-5 hours with 180 rpm speed.
3. After 4.5 hours, the culture was transferred to a centrifuge tube and centrifuged at 4500xg for 10 minute. The supernatant was transferred to a fresh tube and recentrifuged to remove any tissue/bacterial contamination.
4. The upper 80% of supernatant was transferred to a fresh tube and 1/6 volume of 20% PEG/2.5 M NaCl was added to it. The mixture was mixed briefly and the phage was allowed to precipitate overnight at 4°C.
5. Next day, the PEG precipitated phage was recovered by centrifugation at 12,000 g for 15 minutes at 4°C. The supernatant was discarded. The tube was again centrifuged briefly to remove residual supernatant.
6. The pellet was suspended in 1 ml of TBS and centrifuged at 14,000 rpm for 5 minutes at 4°C to pellet out residual cells.
7. The supernatant was transferred to a fresh microcentrifuge tube and 1/6 volume (167µl) of 20% PEG/2.5 M NaCl was added and incubated on ice for 60 minutes to precipitate phage.
8. Then the content was centrifuged at 14,000 rpm for 10 minutes at 4°C, the supernatant was discarded, re-spinned briefly and residual supernatant was removed with a micropipette.

9. The pellet was resuspended in 200 µl of TBS. Kept it for 20 minute at room temperature to allow the phage to dissolve completely and then centrifuged for 5 minutes to pellet out any remaining insoluble material the supernatant was transferred to a fresh tube and kept at 4°C until it is titered and used. For long-term storage of this amplified phage, it is recommended that the phage be stored in 50% glycerol at -20°C.
10. The amplified eluate was titrated as described earlier on LB/IPTG/Xgal plates.
11. In the similar pattern 1<sup>st</sup> three rounds of surface panning were conducted to enrich peptides with capability to bind PPRV. After five rounds of selection, individual blue plaques were amplified to get ss-DNA of phage.

### **3.5.5: Plaque Amplification and isolation of single stranded phage DNA for Sequencing**

1. Overnight culture of ER2738 was diluted in LB in ratio of 1:100. This 1 ml of diluted culture was dispensed into culture tubes, one for each plaque/clone to be characterized. Randomly 80-100 clones from the fifth round of panning were selected which is sufficient to detect a consensus binding sequence.
2. Well-separated blue plaques were picked from titration plate with the help of pipette tip and transferred to tube containing the diluted overnight culture.
3. Tubes were incubated at 37°C with shaking for 4.5–5hours.
4. After incubation cultures were transferred to micro-centrifuge tubes and centrifuged at 14,000 rpm for 10 minutes to remove bacteria.
5. The supernatant was transferred to a fresh tube and re-centrifuged to remove any leftover bacteria.
6. Upper 80% of the supernatant containing phage was transferred to a fresh tube.
7. To the supernatant 200 µl of PEG/NaCl was added, inverted for several times and allowed to stand for 30 min at room temperature.
8. The mixture was centrifuged at 14000 rpm for 10 min at 4°C. Supernatant was decanted and re-centrifuged to remove all the supernatant.

9. The phage pellet was suspended in 100 µl TE buffer.
10. Equal volume of equilibrated phenol (100 µl) was added, mixed, vortexed and allowed to stand for 1min.
11. Then 100 µl of chloroform was added, mixed, vortexed and allowed to stand for 1 min.
12. The final mixture was centrifuged at 13000 rpm for 15 min at room temperature.
13. Carefully aqueous phase was taken out and 300 µl of 25:1 solution of ethanol: 3M sodium acetate (pH 5.2) was added.
14. Finally, single stranded DNA was recovered by centrifugation at 13000 rpm for 15 min at 4°C.
15. The pellet thus formed was washed with chilled 70% ethanol and again centrifuged at 7500 rpm for 5 min at 4°C.
16. The pellet was allowed to dry and suspended in 40 µl TE buffer.
17. After the DNA was dissolved, it was incubated at 65°C for 1 hour to inactivate DNAses and other nucleases.
18. Quality and quantity of DNA was checked using the spectrophotometer (NanoUve) at 260 and 280 nm wavelength.

### **3.5.6: PCR for the amplification of single stranded DNA of Phage**

The primers were synthesized commercially and were diluted to 100µM stock and again diluted to 10 µM as working concentration using nuclease free water. PCR reaction mixture was prepared by adding components into a sterile 0.2 ml tube in the sequential manner as mentioned in table 1 All the reaction was set up on ice. A negative template control was set up to check PCR contamination if any. Primers sequences for single stranded M13 amplification were adopted as below

Forward primer- 5' TTCGCAATTCCTTTAGTGGTA 3' (21 mer)

Reverse primer- 5' GCGGGGTTTTGCTCAGTAC 3' (19 mer)

Product size- 416bp

**Table 3. 1: PCR reagents**

Reagent	Volume (50 µl)
Forward primer (10 pm/µl)	1.0 µl
Reverse primer (10 pm/µl)	1.0 µl
PCR Master mix (2x)	25µl
PCR grade water	20.5 µl
DNA template	2.5 µl

The tubes with PCR reaction mixture were tapped to mix the ingredients, snap spinned and were placed on thermal cycler programmed for following cycling conditions:

**Table 3. 2: PCR cycling condition**

Steps	Parameters
Initial Denaturation and time	95°C, 10 min
Denaturation	95°C, 30 sec
Annealing temperature and time	50°C, 30 sec
Extension	72°C, 30 sec
Total no. of PCR Cycles	40
Final extension	72 °C, 10 min

### 3.5.7: DNA sequencing of amplified phage DNA and analysis:

PCR products were separated on a 1% agarose gel, stained with ethidium bromide, and visualized under ultraviolet (UV) light and sent for sequencing. The phage displayed peptide sequences were translated and aligned to find the homology and sequence variation by Clustal W using the Bioedit software.

### 3.6: Phage ELISA:

1. Target was dissolved in 0.1M NaHCO<sub>3</sub> buffer to make a solution of 10µg/ml concentration. Control was having same concentration of BSA in 0.1M NaHCO<sub>3</sub>.

100 µl of these solutions were added in respective wells. For each phage clone, target as well as control wells were taken in triplicates.

2. For coating the plate with target, it was kept at 4°C for overnight incubation in a humidified container.
3. Next day, the coating solution was removed from the plate by pouring it off and washing plate once with TBST (TBS+0.05% Tween-20). Now each well was filled with 250µl of blocking buffer (1% BSA in TBS). It was incubated for 1½ hour at 37°C.
4. Blocking solution was discarded as in step 4. Each well was washed thrice with TBST.
5. Dilution of each phage clone was made in TBST @ 10<sup>11</sup> phage/ml solution. 100µl of this was added in each well and plate was kept in incubator at 37°C for 1 hour.
6. Unbound phages were discarded by pouring off and slapping plate face down onto a clean paper towel, followed by washing of each well 6 times with TBST.
7. Mouse raised anti M13 phage antibody was diluted 1: 3000 times in diluting fluid (TBS having 0.5% BSA). This antibody solution was added in each well @ 100µl/well and incubated at 37°C for 1 hour. After one hour plate was washed 5 times with TBST.
8. Anti mouse antibody (2° antibody) was diluted 1: 3000 times in diluting fluid and 100µl of this was added in each well followed by incubation at 37°C for 1 hour. After one hour plate was washed 5 times with TBST.
9. In dark 50µl TMB was added in each well using multi-channel pipette and plate is kept for 15 minutes at room temperature, maintaining the dark condition.
10. 50 µl H<sub>2</sub>SO<sub>4</sub> (1M) was added in each well using multi-channel pipette.
11. O.D. was taken at 450nm.

### **3.7: Peptide synthesis:**

Solid phase peptide synthesis (SPPS) was introduced by Merrifield in 1963 (Merrifield, 1963) which simplified the synthesis of peptides. The principal of SPPS is the stepwise addition of amino acids on a solid support (Fig. 3.1). Peptide sequences were synthesized by Solid Phase Peptide Synthesis using standard 9-fluorenylmethoxycarbonyl chemistry devised by

### Solid Phase Peptide Synthesis Scheme

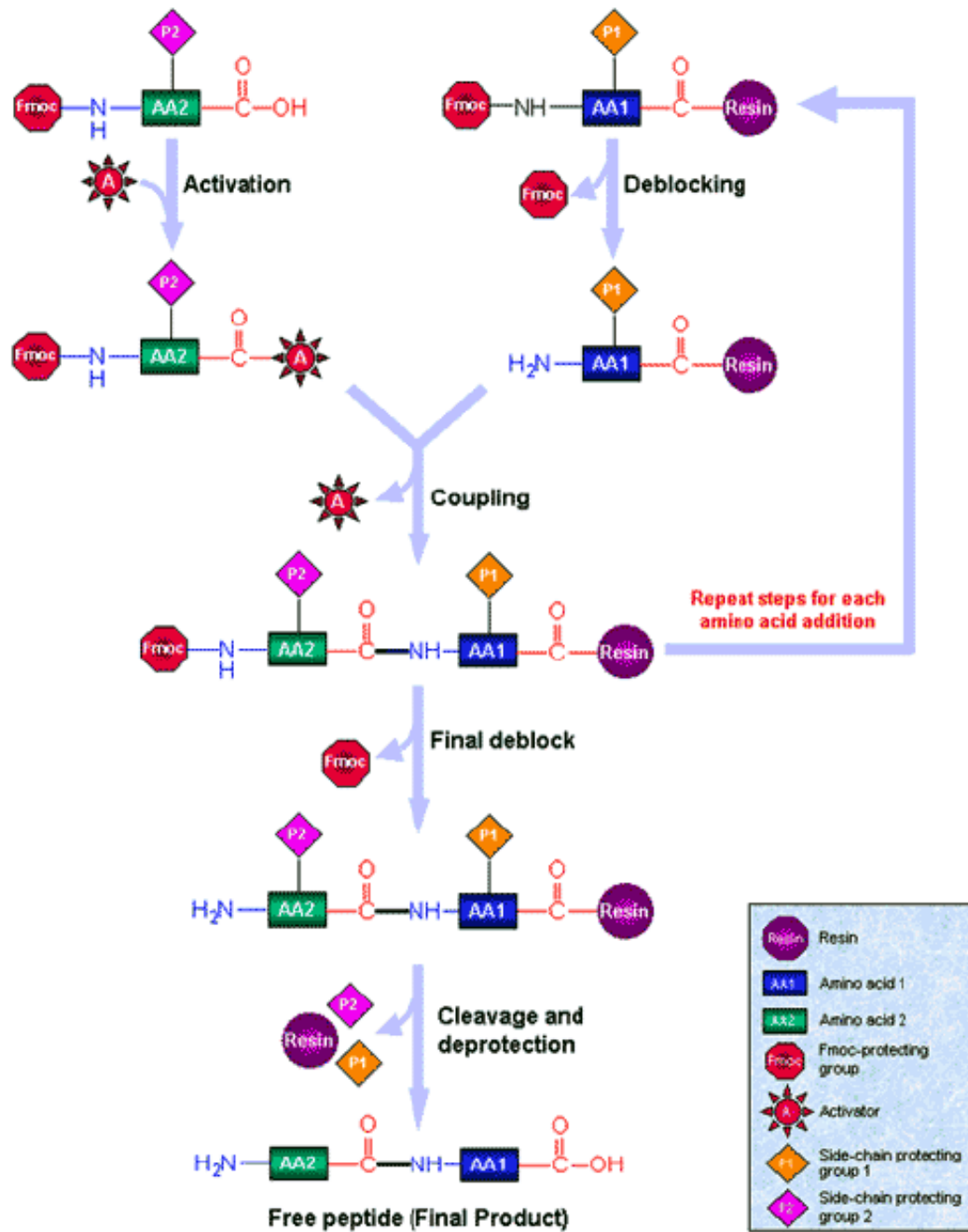


Fig. 3.1 : Solid phase peptide synthesis scheme

Merrifield. The successive addition of Fmoc amino acids was carried by using HOBT-HBTU on Rink amide resin (a modified Wang resin with 0.42 mmol/g loading efficiency of 100-200  $\mu\text{m}$  size of beads). For Peptide synthesis Fmoc-amino acids and Rink amide resin were procured from Novabiochem (Germany). Chemicals and reagents used were of analytical and molecular biology grade.

### **3.7.1: Solvents for peptide synthesis**

Analytical grade and dried Dimethylformamide (DMF), Dichloromethane (DCM), dried ethanol, methanol and diethyl ether were obtained from SD-fine chemicals (India). Dimethyl amino pyridine (DMAP), piperidine and Thioanisol were from Spectrochem (India). Trifluoroacetic acid (TFA) and N,N-diisopropoyl carbodiimide (DIPC) were used form Sigma(USA). Molecular biology grade reagents for preparation of buffer used in cell culture work such as  $\text{MgCl}_2$ , NaOH,  $\text{NaHCO}_3$ ,  $\text{Na}_2\text{CO}_3$ ,  $\text{Na}_3\text{HPO}_4$ ,  $\text{KH}_2\text{PO}_4$  were form Sigma (USA) and cell culture medium Dulbecco's Modified Eagles medium (DMEM) and Fetal bovine serum were from Gibco. Coupling reagents such as 1-hydroxy benzotriazole (HoBT) was form Orpegen pharma (Germany), 2-(1H-benzotriazolyl-1-yl)-1,1,3,3-tetramethyluronium hexafluoro phosphate (HBTU) was purchased from GL Biochem (Shanghai, China) and Nova Biochem (Switzerland).

The solid phase peptide synthesis used, involving following steps:

### **3.7.2: Loading of first Fmoc-amino acid to Rink-amide Resin**

The first Fmoc-amino acid suitably protected at the side chain was coupled to Rink amide resin using preformed. The protocol steps used were as follows:

1. To 1 g of Rink amide resin beads taken in modified Merrifield apparatus, added sufficient amount of DMF and allowed to swell for 2 hours.
2. Relative to loading efficiency of resin, first Fmoc-amino acid at C-terminal was dissolved separately in 5 ml of dry DMF and cooled at  $0^\circ\text{C}$  over ice bath.
3. For activation of amino acid 3 eq. HOBT and 2.9 eq. HBTU were added and kept at  $0^\circ\text{C}$  for 15 minutes. along with Fmoc amino acid dissolved in DMF

4. Then this solution was added to Rink amide resin in reaction vessel and stirred for 2 hr at room temperature (i.e, 25°C) at 160 rpm
5. After 2 hours Rink amide resin was washed 5 times with DMF and 5 times with DCM to remove excess amino acid.

**3.7.3: Estimation of loading efficiency of first amino acid:**

1. From the reaction vessel, 20mg of Rink amide resin was removed and washed 5 times with dry diethyl ether and dried under vacuum.
2. About 1 mg of dried Rink amide resin was taken and 3 ml of 20% piperidine solution was added to it with occasional swirling for 5 minutes. Resin was allowed to settle at the bottom. At least three repeat samples were taken.
3. The supernatant solutions were taken in silica UV cell of 10 mm path length.
4. The absorbance at 290 nm was measured by comparing with reference i.e 20 % piperidine.
5. The average value of Fmoc amino acid loading into resin obtained using standard reference table given below.

<b>Fmoc (μM)</b>	<b>0.1</b>	<b>0.2</b>	<b>0.3</b>	<b>0.4</b>	<b>0.5</b>	<b>0.6</b>	<b>0.7</b>	<b>0.8</b>	<b>0.9</b>	<b>1.0</b>
Absorbance	0.165	0.330	0.495	0.660	0.825	0.990	1.115	1.320	1.485	1.650

Fmoc loading efficiency was also calculated by formula:

$$\text{mmol/g} = \mu\text{mol Fmoc/mg of resin}$$

**3.7.4: End capping of un-reacted ends of resin**

End capping of un-reacted functional group on Rink amide resin was done to avoid formation of truncated peptide fragments. About 500 μl of End capping solution (DMF : acetic anhydride : DIEA (193 : 6 : 1) was added to above vessel and stirred at 25°C for 15 minute at 150 rpm. The beads were washed 3 times with DMF.

### **3.7.5: Deprotection of Fmoc from N-terminal**

For addition of subsequent amino acid deprotection of amino was done as below:

1. The Fmoc amino acid- Rink amide resin was treated twice with 20% piperidine in DMF (v/v) and agitated for 15 min each at room temperature.
2. The beads were washed 3 times each with DMF and one time with DCM and again 2 times with DMF
3. The Rink amide resin with first amino acid was ready for next amino acid coupling.

### **3.7.6: Successive coupling of next amino acids**

1. Rink-amide was taken in dry DMF.
2. Fmoc-amino acid (2nd amino acid) was taken 3 eq. amount and dissolved in dry DMF. For activation of amino acid 3 eq. HOBT and 2.9 eq. HBTU were added and kept at 0°C for 15 min.
3. Then this solution was added to Rink amide resin in reaction vessel and stirred for 2 hr at room temperature (i.e, 25°C) at 160 rpm.
4. Unreacted amino acids and other reagents were washed off 2 times with DMF. Coupling was checked using Kaiser test. In case of negative reaction coupling procedure was repeated without removing Fmoc group from the added amino acid on rink amide resin.
5. After successful coupling and deprotection next amino acid was added by repeating all the steps of deprotection, coupling and end capping to get peptide of desired length.
6. Finally, excessive reagent was removed and resin was washed thoroughly with DMF and then dried by washing with dry methanol and stored in dried form in desiccators until further use.

**Kaiser Test.** The “Kaiser Test” is a colorimetric test for the presence of amino groups; we use it to make sure that each coupling step in peptide synthesis goes to completion. It is based on the reaction of ninhydrin with amino groups to form a blue adduct. Therefore, an incomplete coupling cycle will lead to a positive Kaiser test, demonstrated by the development of a blue colour, while coupling to completion will yield a negative (yellow) test.

### **3.7.7: Labeling bead bound peptide with biotin**

1. Peptide was treated with 20% piperidine in DMF to remove Fmoc group from N terminal end.
2. Bead bound peptide was washed with DMF three times and kept in dry till labeling.
3. The beads were allowed to swell resin in DMF for 1 hr in eppendroff tube.
4. D-Biotin solution was prepared by adding DIPIC (3 equivalent) and DMAP (0.1 equivalent) in DMF and 6 equivalent concentration of biotin.
5. Swelled beads were centrifuged to remove DMF and resuspended in biotin solution prepared in step 4. The mixture was kept in shaker incubator at 110 rpm for overnight at 25°C.
6. Completion of biotin labeling was checked by using ninhydrin test (incomplete coupling of biotin gives a blue color).
7. Resin was washed twice each with DMF, isopropanol and DCM, followed by cleavage

### **3.7.8: Final deprotection and cleavage of peptide from resin**

1. Dried resin bound peptide was taken into an Eppendorf tube. Cleavage solution containing TFA: Water: Thioanisol: phenol: EDT (92:2:2:2:2) was added @ 200µl/ tube to submerge the peptide bound resin and kept on vortex for 4 hours.
2. After 4 hours, the tubes were centrifuged at 10,000 rpm at room temperature for 5 minutes and TFA extract containing cleaved peptide was collected and peptides were precipitated by pouring in dry and chilled diethyl ether in separate tubes and washed five times with diethyl ether, vacuum dried and the white powder thus obtained was stored under dry condition in desiccator until further use.

### **3.8: MAP Synthesis:**

4 armed MAP formats were synthesised of few selected peptides, whose phage clones (No. 4, 8, 9 & 12) were giving better results in phage ELISA. For this, chosen peptide sequences were synthesised in MAP format with cysteine at the C-terminal and lysine mosaic (Figure 3.2). The protocol used is given below:

### **3.8.1: Coupling of Fmoc-Cysteine to the Wang resin**

1. 1 gm of Wang resin (loading efficiency of 0.6 to 1.0 mmole/gm of resin) was placed in a clean, dry fritted column with sufficient amount of DMF to swell the resin.
2. 2.397 gm of Fmoc-cysteine (6 equivalent to the loading efficiency of the resin) was dissolved in the DMF in the separate flask at 0°C (in ice).
3. A solution of DIPC (0.38 gm, 3 equivalents to the loading efficiency of resin) was added to Fmoc-cys solution and mixture was stirred for 20 min at 0°C.
4. Symmetrical anhydride so prepared was added as such to the already swollen resin kept in a flask.
5. DMAP (12.2 mg, 0.1 equivalents to the loading efficiency of resin) was added to above solution. Shaking was continued for 5 hours at room temperature.
6. Resin was washed five times with DMF to remove unreacted components.
7. After coupling of Fmoc-cysteine to resin end capping of unreacted functional group on Wang resin was done to avoid truncated peptide fragments in further synthesis.

Acetylation mixture was made (193 DMF: 6 acetic anhydride: 1 DIEA) and mixed with dried resin and kept in shaker at 37°C for 1 hour. After that beads were washed five times with DMF and deprotection was done to remove N-terminal protection from Fmoc-Cys-Wang resin as given next.

### **3.8.2: Removal of N-terminal protection from amino acid coupled to resin**

1. 20% piperidine in DMF was added to the resin and allowed to stand for 20 minutes at room temperature with occasional shaking.
2. Piperidine solution was drained off and resin was washed five times with DMF.

### **3.8.3: Coupling of di-Fmoc-Lys-OH**

1. Cysteine bound resin was taken in modified Merrifield flask and 1.4767 gm of di-Fmoc-lys-OH (2.5 mmol) along with 0.324 gm HOBt (2.5 mmol) was dissolved

separately in minimum amount of DMF at 0°C. HBTU, 0.9932 gm (2.4 mmol) was added to activate the di-Fmoc-lys-OH.

2. This activated di-Fmoc-lys-OH was added to the resin and left for coupling for 2 hours at 37°C in shaker.
3. Excess reactants were removed by filtration and resin was washed several times with DMF.

Coupling efficiency was determined as previously described and found to be 90%. At this stage HBTU was added for the end capping of left over unreacted amino groups on cys-Wang, if any.

In the next coupling, di-Fmoc-lys-OH was added again to give four arms to the MAP core. The coupling was done in following ways.

1. The di-Fmoc-lys-OH (1.4767 gm, 2.5 mmol) and HOBt (0.324 gm, 2.5 mmol) were dissolved in DMF at 0°C and activated using 0.9932 gm HBTU (2.4 mmol) for 10 minutes.
2. Activated mixture was added to lys-cys-Wang resin and coupling was allowed for 2 hours at 37°C with continuous shaking. Now the coupling efficiency was determined again.
3. This provided a MAP core having four arms.

#### **3.8.4: Sequential synthesis of full length peptide on MAP core**

After determining the coupling efficiency, peptides were synthesised by sequential addition of Fmoc amino acids on the MAP core, as per the sequence in the same manner described previously. MAP core on 100 mg resin beads was utilised to synthesize each MAP peptide. Once the desired length of peptide was achieved, N-terminal end was deprotected and acetylated before cleavage from the resin.

#### **3.8.5: N-terminal acetylation of resin bound MAP peptides**

1. After addition of last amino acid as per the sequence, deprotection was done using 20% piperidine. To the resin bound peptide a mixture of DMF : acetic anhydride : diisopropyl ethylamine (193:6:1) was added.

2. The mixture is kept at room temperature with constant shaking for 2 hours.
3. Excessive reagent was removed and beads were washed thoroughly with DMF and finally dried by washing with dry methanol.

### 3.8.6: Side chain deprotection and cleavage of MAP peptide from resin

The acetylated MAP peptides were deprotected and cleaved by preparing a cleavage mixture comprising TFA: thioanisole: water: phenol: EDT (92:2:2:2:2, v/v). Cleavage mixture was added (@ 200  $\mu$ l per tube) to the resin bound peptide and left at room temperature for 5 hours with continuous shaking at moderate speed.

The tubes were centrifuged at 10,000 rpm for 5 minutes and TFA extract was transferred to different tubes after labelling them. TFA solution was poured in chilled dry ether and peptides were precipitated. The precipitated MAP peptides were washed several times with dry and chilled ether, vacuum dried as white powder and stored under dry condition for further use.

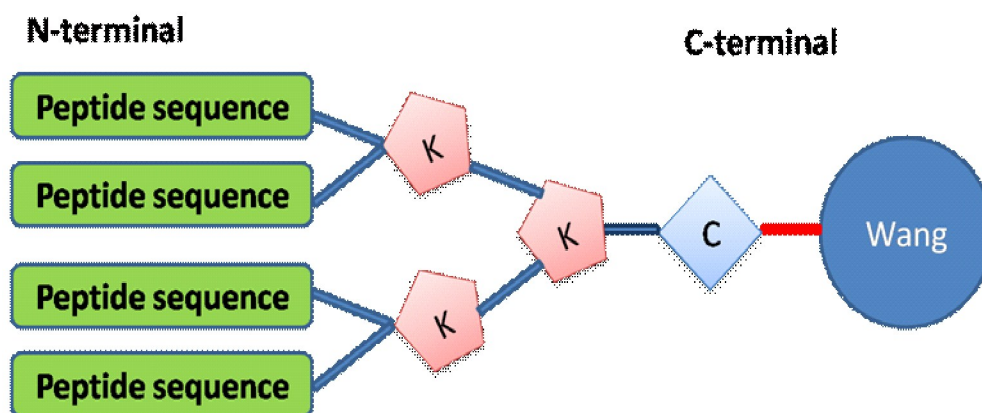


Figure 3.2: Schematic diagram of MAP core

### 3.9. Analysis of peptide purity using Reverse Phase HPLC (RP-HPLC)

1. Peptides were purified on semi-preparative RP-HPLC (Ultropac column, TSK ODS, 120T, 10  $\mu$ m, 7.8X300mm) with the following elution gradient of water (A) and acetonitrile (B) having 0.1% TFA (v/v)
2. After semi-preparative RP-HPLC peptides were analysed for their purity on analytical RP C-18 column (4X150 mm; 5  $\mu$ m particle size) in an isocratic manner at 80% solution B conc.

3. The flow rate was kept 1.0 ml/min for preparative purifications and 0.5 ml/min for analytical HPLC (isocratic). Chromatograms were monitored in UV at wavelength of 220 & 280 nm using PDA as detector.
4. Eluted peptide from semi-preparative HPLC was collected and concentrated in speed vacuum concentrator. These peptides were studied in CD spectroscopy, ELISA and other experiments.

**Table 3.3 Solvent gradient in semi-preparative RP-HPLC**

Time (mins)	Solvent A (%)	Solvent B (%)
0.01	99	1
10	50	50
20	20	80
25	5	95
30	0	100
34	20	80
37	70	30
39	99	1
40		STOP

### 3.10: Circular Dichroism (CD) spectroscopy

CD spectra of peptide solutions (0.1 mg/mL concentration) were recorded in wavelength range of 190-250 nm using CD spectropolarimeter (J-810 Model, JASCO, Japan) with rectangular quartz cell of 0.1 cm path-length. The CD machine was calibrated using d-10 campho sulphonic acid (60mg/100ml water). The CD spectra were expressed in molar ellipticity,  $[\Theta]$ , in  $\text{degcm}^2\text{dmol}^{-1}$  calculated using the equation  $[\Theta] = 100\psi/c.l$ , where  $\psi$  is observed ellipticity (millidegree),  $c$  is the peptide concentration (mole/liter) and  $l$  is the pathlength (cm). Data analysis and acquisition were performed using inbuilt spectra manager software. An

average of four scans was recorded with scanning speed of 100 nm/minute and response time was 1 second. The CD spectra were recorded in water and TFE to ascertain the conformation acquired by the peptide in polar and non-polar environment.

### **3.11: Virus Capture ELISA**

1. MAP or linear peptide were dissolved in coating buffer (i.e, 0.1M NaHCO<sub>3</sub>, pH 8.5) and added in the wells of ELISA plate @ 1 µg/well. For coating overnight incubation was done at 4°C. In control well BSA was coated.
2. Next day, the coating solution was removed from the plate by pouring it off and washing plate once with PBST (PBS+0.05% Tween-20). Now each well was filled with 250 µl of blocking buffer (1% BSA in PBS). blocking was done by keeping the plate in incubator for 2 hours.
3. Blocking solution was discarded as in step 2. Each well was washed thrice with PBST.
4. PPRV was diluted in PBS to make conc. of 1 µg/100 µl. 100 µl of this solution was added in each well in order to make amount of virus 1 µg in each well. 1 hour incubation was done at 37°C. Washing was done 6 times with PBST.
5. Polyclonal sera against PPRV was diluted 1:200 in diluent (PBS + 0.5% BSA) and 100 µl/well was added. Plate was kept in incubator for 1 hour.
6. Wells were probed with 1:2000 dilutions of secondary antibody chicken anti-goat IgG-HRPO conjugate for for 1 hr at 37°C and then washed five times with PBS.
7. The TMB substrate (Amresco) was used (50 µl per well) and 10 mins incubation was done at room temperature to develop the color.
8. The reaction was stopped by adding 1M H<sub>2</sub>SO<sub>4</sub> (50 µl per well).
9. The absorbance readings were taken at 450nm. The average values for the triplicates were used for plotting the result.

#### **3.12.1: Gold Nanoparticle synthesis using citrate reduction method:**

1. Before going for synthesis of gold nanoparticles, all the glasswares were treated with aquaregia.

2. Citrate stabilized Gold Nanoparticles were synthesized using standard protocol with minor modifications. 1mM hydrogen tetrachloroaurate (HAuCl<sub>4</sub>) was dissolved in 50 ml of double distilled water and the solution was brought to boiling on hot plate with vigorous stirring using magnetic stirrer.
3. While boiling, about 50 mL of 38.8 mM of trisodium citrate was added rapidly to the stirring solution and further heated with constant stirring for 10 min.
4. The solution was allowed to cool but continued to stir for an additional 15 minutes till brick red colour appears in the solution.
5. Finally, the solution was allowed to cool down to room temperature and filtered through 0.8 µm membrane filter. Storage was done at 4°C.

### **3.12.2: Conjugation of Peptide on Gold nanoparticles:**

1. AuNP suspension was treated with 0.1% Tween-20 for 1 hour with continuous stirring.
2. For surface modification, different concentrations (1-10µM) of peptides were added to 1ml aliquots of pre-treated AuNP suspension.
3. The solution was stirred for overnight, washed and resuspended in distilled water.

### **3.12.3: Colorimetric assay AuNP-Cys-Peptide conjugate:**

PPRV stock virus suspension was added to each 100µl of AuNP-peptide conjugate. To check the selectivity of the test, controls were included; plain DMEM and PBS alone. The visible color change was observed. Further, the solutions were subjected to UV-Visible spectrometer and the absorption spectra were recorded for the range of 400nm to 700nm.

### **3.13.1: RNA isolation of PPRV:**

1. Virus was captured by coated MAPs in the ELISA plate.
2. 100 µl/well Trizol was added and kept for 5-10 minutes. This solution is then pipette out and collected in nuclease free sterile microfuge tube.
3. 20% (i.e, 200µl in 1ml) chloroform is added into the tube and mixed properly. These tubes were then centrifuged at 13000 rpm for 15 minutes at 4°C.

4. Aqueous phase was collected in which equal amount of isopropanol was added. Incubation was done at room temperature for 10 minutes.
5. Again centrifugation was done at 13000rpm for 15 minutes.
6. Supernatant was decanted and pellet was washed by 70% ethanol.
7. The pellet was the air dried and resuspended in DEPC treated NFW.
8. The purity of RNA was measured by Nanodrop by O.D. at 260/280.

### **3.13.2: Viral cDNA synthesis.**

From viral RNA, cDNA was synthesized using Revert Aid first strand cDNA Synthesis Kit (Thermo Scientific). Equal quantity (500ng) of the RNA for each of the control and treated groups were taken using spectrophotometer (NanoDrop, Thermo Scientific) readings followed by appropriated dilution of the samples. cDNA was synthesized in two steps as mentioned below following manufacturers instructions.

#### **First step:**

Viral RNA = 500ng + Random primer = 20pmol + Nuclease free water = up to 12µl

Mixed gently, and incubated at 65°C for 5 min, spin down and placed the vial back on ice.

#### **Second step:**

5X Reaction Buffer 4 µL + RiboLock RNase Inhibitor (20U/µL) 1 µL + 10 mM dNTP Mix 2 µL + RevertAid M-MuLV RT (200 U/µL) 1 µL = Total volume 20 µL

Mixed gently and incubate 5 min at 25°C followed for 60 min at 42°C.

Reaction was terminated by heating at 70°C for 5 min. Resulting cDNA was stored in -20°C for further use.

cDNA synthesized was checked by performing a test PCR for the amplification of viral gene.

*✍ ✍ ✍*



# *Results*



In search of the proof that phage display technology can be used to retrieve peptide sequences which would have tendency to bind with the pathogen target, the present dissertation work entitled '**Identification and characterisation of peptides binding to *Peste des petits ruminants (PPR) virus using phage display***' was undertaken in which we took PPR virus as model. This section describes the findings revealed while undertaking each objective.

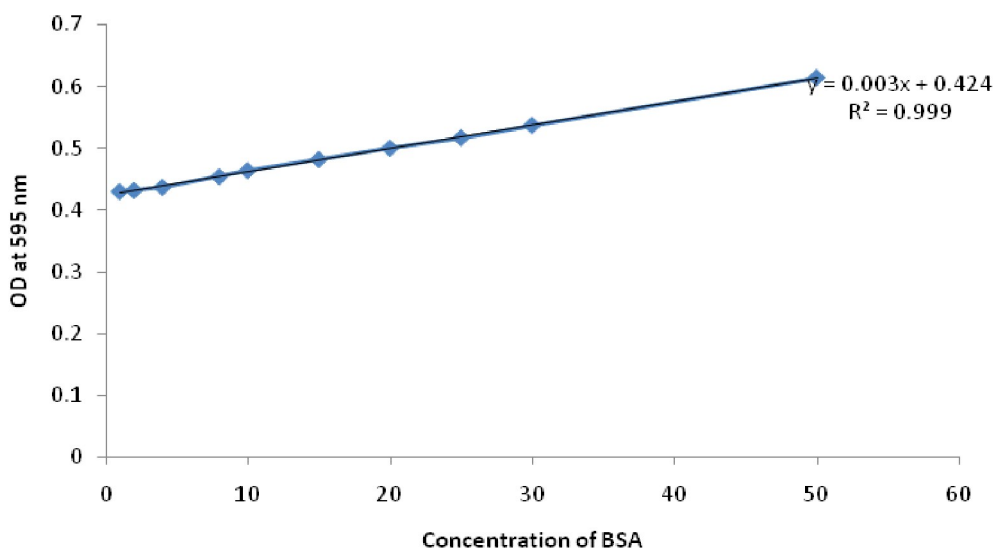
**Objective 1: To identify the peptide binding to PPR virus using phage display technology.**

#### **4.1 Propagation and purification of viral antigen**

In order to perform Phage display by direct surface panning method, PPR virus was propagated to sufficient quantity. It was done by infecting the Vero cells with PPRV. Visible CPE was observed after fifth day post infection characterized by cell rounding and aggregation of cells. By sixth day post infection, CPE was generalized with formation of syncytia which concurred with earlier reports of Lefevre and Diallo (1990). The propagated virus was then ultra centrifuged. The PPRV pellet was resuspended in PBS and concentration of virus in suspension was measured by Bradford assay.

**Table 4.1: Bradford assay**

S. No.	Std. (BSA in $\mu\text{g}$ )	Amount of Std. (in $\mu\text{l}$ )	PBS ( $\mu\text{l}$ )	Volume of Bradford reagent ( $\mu\text{l}$ )	O.D. at 595 nm
1	1	1	59	900	0.43
2	2	2	58	900	0.432
3	4	4	54	900	0.437
4	8	8	52	900	0.454
5	10	10	50	900	0.464
6	15	15	45	900	0.482
7	20	20	40	900	0.5
8	25	25	35	900	0.517
9	30	30	30	900	0.537
10	50	50	10	900	0.614

**Fig. 4.2: Standard curve plotted in Bradford Assay**

#### 4.2: *in vitro* panning to identify virus specific peptides

To identify the PPRV specific peptides, PhD library having random projection of 12-mer was used. Phage display was done according to the manufacturer's instructions (New England Biolabs) with minor modifications. Screening phage displayed peptide libraries against

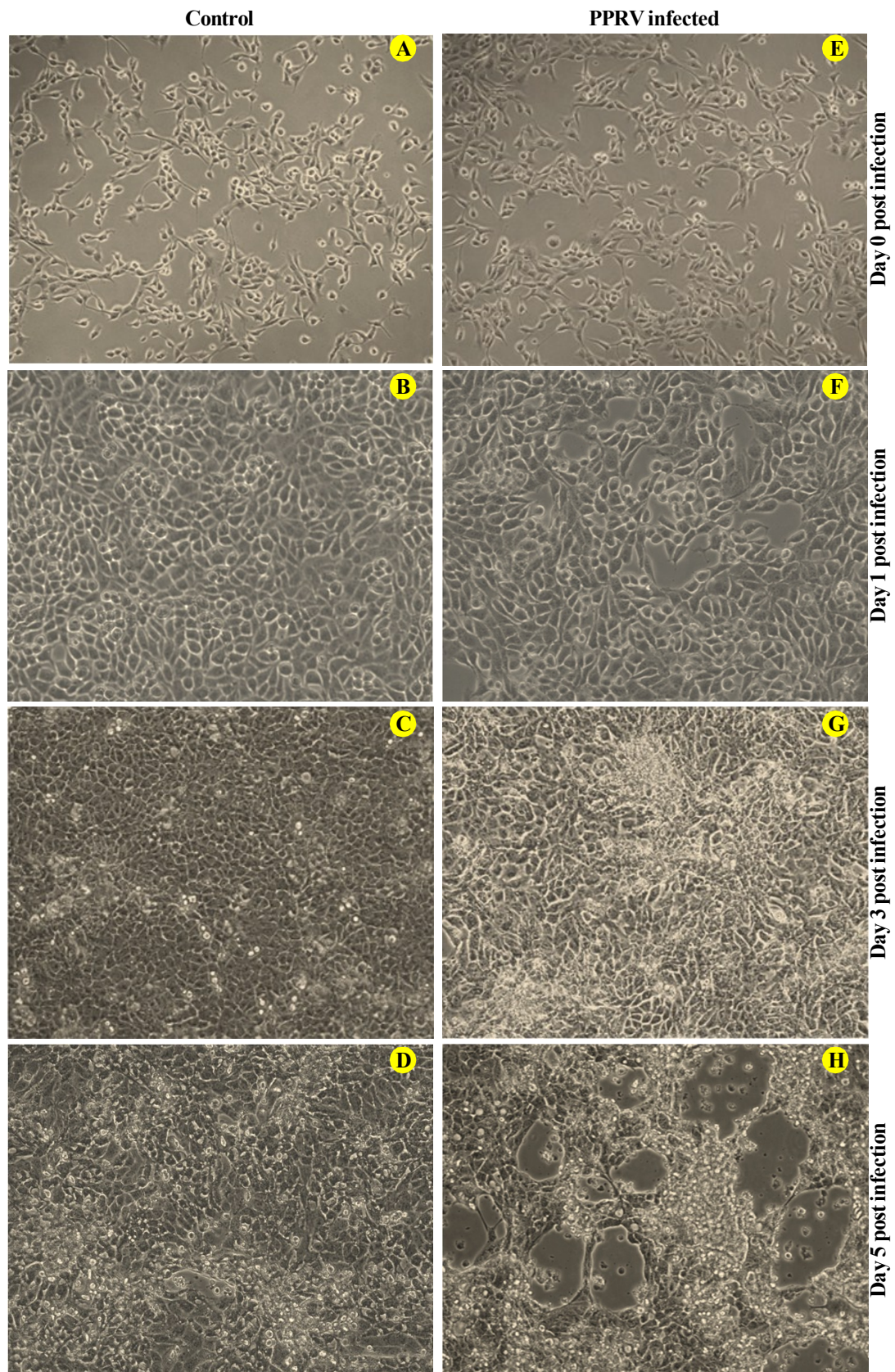


**Fig. 4.1 :** Propagation of PPRV in Vero cells. Cytopathic effects were observed after 5 day post infection.

specific target antigen is a direct and fast method of identifying novel peptide sequences with target specificity.

#### **4.2.1 Phage titration**

Before performing biopanning, the titer of phage stock should be known. For titration of phage, the manufacturer's protocol was followed with modification described in detail in material and method section. The host ER 2738 supplied with the kit was revived in LB-Tet plate and culture was maintained in LB- broth containing tetracycline as this bacterium is tetracycline resistant. There are many critical factors which need attention while performing titration of the phage like keeping the temperature of top agar to the optimum. Agar exhibits hysteresis which is a state transition when melting and freezing temperature do not agree. In other words, typically agar melts at 85°C and solidifies from 32 to 40°C. But once agar is melted while autoclaving from the temperatures of 40 to 85°C, agar can be either liquid or solid, depending on which state it was before (Mielke and Roubicek, 2003). This gives us a tough time to find out the optimum temperature for top agar to get optimum fluidity. As higher temperature will kill the host i.e, ER 2738 and at lower temperature the top agar will solidify in which phage would be unable to migrate and attack new host. In both conditions we won't get any blue plaque. In addition the mutant phage displaying the 12-mer amino acid on the coat protein is less infective than its wild counterpart. Hence there is possibility of environmental wild phage contamination which will give white colony unlike the blue plaques of mutant phage.

The phage stock was 10 fold serially diluted to make dilutions i.e, 10<sup>1</sup>, 10<sup>2</sup>, 10<sup>3</sup>, 10<sup>4</sup>, 10<sup>5</sup>, 10<sup>6</sup>, 10<sup>7</sup>, 10<sup>8</sup>, 10<sup>9</sup>, 10<sup>10</sup>, 10<sup>11</sup> and 10<sup>12</sup>. These dilutions were then titrated on LB/XGal/IPTG plates. In the dilution 10<sup>11</sup> we got 2 plaques.

Hence titer of the phage supplied with the phage library kit was:

$$\text{No. of pfu/ml} = \text{No. of plaques} \times \text{Dilution factor} \times 100$$

$$\text{i.e, } 2 \times 10^{11} \times 100 = 2 \times 10^{13}$$

#### 4.2.2: *in-vitro* (surface) panning:

The target (PPRV) was coated in wells of microtiter plate and a population of approximately  $1 \times 10^{11}$  phage were added in each well. After 30-45 minutes incubation at room temperature, non binding phage clones were discarded and bound phage were collected using Glycine-HCl (pH 2.2) and neutralised by Tris-HCl.

Three rounds of direct panning were conducted taking PPRV as target. After each round of panning population of the phage binding to PPRV was rescued by ER-2738, amplified, purified and titrated according to the manufacturer's protocols (NEB) with lab modification. Phage titer before panning, after panning and after phage amplification is given in Table 4.2. Here we report that there was decrease in the eluted phage titer in 2<sup>nd</sup> round of panning as compared to 1<sup>st</sup> round of panning. It may be due to increased concentration of tween-20 in the washing buffer. In subsequent panning we reported relatively increased titer of the phage in the eluate.

#### 4.3: Phage ELISA

PPRV was coated (1 µg/well) in maxi-sorb ELISA plate. BSA was taken as negative control and BTV was taken as virus control. All the samples were taken in triplicate. Next day, blocking was done with 1% BSA. Binding of all the 12 phage clones was compared by ELISA. O.D. was taken at 450nm. Here we reported that phage 4, 8, 9 & 12 show selective affinity towards PPRV, whereas other phage clones i.e, 1, 2, 3, 5, 6, 7, 10 and 11 were non-specific in nature as they were showing high O.D. at 450nm in negative as well as BTV coated wells. Among the 4 phage clones giving desirable results, phage number 8 was showing highest affinity to PPRV followed by 9, 4 and 12 respectively in order of their reactivity. The graph showing affinity of the phage clones was depicted by 2 ways, which are as follows:

1. The O.D. at 450 nm of all the wells is shown in figure 4.6. Here O.D. value of BTV coating group and negative control has also been shown in order to show the nature of specificity of the phage clones.
2. The ratio of O.D. values of PPRV and BTV with respect to that of BSA (negative control group) has been shown as P/N ratio in figure 4.7. Phage clones having P/N ratio of more than four were taken further for phage-ELISA.

**Table 4.2a: PPRv binding phage titer before and after panning and after phage amplification**

Rounds of Biopanning	Input titer (pfu/ml)	Collected (eluted/non binding) Phage titer in (pfu/ml)	Phage titer after amplification (pfu/ml)
1 <sup>st</sup> round	$2 \times 10^{13}$	$1.1 \times 10^5$ (eluted)	$1 \times 10^{12}$
2 <sup>nd</sup> round	$1 \times 10^{12}$	$5 \times 10^4$ (eluted)	$2 \times 10^{12}$
3 <sup>rd</sup> round	$2 \times 10^{12}$	$3 \times 10^5$ (eluted)	Not amplified
4 <sup>th</sup> round	$3 \times 10^5$		
(Negative panning)	(unamplified phage from 3 <sup>rd</sup> round)	$1.1 \times 10^3$ (Non binding)	$1.7 \times 10^{11}$
5 <sup>th</sup> round	$1.7 \times 10^{11}$	$2.3 \times 10^5$ (eluted)	-

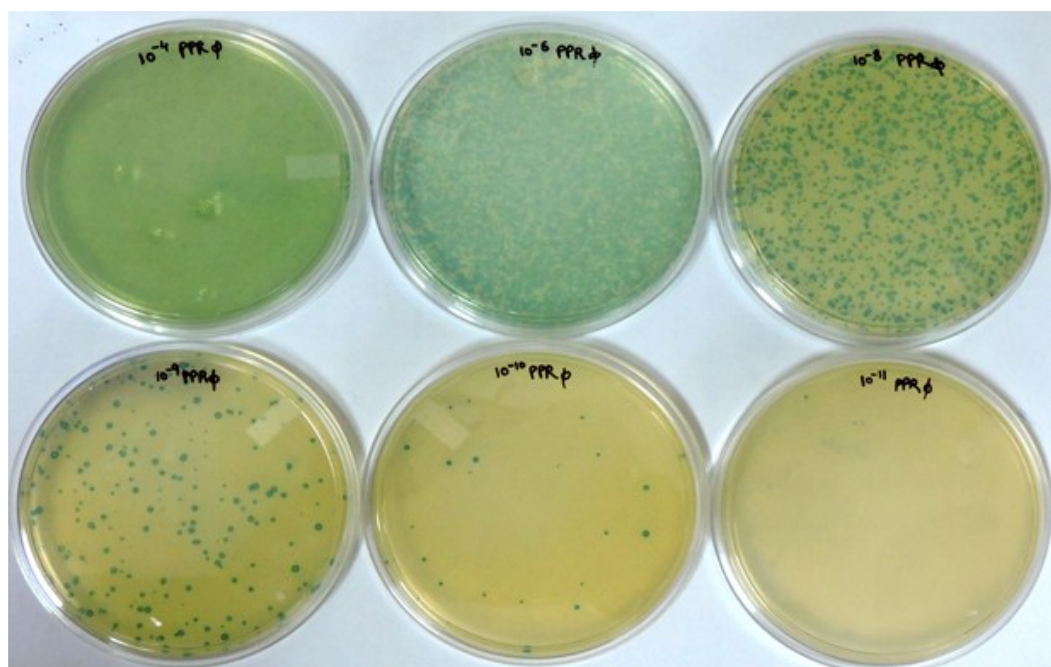


**Fig. 4.3 :** LB/Tet/Xgal/IPTG plates showing blue colonies (plaques) of phage grown on  $\alpha$ -Complementing host ER2738.

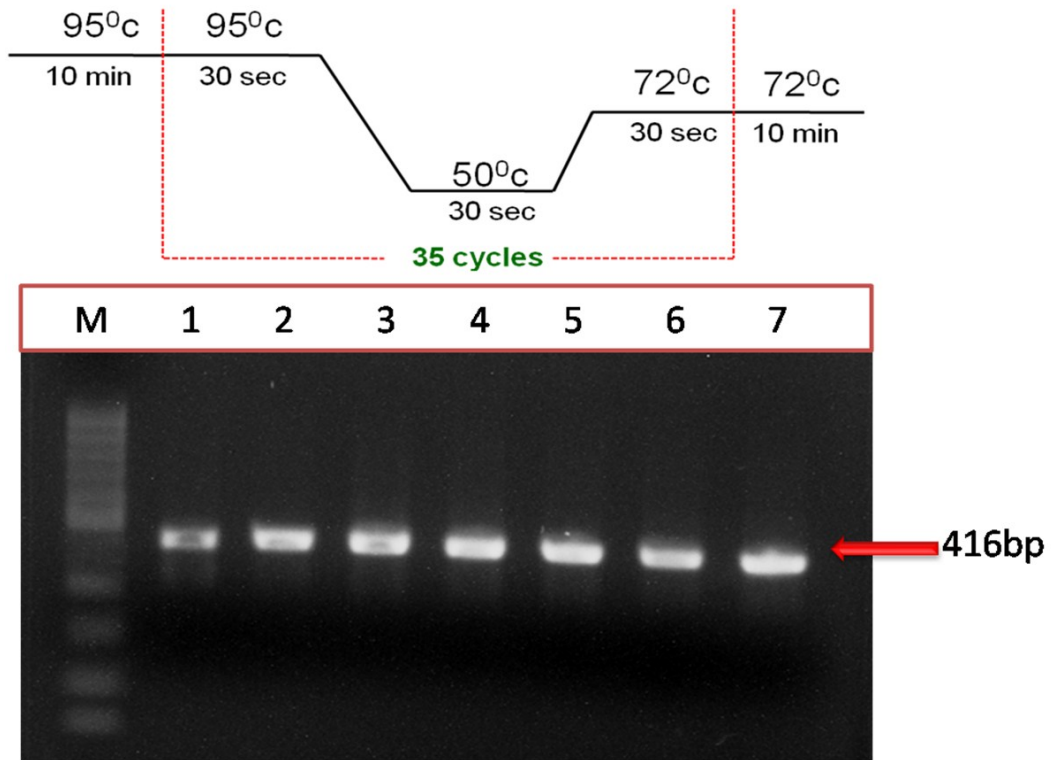
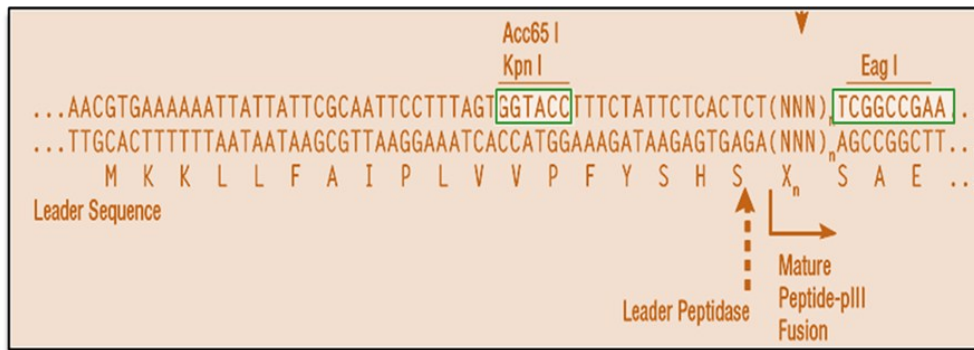


**Fig. 4.4 :** Agarose gel electrophoresis of amplified ss-DNA of phage showing 416 bp PCR product. lane M: 100bp DNA ladder, lane 1-7 shows representative amplicon from 40 plaques



### Schematics: peptide cloning site

```

ACCCTCGTCCGATGCTGTCTTTCGCTGCTGAGGGTGACGATCCCGCAAAGCGGCCTTAACTCC
CTGCAAGCCTCAGCGACCGAATATATCGGTTATGCGTGGGCGATGGTTGTTGTCATTGTCGGCGCA
ACTATCGGTATCAAGCTGTTAAGAAATCACCTCGAAAGCAAGCTGATAAACCGATAACAATTAAG
GCTCCTTTTGGAGCCTTTTTTTGGAGATTTCAACGTGAAAAAATTATTATTCGCAATTCCTTTAGT
GGTACCITTCTATTCTCACTCTGATTACCTCAGAAGTTAATAATAATTTATGTCGGTGGAGGT
TCGGCCGAAACTGTTGAAAGTTGTTTAGCAAATCCCATACAGAAAATTCATTACTAACGTCTGAA
AGACCGCCCCATTG

```

**Fig. 4.5 :** Schematics of sequence map of peptide displayed on minor coat protein of M13 phage a; text highlighted in blue- restriction site for ACC65I and KpnI; text in green blue is 36 bp random oligonucleotides sequence insert; text in red- tri Gly linker, text highlighted in green leader peptidase site codes for Ser-Ala- Glu.

**Table 4.3: PPRV binding phage-DNA and translated Peptide sequences after 5th round of panning**

Nucleotide Sequence retrieved	Sequence translated (Peptide sequence)	Frequency	Nomenclature given
5'TGTATTTGGTGTGTGGGGGAGCCTTGGGGAGCCTTTT3'	<b>CIWCVGELAEPF</b>	8	P1
5'GTGCAITGGGAITTTCCGGCAGTGGTGGCAGCCCTTCT3'	<b>VHWDFRQWWQPS</b>	10	P2
5'GCTTATGATCCATATTCAGTATTGGATTGAGCGGT3'	<b>AYDPHIQYWIER</b>	6	P3
5'CAGAAATAGTCCGAICTTTCAGTATTGGTTGGCCGGG3'	<b>QNSPILQYWLAR</b>	2	P4
5'GATTTGGAGTTCGTGGGTGTATAGGGATCCCGCAGACT3'	<b>DWSSWVYRDPQT</b>	1	P5
5'GATCATTCGGTGTTTCATGCTTGGCATAACGTAITTTT3'	<b>DHSVFHAWHTYF</b>	5	P6
5'TGGCAITGGGGGGCCCTGTGATTTATAGTTGGCCT3'	<b>WHWRAPVIYSWP</b>	2	P7
5'TCTGATCCTGTTCCTTTGCTCTTATTGGCTGGCTCGT3'	<b>SDPVALSYWLAR</b>	1	P8
5'GAGCCCTTGGGTGCATTTGAATTAITGGGTTAGTAGG3'	<b>EPWVHLNYWVSR</b>	1	P9
5'TGGAATAATCTGTTTTGGATTAITGGCTGCAGAGG3'	<b>WNNSVLDYWLQR</b>	1	P10
5'TGGCAITGGTGGGGCGGTTGATTCATAGTTTTCTG3'	<b>WHWWGRLIHSFL</b>	1	P11
5'GTATTTGGTGTGGGGGAGCCCTTGGGGAGCCTTTTT3'	<b>VFGVWGSLEAEPF</b>	1	P12

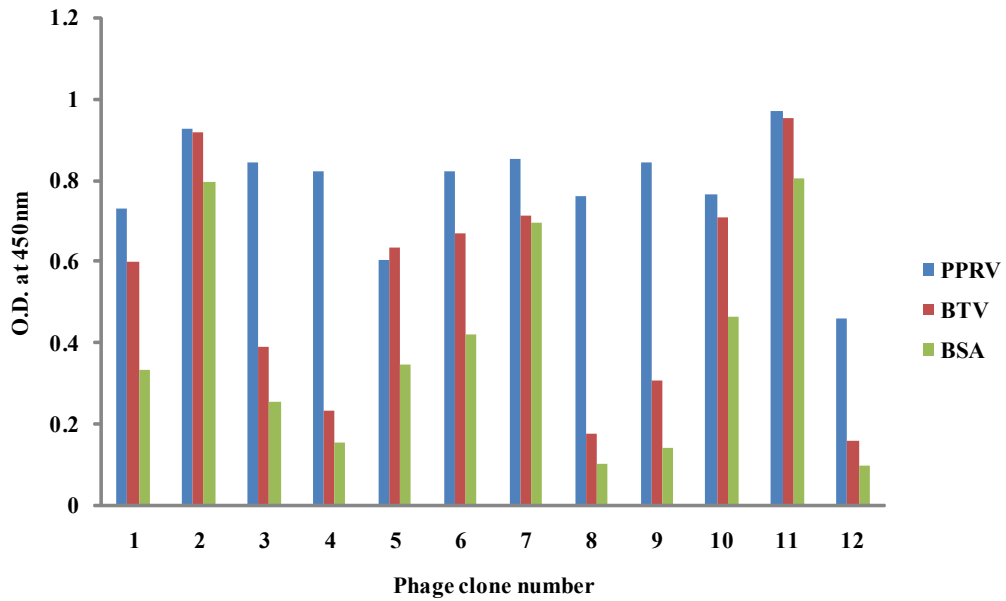


**Fig. 4.6 :** Histogram representing affinity of all the 12 phage clones through Phage ELISA. Phage clone number 4, 8, 9 and 12 are having specific binding with PPRV.

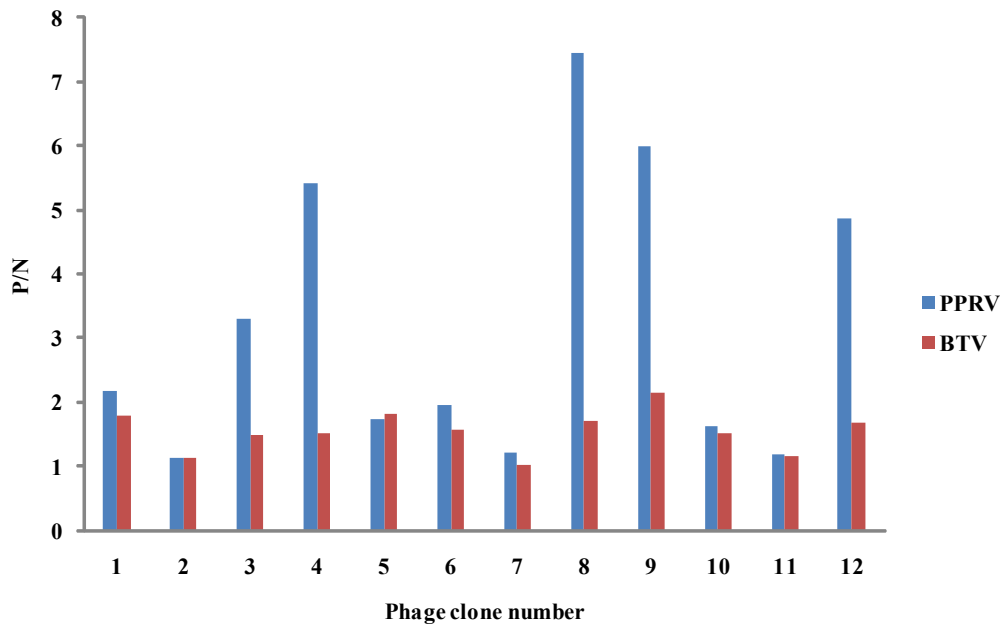


**Fig. 4.7 :** Histogram representing ratio of optical densities at 450nm of all the 12 phage clones. Phage clone number 4, 8, 9 and 12 are having a P/N ratio for PPRV more than four times.

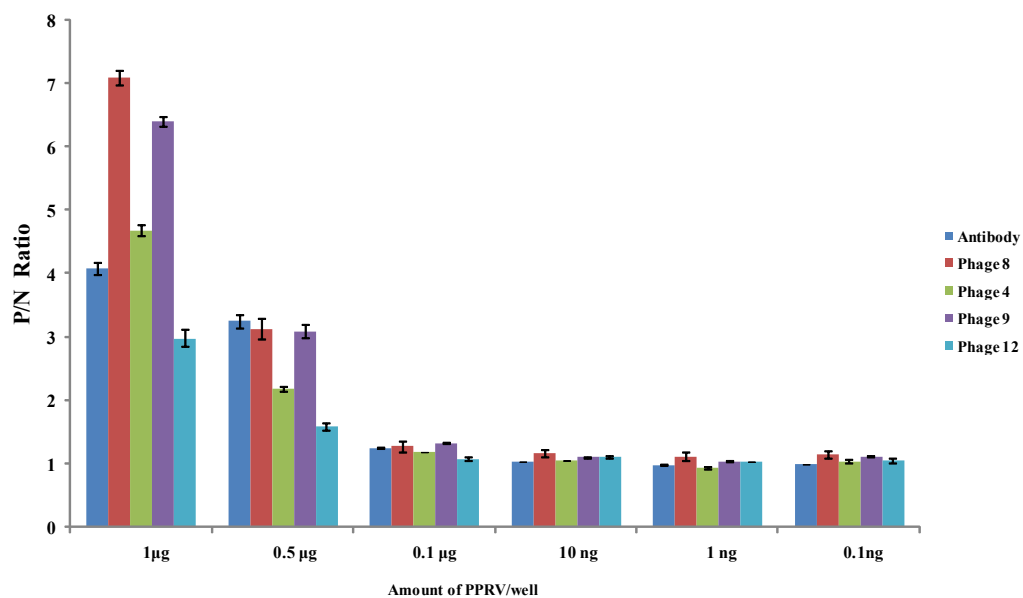


**Fig. 4.8 :** Histogram representing comparison of P/N ratio of Optical densities of antibody with that of phage No. 4, 8, 9 & 12 at 450nm.

**Table 4.4: List of the peptides synthesized and their attributes**

Peptide Sequence	Charge	Attribute	Mol. Wt	pI
P1 Biotin-Ahx-CIWCVGELAEPF	-2	acidic	1706.07	3.61
P2 Biotin-Ahx-VHWDFRQWWQPS	1	basic	2011.3	6.75
P3 Biotin-Ahx-AYDPHIQYWIER	0	neutral	1930.22	5.40
P4 Biotin-Ahx-QNSPILQYWLAR	1	basic	1828.18	8.56
P5 Biotin-Ahx-DWSSWVYRDPQT-GGG	-1	acidic	2050.25	4.11
P6 Biotin-Ahx-DHSVFHAWHTYF-GGG	2	basic	2057.3	6.62
P7 Biotin-Ahx-WHWRAPVIYSWP-GGG	2	basic	2108.48	8.59
P8 Biotin-Ahx-SDPVALSYWLAR-GGG	0	neutral	1888.19	5.55
P9 Biotin-Ahx-EPWVHLNYWVSR-GGG	1	basic	2096.43	6.75
P10 Biotin-Ahx-WNNSVLDYWLQR-GGG	0	neutral	2104.41	5.55
P11 Biotin-Ahx-WHWWGRLIHSFL-GGG	3	basic	2148.57	10.03
P12 Biotin-Ahx-VFGVWGS LAEPF-GGG	-1	acidic	1819.14	3.85

In another modified form of Phage-ELISA, phage clone number 4, 8, 9 and 12 were compared with polyclonal sera generated against PPRV for their affinity at different amount of virus coated per well. The comparison was made using ratio of their O.D. values at 450 nm with respect to that of negative control group and it was shown by P/N ratio. The graph of this form of phage ELISA is depicted in Figure 4.8.

The results showed that at 1 $\mu$ g/well concentration phage 4, 8 and 9 were having higher P/N ratio than that of polyclonal sera against PPRV collected from a strong positive case, whereas phage 12 was having lower P/N ratio than that of polyclonal sera. At 0.5 $\mu$ g/well concentration phage 8 and 9 showed same level whereas phage 4 and 12 showed lower level of P/N as compared to that of the polyclonal sera. At lower concentrations the ratio became equal for all 4 phage clones with polyclonal sera.

## **Objective 2: To characterize PPRV specific peptides and testing their binding efficacy**

### **4.4: Peptide synthesis**

All the 12 peptide sequences represented by the phage clones were synthesised using solid phase peptide synthesis protocol using Rink amide MBHA resin. These sequences show 2 types of consensus sequenses i.e, L\_YW\_\_R and G\_LAEPF at C- terminal end. Further, those phage clones (i.e, phage number 4, 8, 9 & 12) which were giving better results than other clones, their sequences were also prepared in MAP formats. The logic behind doing this was to mimic the binding site of pentavalent phage with that of the 4 armed MAP. MAP-core was having lysine mosaic with cysteine at the C-terminal end. We found that out of the 4 chosen peptides, 3 were showing consensus sequence (L\_YW\_\_R) with each other and MAP 12 was having 2nd consensus sequence i.e, G\_LAEPF. The sequence of source linear peptide and molecular weights of the MAPs are as follows-

**Table 4.5: List of MAP synthesized**

S. No.	Name given	Sequence of linear peptide										Mol. Wt. (gm/mol)		
1	MAP-4	Q	N	S	P	I	L	Q	Y	W	L	A	R	6415.12
2	MAP-8	S	D	P	V	A	L	S	Y	W	L	A	R	5970.44
3	MAP-9	E	P	W	V	H	L	N	Y	W	V	S	R	6803.40
4	MAP-12	V	F	G	V	W	G	S	L	A	E	P	F	5694.24

#### 4.5: High performance Liquid Chromatography

Cleaved peptides were subjected to semi-preparative RP-HPLC. The chromatograms were monitored with absorbance at 220nm and 280nm. The results for each of these peptides showed a major peak along with some minor peaks. The major peak (with 280nm) in each of the chromatogram represented the peptide of interest. The sequence of these peptides had tyrosine and tryptophan. The aromatic rings of these peptides gave specific and maximum absorbance at 280nm. The minor peaks indicated the presence of some salt impurities which also had some absorbance.

**Table 4.6: Retention time and % ACN on which peptide eluted**

Peptide	Retention time (minutes)	Elution % ACN
P1	21	82
P2	20	80
P3	21	82
P4	21	83
P5	20	80
P6	20	80
P7	27	84
P8	21	83
P9	26	84
P10	21	83
P11	23	89
P12	24	90
MA-4	21.5	85
MAP-8	21	83
MAP-9	20	80
MAP-12	22	87

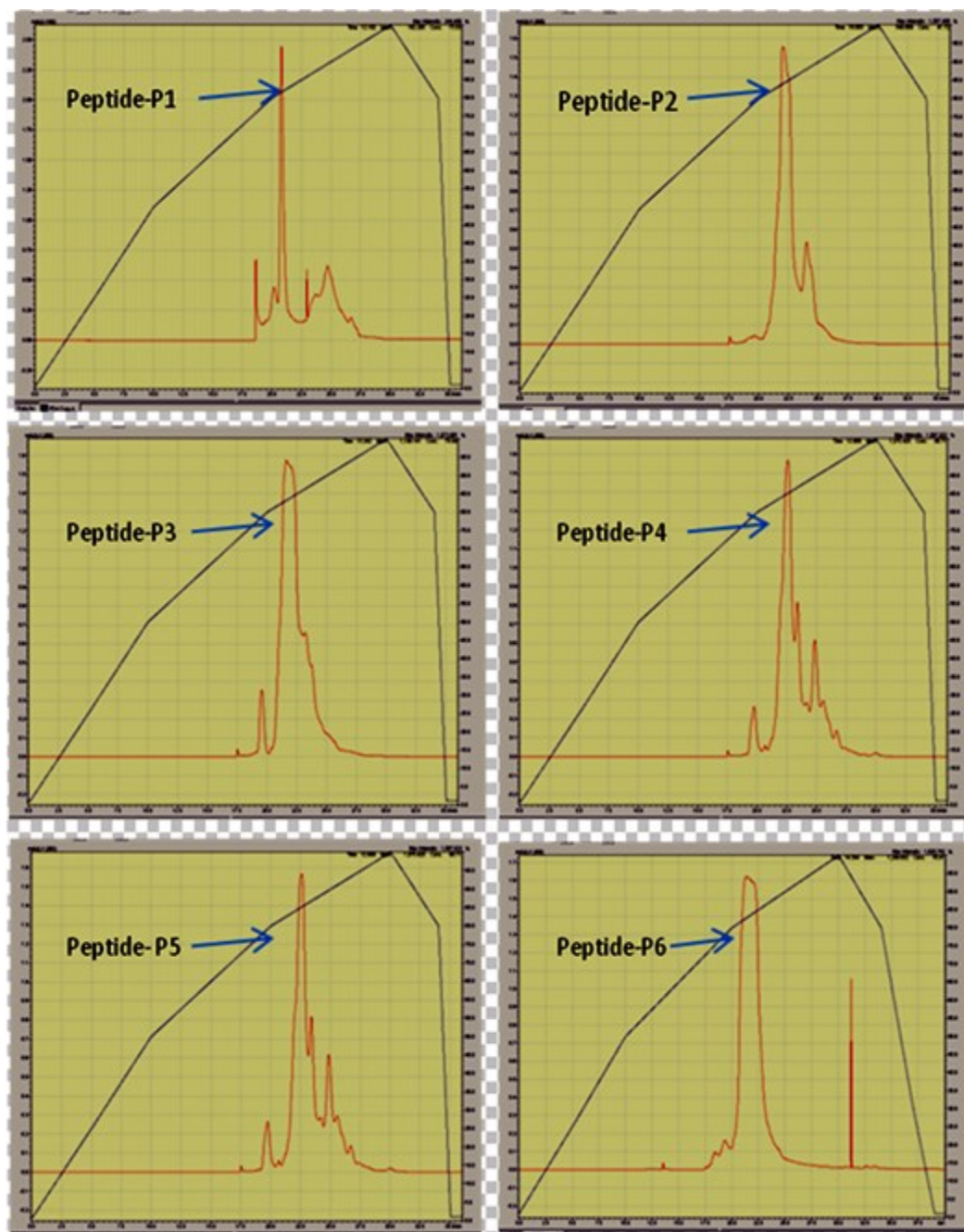


**Fig. 4.9 :** RP-HPLC chromatogram of PPRV binding peptides (P1, P2, P3, P4, P5 and P6) on a semi-preparatory column (Ultropac column, TSK ODS, 120T, 10 $\mu$ m, 7.8X300mm) tented line (black) indicates the gradient profile of solvent B (ACN with 0.1% TFA, v/v) in solvent A (H<sub>2</sub>O with 0.1% TFA, v/v)

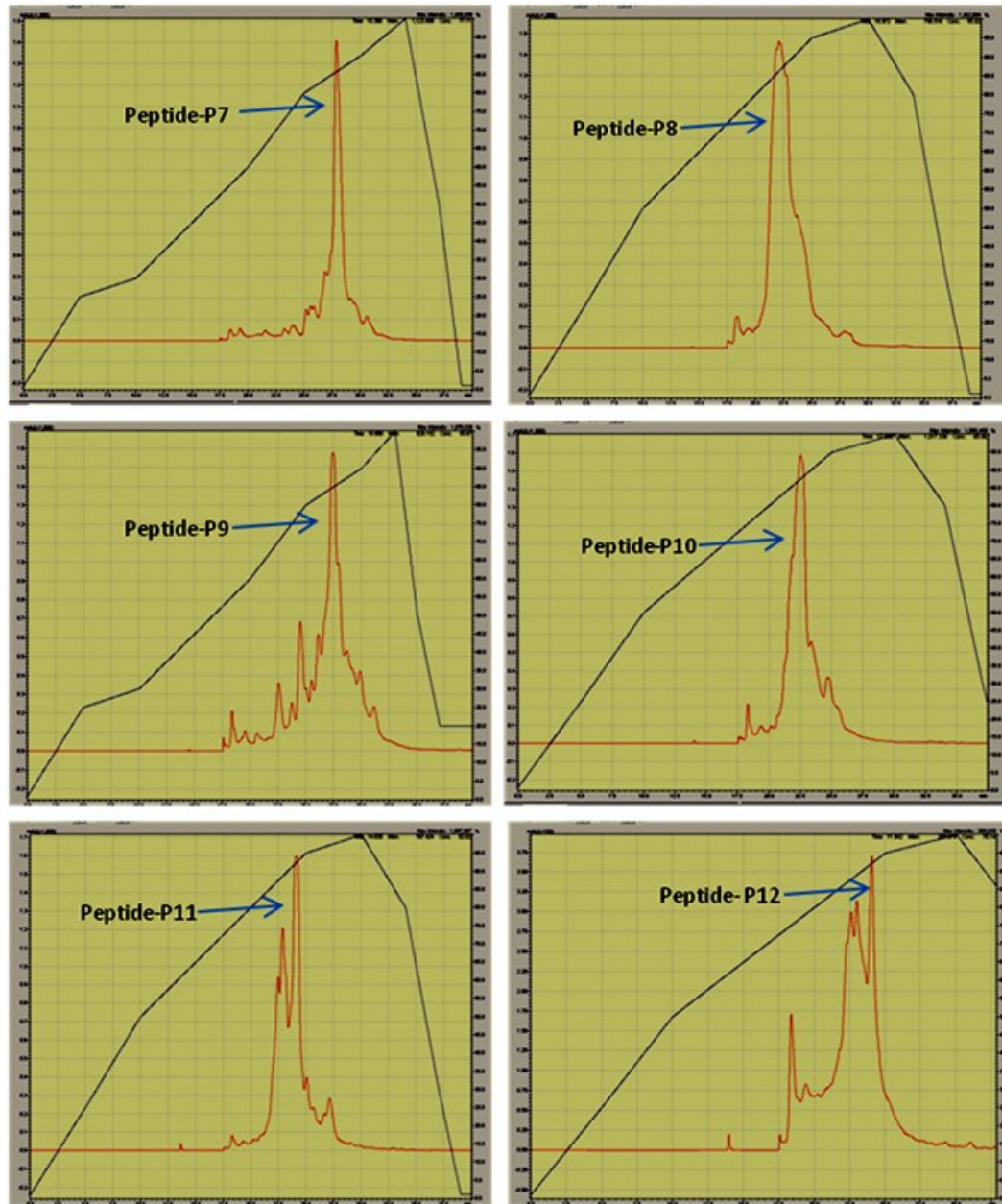


**Fig. 4.10 :** RP-HPLC chromatogram of PPRV binding peptides (P7, P8, P9, P10, P11 and P12) on a semi-preparatory column (Ultropac column, TSK ODS, 120T, 10 $\mu$ m, 7.8X300mm) tented line (black) indicates the gradient profile of solvent B (ACN with 0.1 % TFA, v/v) in solvent A (H<sub>2</sub>O with 0.1% TFA, v/v)

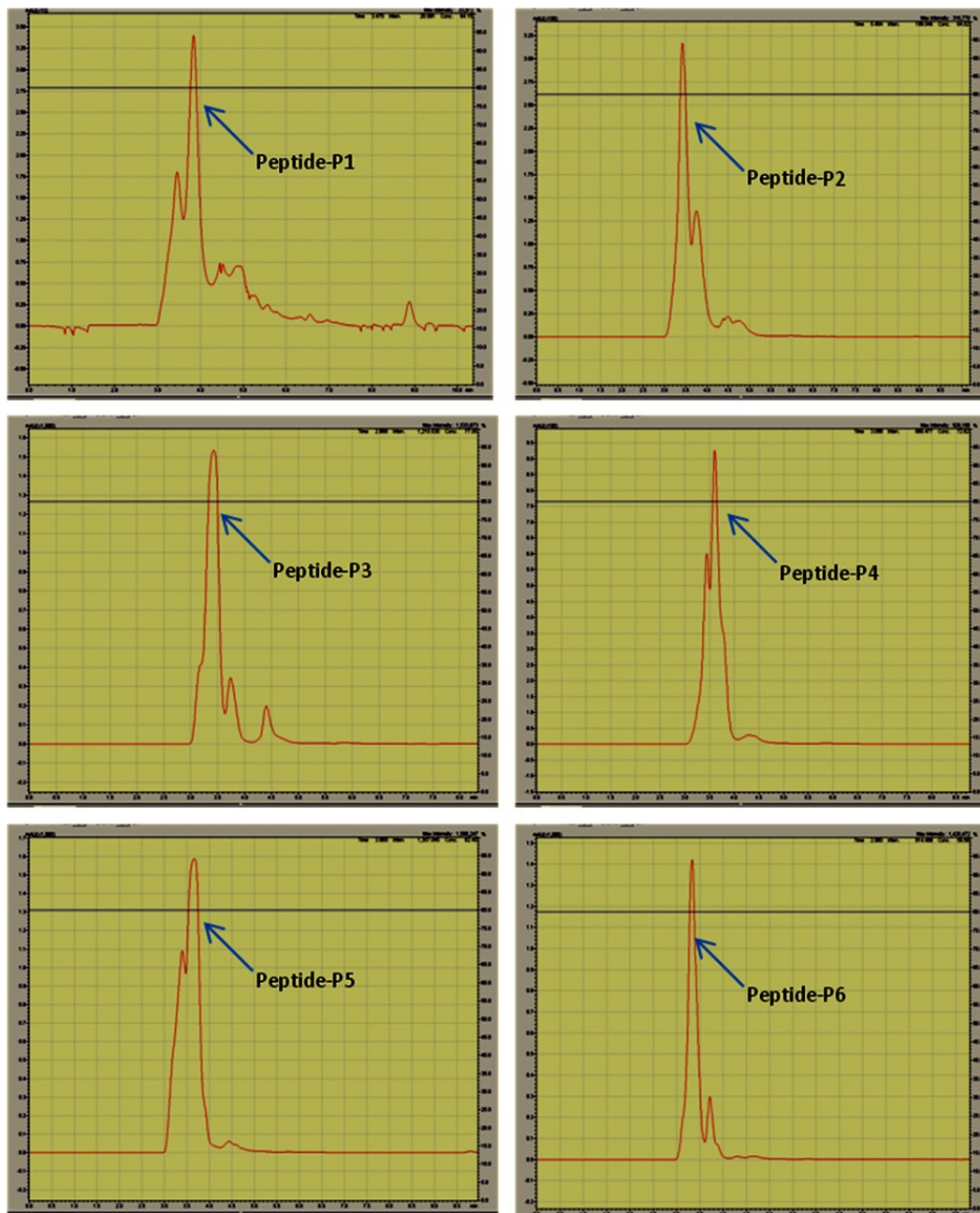


**Fig. 4.11** : RP-HPLC chromatogram of PPRV binding peptides (P1, P2, P3, P4, P5 and P6) on a analytical coulumn (Phenomenex, Luna, , C18, 150 x 4.6 mm with 5 $\mu$  size) at 80% ACN. Black line indicates the isocratic profile of solvent B ( ACN with 0.1 % TFA, v/v) in solvent A (H<sub>2</sub>O with 0.1% TFA, v/v)

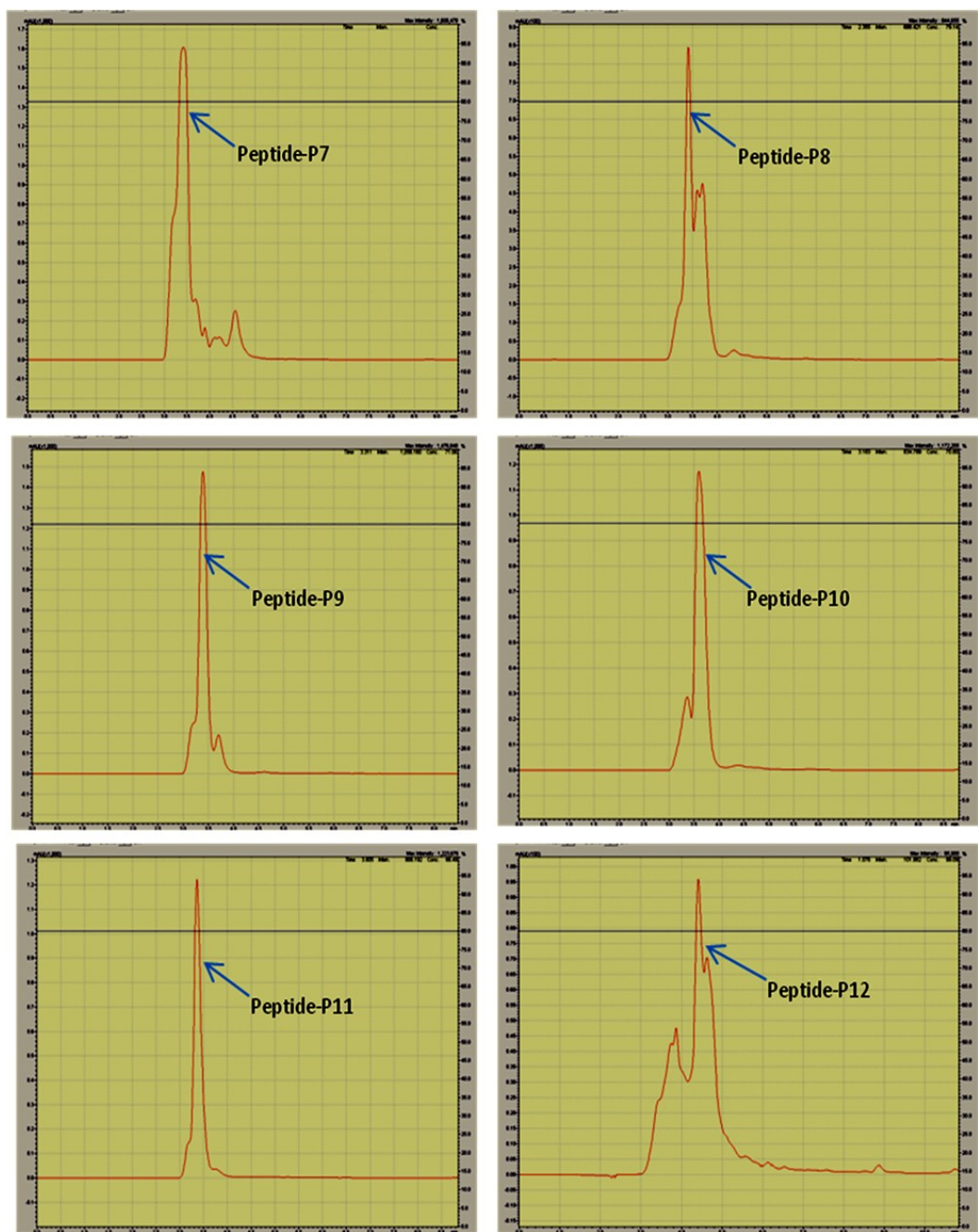


**Fig. 4.12 :** RP-HPLC chromatogram of PPRV binding peptides (P7, P8, P9, P10, P11 and P12) on an analytical column (Phenomenex, Luna, C18, 150 x 4.6 mm with 5 $\mu$  size) at 80% ACN. Black line indicates the isocratic profile of solvent B (ACN with 0.1 % TFA, v/v) in solvent A (H<sub>2</sub>O with 0.1% TFA, v/v)

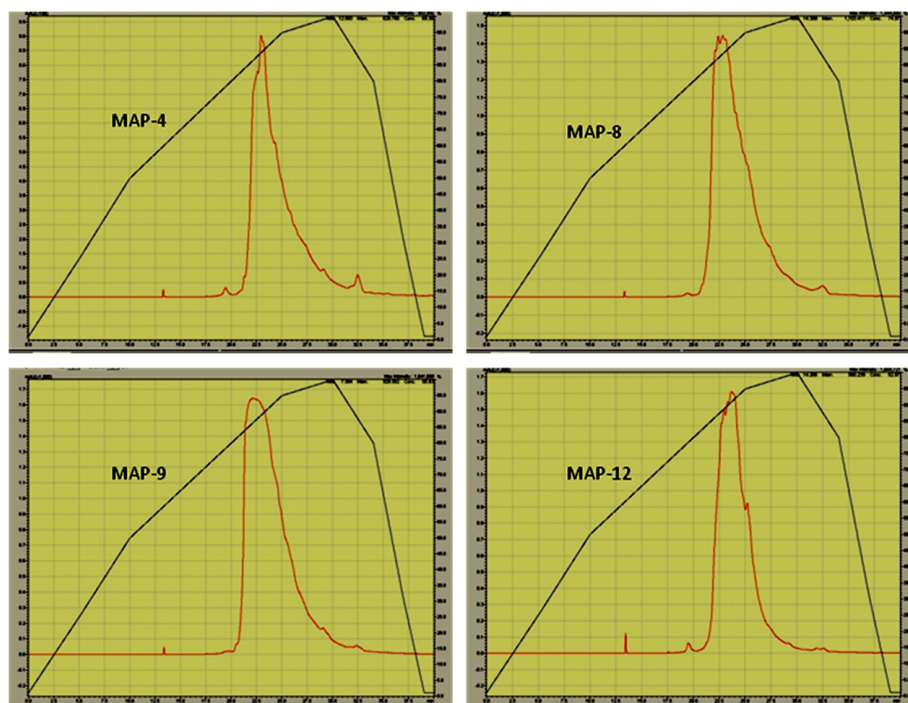


**Fig 4.13 :** RP-HPLC chromatogram of MAP format of selected PPRV binding peptides (MAP-4, 8, 9 & 12) on a semi-preparatory column (Ultropac column, TSK ODS, 120T, 10 $\mu$ m, 7.8X300mm) tented line (black) indicates the gradient profile of solvent B (ACN with 0.1 % TFA, v/v) in solvent A (H<sub>2</sub>O with 0.1% TFA, v/v)

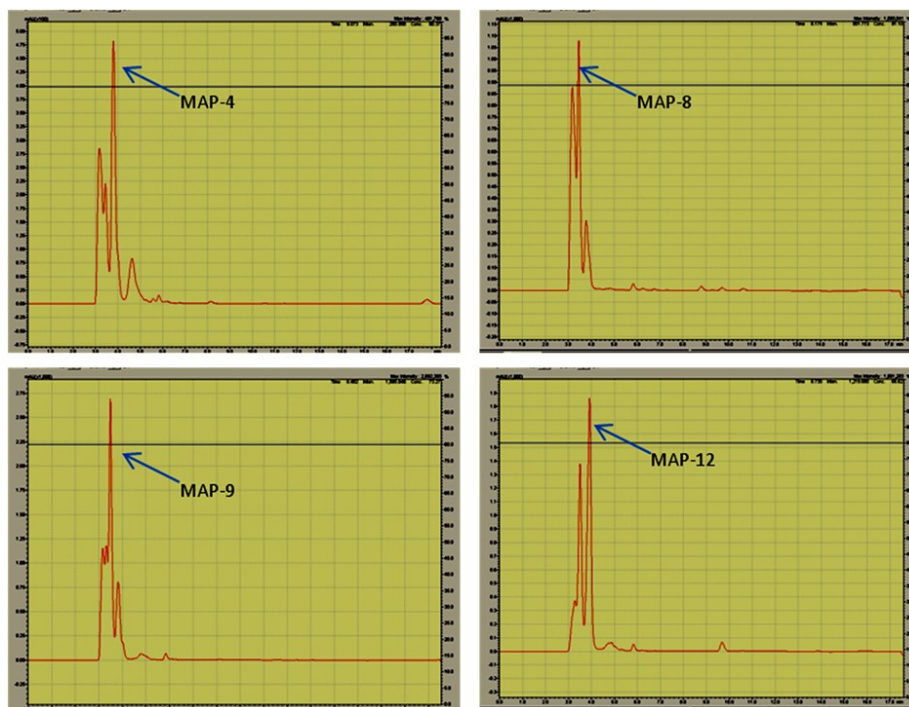


**Fig. 4.14 :** RP-HPLC chromatogram of MAP format of selected PPRV binding peptides (MAP-4, 8, 9 & 12) on an analytical column (Phenomenex, Luna, C18, 150 x 4.6 mm with 5 $\mu$  size) at 80% ACN. Black line indicates the isocratic profile of solvent B (ACN with 0.1 % TFA, v/v) in solvent A (H<sub>2</sub>O with 0.1% TFA, v/v)

The RP-HPLC chromatogram of biotinylated PPRV binding peptides (Linear and MAP) are depicted in Figure 4.9, 4.10, 4.11, 4.12, 4.13, 4.14 respectively. The retention time and % ACN on which peptide eluted is given in table 4.6. Thus, peptides have more than 90 % purity and used for further studies.

#### 4.6: Characterisation of Peptides using MALDI:

The peak-fraction of selected peptides in HPLC was concentrated in speed-vac concentrator and analyzed for expected mass of the peptide using MALDI spectrometry. Estimated mass and observed mass of each peptide in table 4.7.

**Table 4.7: Calculated mass and observed mass using MALDI**

Peptide	Calculated mass (gm/mole)	Observed mass (gm/mole)
P4	1828.18	1826.90
P8	1888.19	1888.86
P9	2096.43	2098.3
P12	1819.14	1839.8

#### 4.7: Virus capture ELISA

##### 4.7.1: Peptide-ELISA:

Linear peptides were coated on the surface of microtiter plate. PPRV was allowed to incubate on these coated peptides for 1 hour. Unbound virus was washed away by TBST. Then with the help of polyclonal sera and anti goat antibody captured virus was detected by addition of TMB and 1M H<sub>2</sub>SO<sub>4</sub>. O.D. at 450 nm was taken. Here, no significant difference in the O.D.450 between test and negative control wells was there. This loss of affinity of linear peptides may be attributed to their poor coating efficiency or change in their conformation during coating.

##### 4.7.2: MAP-ELISA:

When in virus capture ELISA, MAP format of peptides were used instead of monovalent linear peptides, significant reactivity with PPRV was shown by the MAP peptides. The graph depicting the O.D. values at 450nm are shown in figure 4.16.

#### 4.8: Elucidation of Secondary Structure using CD spectroscopy

To predict the conformation of peptides in solution, CD spectra of linear and MAP formats of peptides were recorded in water, 50%, 100% trifluoroethanol (TFE) and PBS. CD spectra obtained in these solutions is depicted in figures 4.17, 4.18, 4.19, 4.20 and 4.21 respectively. The quantitation of different secondary structures was carried out by CD structure quantitation software. The percentage of different secondary structures of PPRV binding peptides in different concentration of TFE are given below in table no.4.8, 4.9, 4.10, 4.11 and 4.12 respectively.

The spectra indicate that, all these peptides (linear as well as MAPs) comprise mainly  $\beta$ -structures. The percentages of  $\alpha$ -helices are very low as compared to random and turn structures. These beta structures may be responsible for the binding of our peptides with PPRV.

#### 4.9: Visual Plasmon change in AuNPs

The MAP was conjugated on AuNPs and the conjugation was confirmed by red shift in  $\lambda_{\max}$  in UV-Vis spectra (Figure 4.22). After proper washing, MAP-activated gold nanoparticle solution PPRV was added at a final concentration of 0.01  $\mu\text{g}/\mu\text{l}$ . In control tubes, same volume of PBS was added (as stock virus was suspended in PBS) in AuNPs. In test, where PPRV was added, the colour of solution changed from wine red to purple (Figure 4.23). No colour change was observed in control tubes. Colour change may be attributed to the change in surface plasmon due to networking between MAP conjugated AuNPs and PPRV.

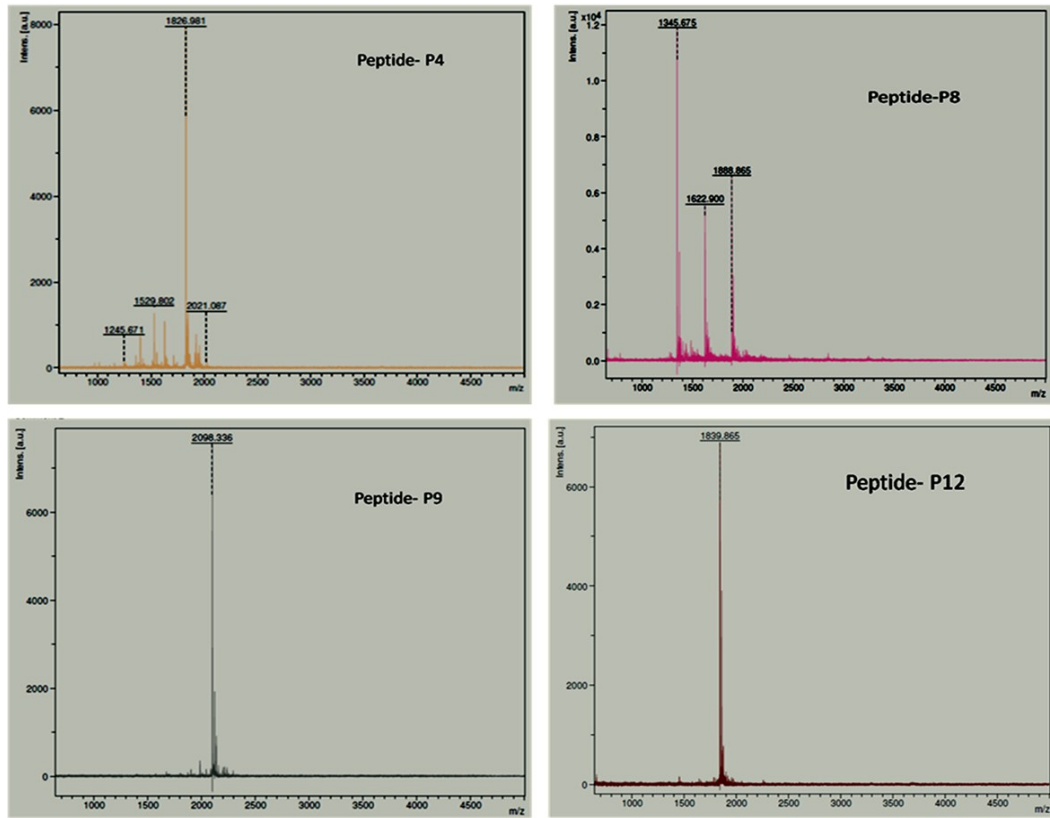


**Fig. 4.15 :** MALDI-TOF of peptides showing different charged fragments with average mass in dalton

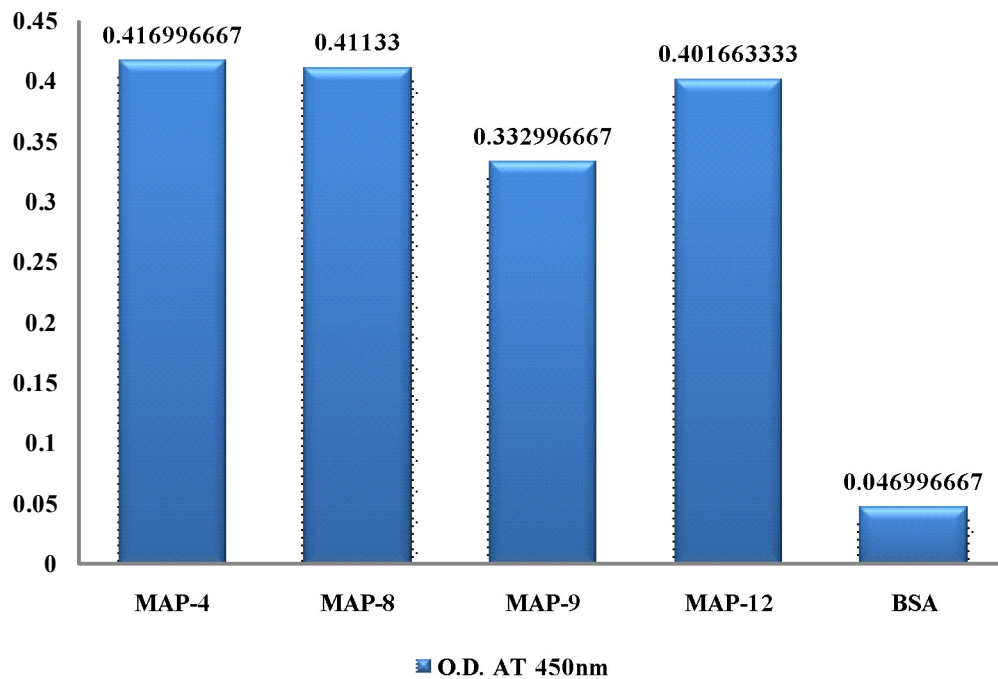


**Fig. 4.16 :** Histogram representing virus capture ELISA using MAP for capturing PPRV and polyclonal sera & HRP conjugated anti goat antibody for detecting PPRV

**Table 4.8: Elucidation of Secondary Structure of biotinylated PPR binding peptides (P1, P2 & P3) using CD spectroscopy**

<b>P1</b>	<b>Biotin-Ahx-CIWCVGELAEPF</b>			mol. wt.-1706.07 g/mol
	Water	50% TFE	100% TFE	PBS
	%	%	%	%
<b>Helix</b>	0.0	0.0	0.4	1.7
<b>Beta</b>	82.7	82.5	81	73.2
<b>Turn</b>	0.0	0.0	0.0	2.9
<b>Random</b>	17.3	17.5	18.6	22.3
<b>P2</b>	<b>Biotin-Ahx-VHWDFRQWWQPS</b>			mol. wt.- 2011.3 g/mol
	Water	50% TFE	100% TFE	PBS
	%	%	%	%
<b>Helix</b>	3.9	4.5	7.0	0.0
<b>Beta</b>	48.3	60.1	57.4	71.0
<b>Turn</b>	13.8	7.1	8.2	8.6
<b>Random</b>	33.9	28.3	27.4	20.4
<b>P3</b>	<b>Biotin-Ahx-AYDPHIQYWIER</b>			mol. wt.- 1930.22 g/mol
	Water	50% TFE	100% TFE	PBS
	%	%	%	%
<b>Helix</b>	0.0	3.8	2.6	2.5
<b>Beta</b>	66.7	75.5	78.0	6.1
<b>Turn</b>	4.9	0	0.0	4.6
<b>Random</b>	28.4	20.7	19.5	25.7

CD spectra recorded to elucidate the conformation of PPRV binding peptides (P1, P2 & P3) in water (polar) and apolar environment using solvent like TFE is shown in Figure 4.17.

**Table 4.9: Elucidation of Secondary Structure of biotinylated PPR binding peptides (P4, P5 & P6) using CD spectroscopy**

<b>P4</b>	<b>Biotin-Ahx-QNSPILQYWLR</b>			mol. wt.-1828.18 g/mol
	Water	50% TFE	100% TFE	PBS
	%	%	%	%
<b>Helix</b>	5.6	7.3	5.3	0.0
<b>Beta</b>	46.2	66.3	71.4	81.3
<b>Turn</b>	12.8	2.0	0.9	0.0
<b>Random</b>	35.4	24.4	22.4	18.7

<b>P5</b>	<b>Biotin-Ahx-DWSSWVYRDPQT-GGG</b>			mol. wt.- 2050.25 g/mol
	Water	50% TFE	100% TFE	PBS
	%	%	%	%
<b>Helix</b>	0.0	0.6	2.6	3.6
<b>Beta</b>	66.2	77.4	76.7	58.5
<b>Turn</b>	4.9	0.	0.0	7.6
<b>Random</b>	28.9	22	20.7	30.3

<b>P6</b>	<b>Biotin-Ahx-DHSVFHAWHTYF-GGG</b>			mol. wt.- 2057.3g/mol
	Water	50% TFE	100% TFE	PBS
	%	%	%	%
<b>Helix</b>	4.3	0.0	13.3	0.0
<b>Beta</b>	52.9	82.3	59.5	82.8
<b>Turn</b>	11.8	0.0	4.7	0.0
<b>Random</b>	31.0	17.7	22.5	17.2

CD spectra recorded to elucidate the conformation of PPRV binding peptides (P5, P6 & P7) in water (polar) and apolar environment using solvent like TFE is shown in Figure 4.18.

**Table 4.10: Elucidation of Secondary Structure of biotinylated PPR binding peptides (P7, P8 & P9) using CD spectroscopy**

<b>P7</b>	<b>Biotin-Ahx-WHWRAPVIYSWP-GGG</b>			mol. wt.-2108.48 g/mol
	Water	50% TFE	100% TFE	PBS
	%	%	%	%
<b>Helix</b>	0.0	0.0	0.3	0.0
<b>Beta</b>	65.0	79.4	81.4	69.8
<b>Turn</b>	6.8	0.0	0.0	3.0
<b>Random</b>	28.1	20.6	18.2	27.2

<b>P8</b>	<b>Biotin-Ahx-SDPVALSYWLAR-GGG</b>			mol. wt.- 1888.19 g/mol
	Water	50% TFE	100% TFE	PBS
	%	%	%	%
<b>Helix</b>	3.5	9.5	13.8	0.8
<b>Beta</b>	62.6	59.0	53.4	79.2
<b>Turn</b>	6.8	5.4	6.3	0.
<b>Random</b>	27.1	26.2	26.5	20.0

<b>P9</b>	<b>Biotin-Ahx-EPWVHLNYWVSR-GGG</b>			mol. wt.- 2096.43 g/mol
	Water	50% TFE	100% TFE	PBS
	%	%	%	%
<b>Helix</b>	0.0	11.1	11.8	6.9
<b>Beta</b>	68.7	69.9	70.7	54.8
<b>Turn</b>	4.1	0.0	0.0	8.9
<b>Random</b>	27.1	19.0	17.5	29.5

CD spectra recorded to elucidate the conformation of PPRV binding peptides (P7, P8 & P9) in water (polar) and apolar environment using solvent like TFE is shown in Figure 4.19.

**Table 4.10: Elucidation of Secondary Structure of biotinylated PPR binding peptides (P10, P11 & P12) using CD spectroscopy**

<b>P10</b>	<b>Biotin-Ahx-WNNSVLDYWLQR-GGG</b> mol. wt.-2104.41 g/mol			
	Water	50% TFE	100% TFE	PBS
	%	%	%	%
<b>Helix</b>	2.5	6.2	9.6	0.0
<b>Beta</b>	64.3	69.4	67.6	79.9
<b>Turn</b>	6.0	0.1	0.0	0.0
<b>Random</b>	27.2	24.3	22.7	20.1

<b>P11</b>	<b>Biotin-Ahx-WHWWGRLIHSFL-GGG</b> mol. wt.- 2148.57 g/mol			
	Water	50% TFE	100% TFE	PBS
	%	%	%	%
<b>Helix</b>	0.0	16.0	18.8	6.8
<b>Beta</b>	72.4	64.5	62.4	64.2
<b>Turn</b>	2.8	0.0	0.0	5.3
<b>Random</b>	24.8	19.4	18.8	23.8

<b>P12</b>	<b>Biotin-Ahx-VFGVWGS LAEPF-GGG</b> mol. wt.- 1819.14 g/mol			
	Water	50% TFE	100% TFE	PBS
	%	%	%	%
<b>Helix</b>	0.0	1.9	0.7	0.0
<b>Beta</b>	76.0	70.7	77.6	84.5
<b>Turn</b>	1.9	3.9	0.9	0.0
<b>Random</b>	22.1	23.6	20.9	15.5

CD spectra recorded to elucidate the conformation of PPRV binding peptides (P10, P11 & P12) in water (polar) and apolar environment using solvent like TFE is shown in Figure 4.20.

**Table 4.10: Elucidation of Secondary Structure of biotinylated PPR binding peptides (MAP-4, 8, 9 and 12) using CD spectroscopy**

<b>MAP-4</b>		<b>Mol. Wt.- 6415.12 g/mol</b>			
	<b>Water</b>	<b>50% TFE</b>	<b>100% TFE</b>	<b>PBS</b>	
<b>Helix (%)</b>	0.0	2.3	4.8	5.7	
<b>Beta (%)</b>	80.5	78.3	72.9	55.7	
<b>Turn (%)</b>	0.0	0.0	0.0	8.1	
<b>Random (%)</b>	19.5	19.4	22.3	30.5	

<b>MAP-8</b>		<b>Mol. Wt.- 5970.44 g/mol</b>			
	<b>Water</b>	<b>50% TFE</b>	<b>100% TFE</b>	<b>PBS</b>	
<b>Helix (%)</b>	1.9	8.1	13.6	0.0	
<b>Beta (%)</b>	63.2	57.7	46.1	70.8	
<b>Turn (%)</b>	6.7	6.3	9.6	4.0	
<b>Random (%)</b>	28.3	27.9	30.7	25.2	

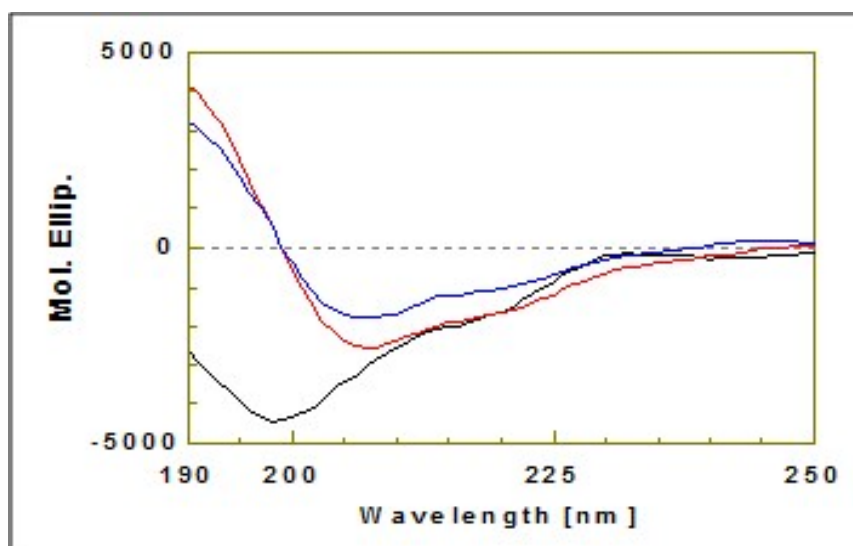
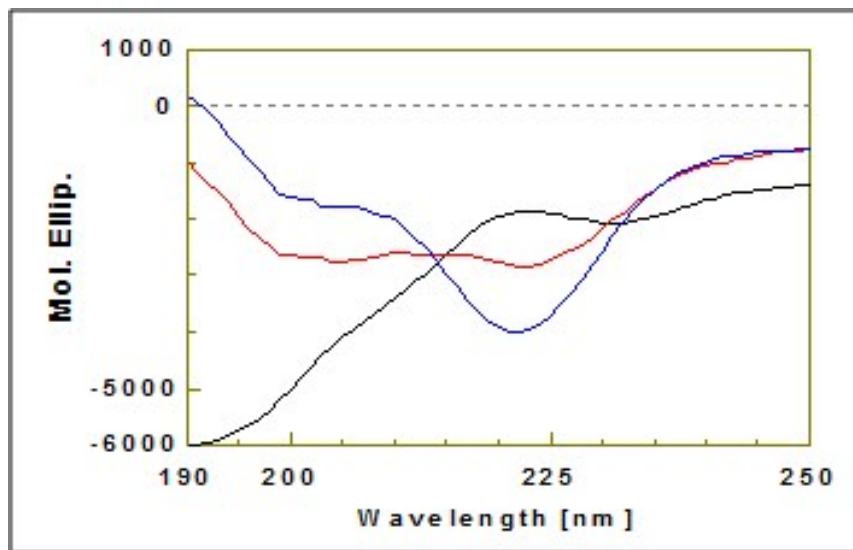
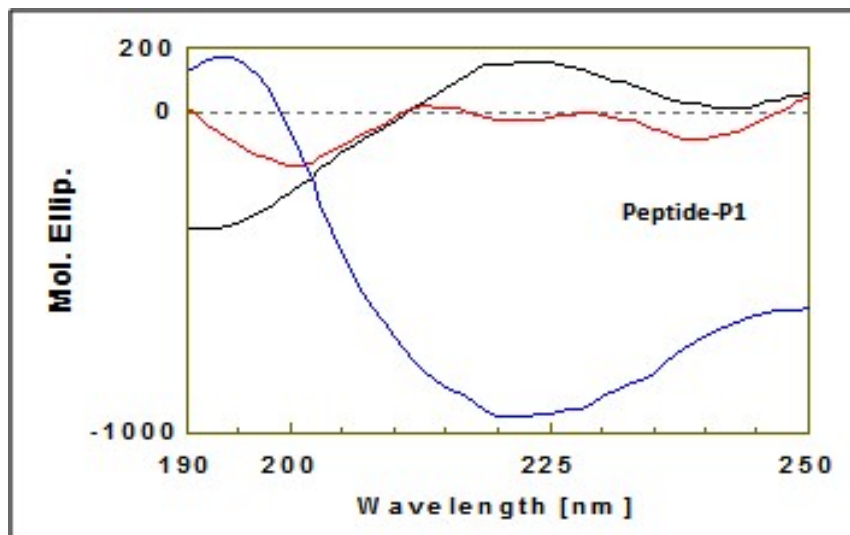
<b>MAP-9</b>		<b>Mol. Wt.- 6803.40 g/mol</b>			
	<b>Water</b>	<b>50% TFE</b>	<b>100% TFE</b>	<b>PBS</b>	
<b>Helix (%)</b>	0.0	1.7	5.8	3.0	
<b>Beta (%)</b>	70.1	75.0	68.9	56.3	
<b>Turn (%)</b>	4.0	0.0	1.2	8.0	
<b>Random (%)</b>	26.0	23.2	24.1	32.6	

<b>MAP-12</b>		<b>Mol. Wt.- 5694.24 g/mol</b>			
	<b>Water</b>	<b>50% TFE</b>	<b>100% TFE</b>	<b>PBS</b>	
<b>Helix (%)</b>	0.0	3.8	5.1	0.0	
<b>Beta (%)</b>	75.2	64.7	64.6	79.3	
<b>Turn (%)</b>	2.3	6.1	5.4	2.5	
<b>Random (%)</b>	22.5	25.4	24.9	18.2	

CD spectra recorded to elucidate the conformation of MAP 4, 8, 9 & 12 are shown in fig 4.21





**Fig. 4.17:** CD spectra of PPRV binding peptides (P1, P2 & P3) in different polar and apolar solutions; water, 50% and 100% TFE

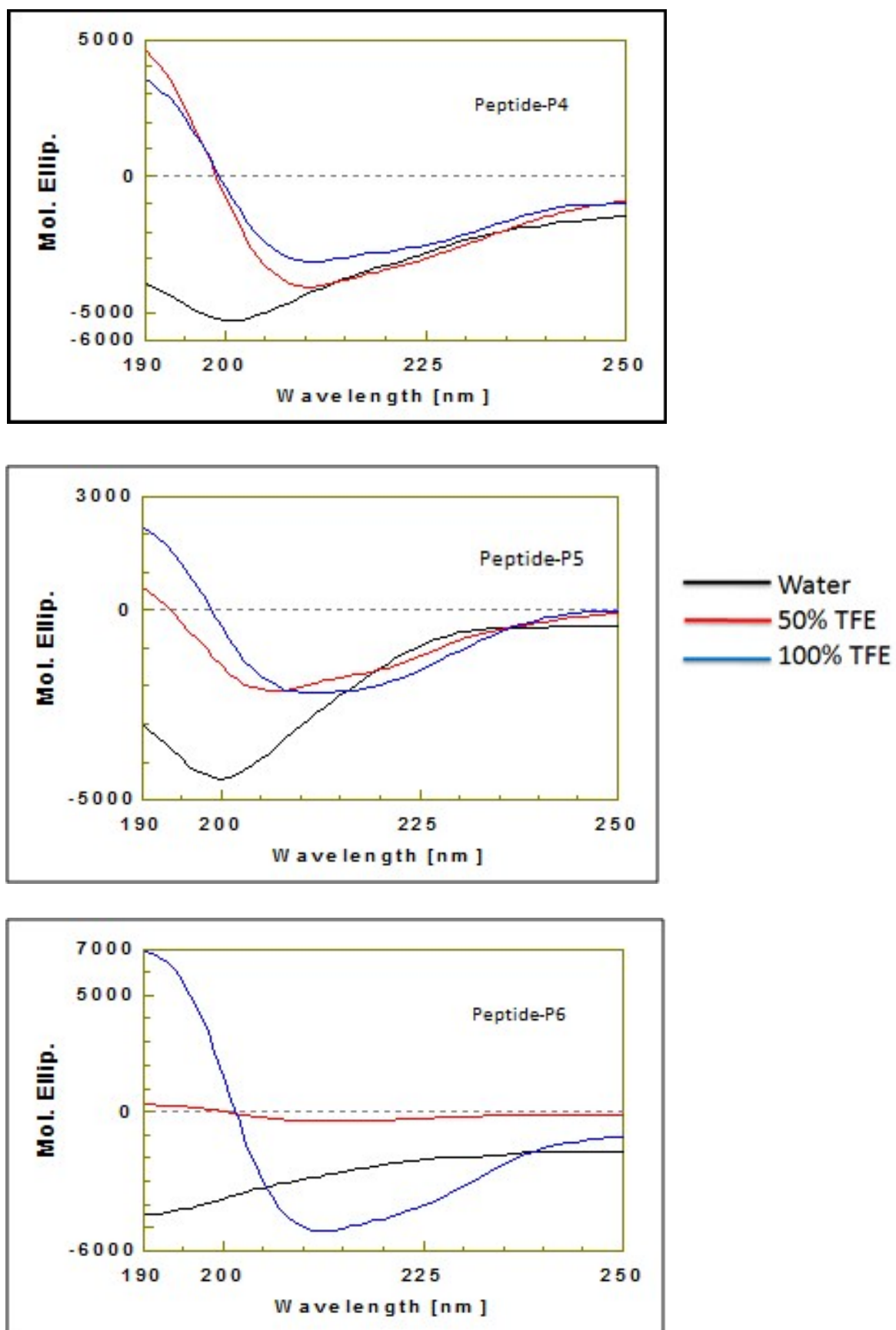


**Fig. 4.18:** CD spectra of PPRV binding peptides (P4, P5 & P6) in different polar and apolar solutions; water, 50% and 100% TFE

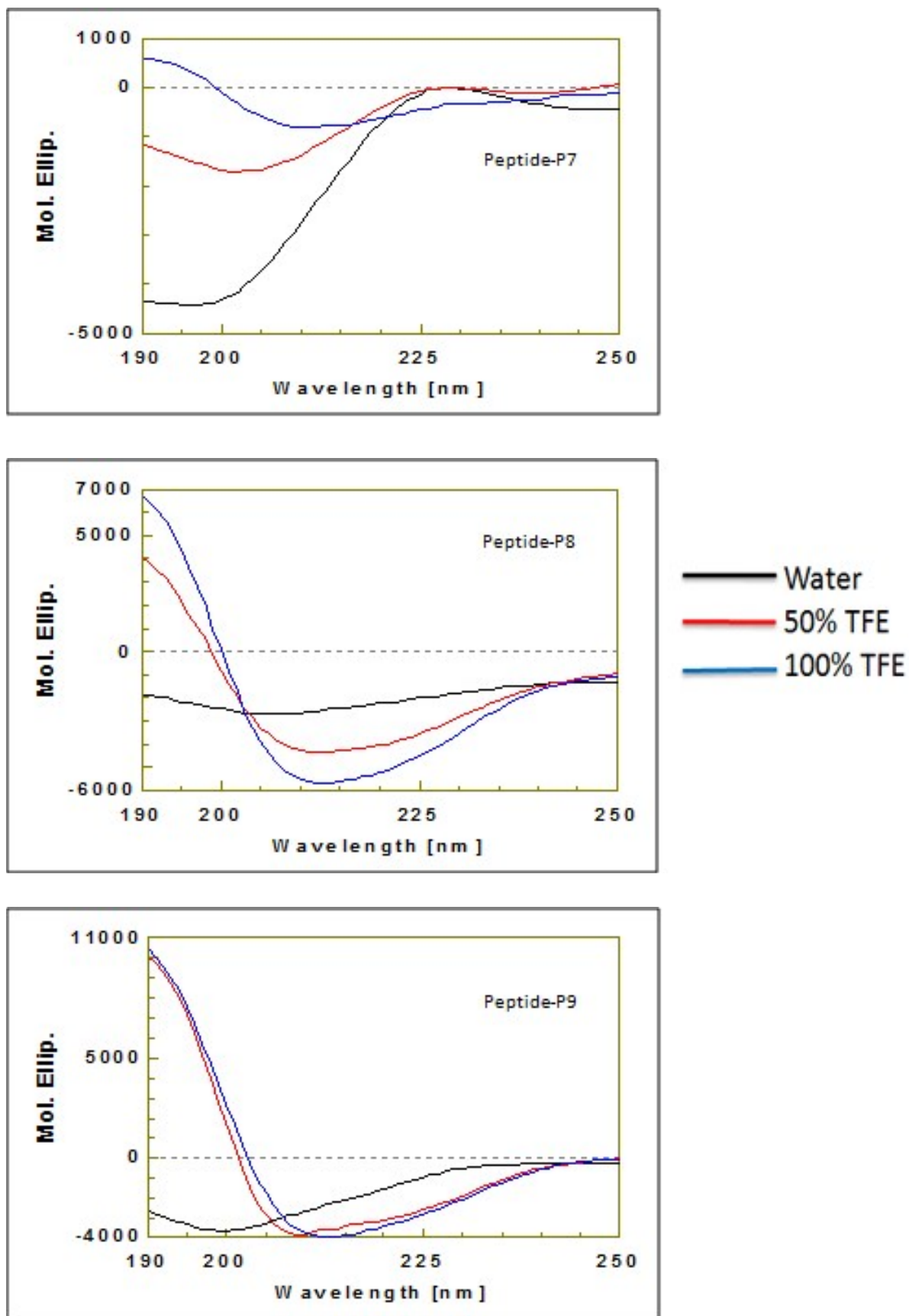


**Fig. 4.19:** CD spectra of PPRV binding peptides (P7, P8 & P9) in different polar and apolar solutions; water, 50% and 100% TFE

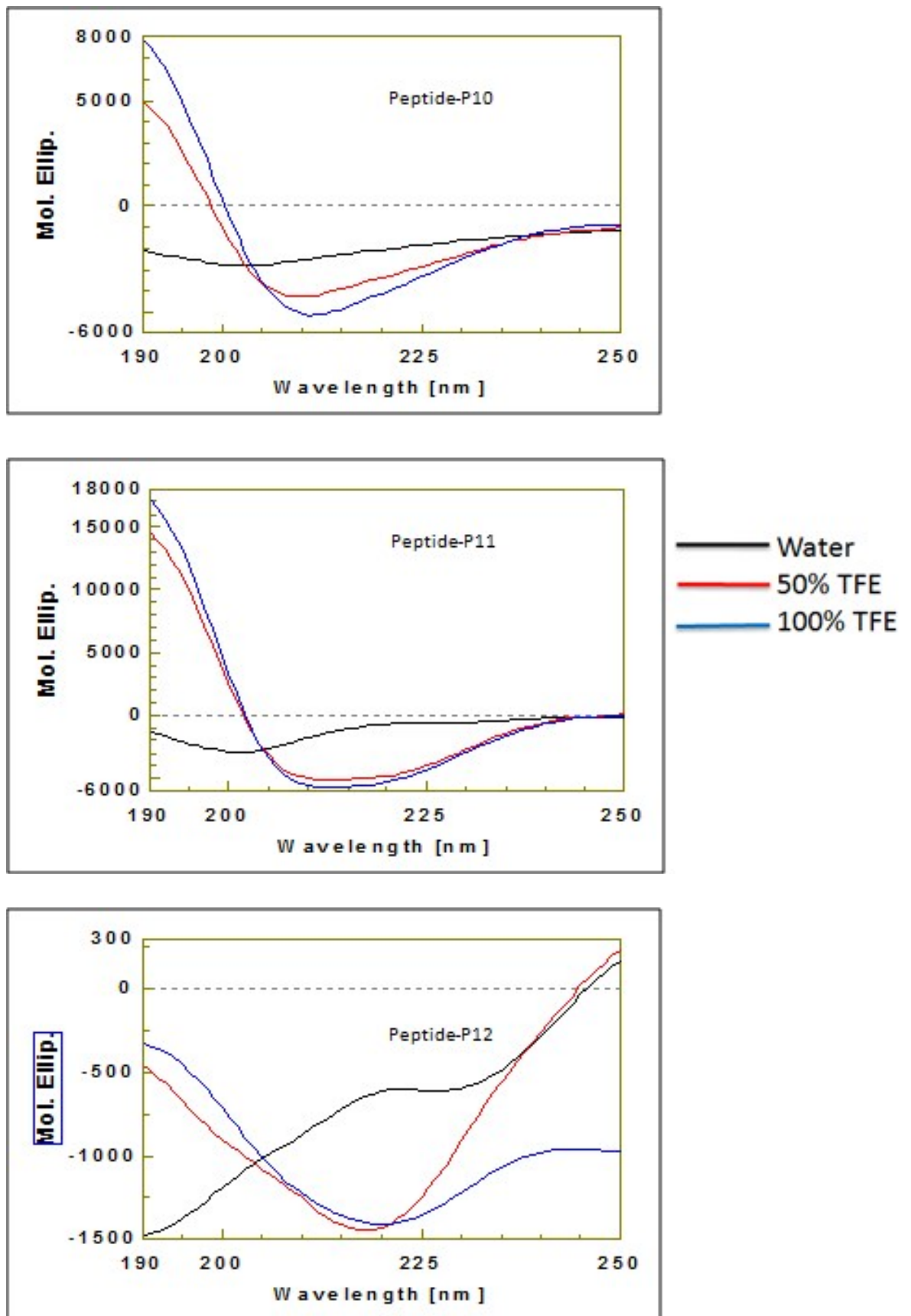


**Fig. 4.20:** CD spectra of PPRV binding peptides (P10, P11 & P12) in different polar and apolar solutions; water, 50% and 100% TFE

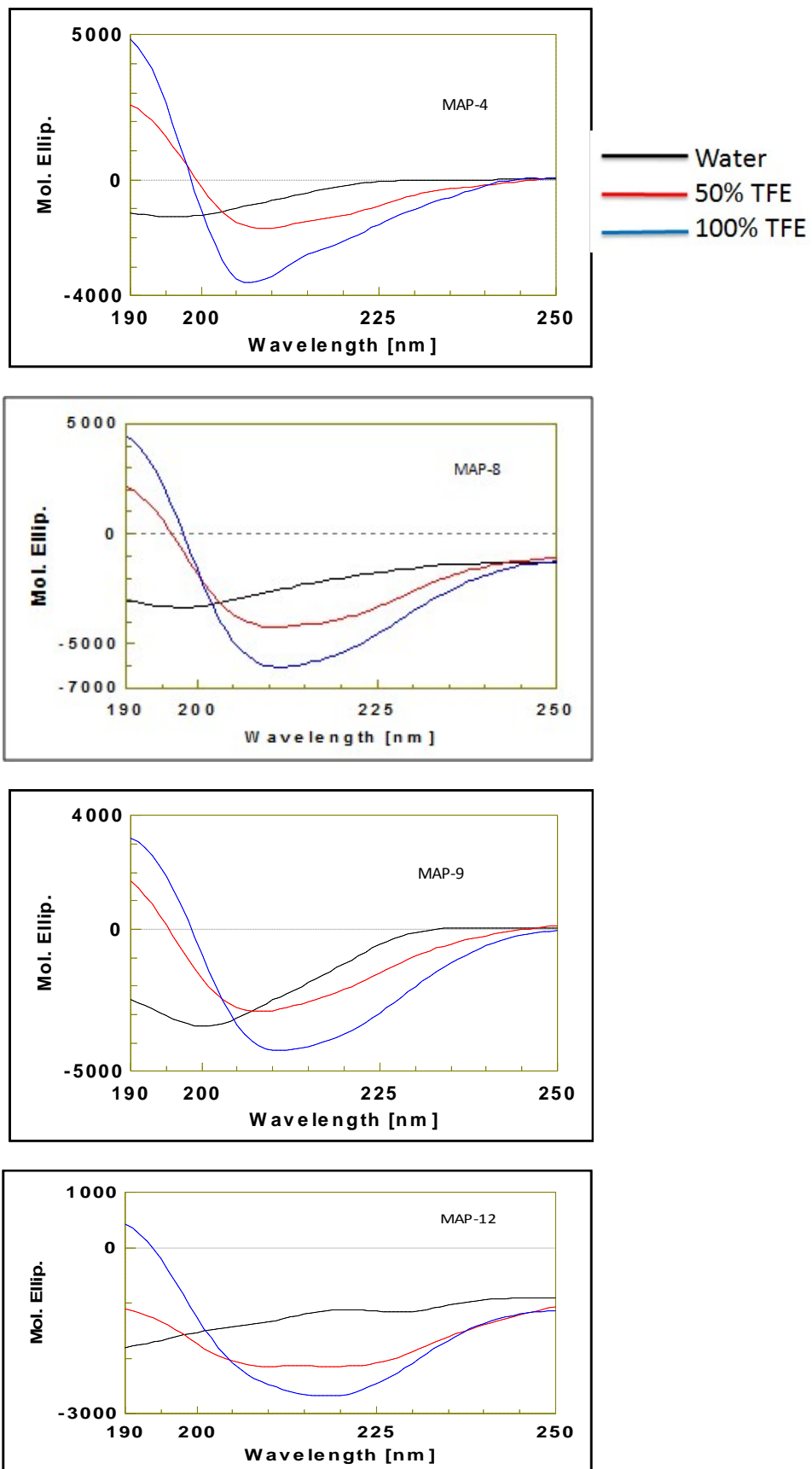


**Fig. 4.21:** CD spectra of PPRV binding peptides (MAP-4, MAP-8, MAP-9 & MAP-12) in different polar and apolar solutions; water, 50% and 100% TFE

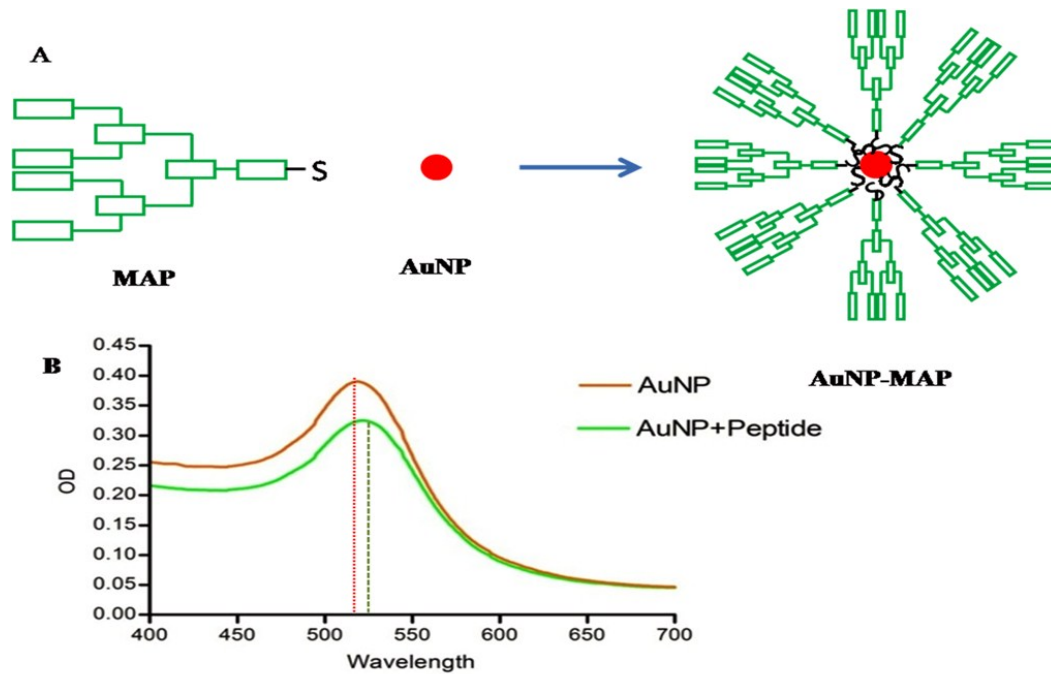


**Fig. 4.22** : Conjugation of MAP cysteine to AuNP (A); UV-Vis spectra of AuNP and AuNP-MAP showing red shift of  $\lambda_{\max}$  (B)

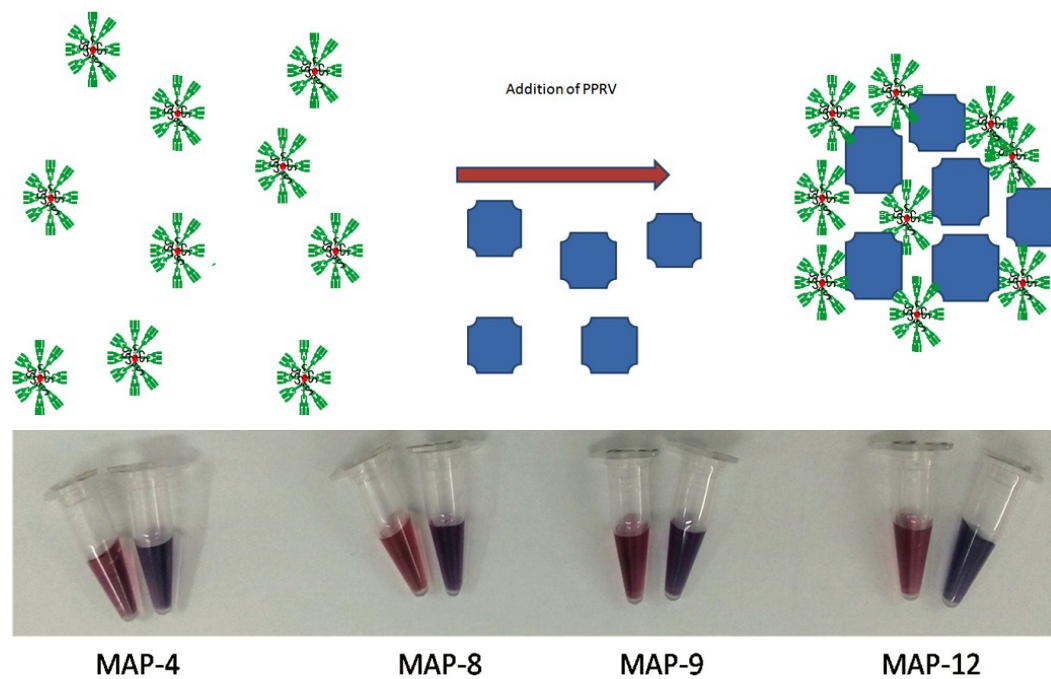
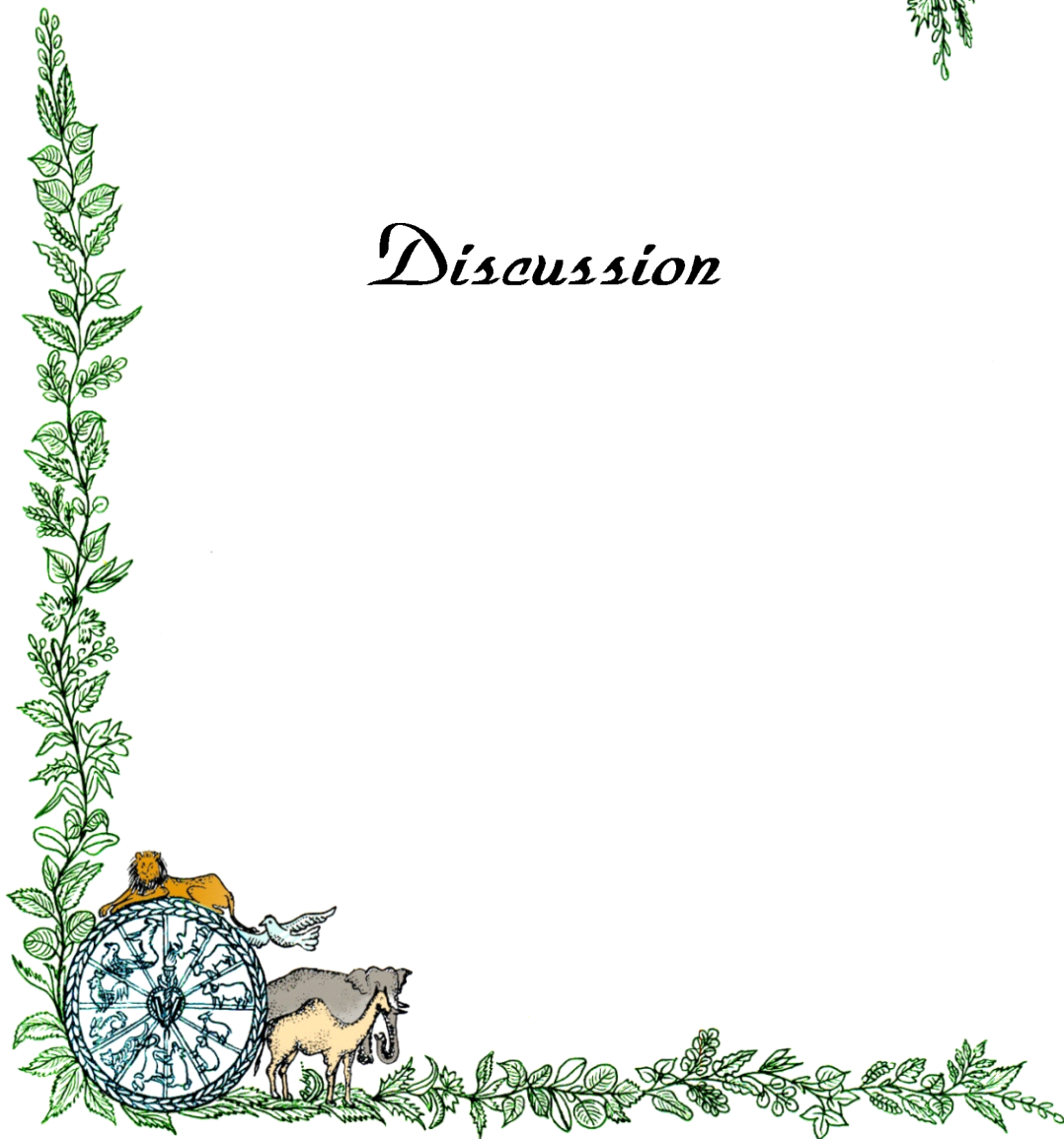


**Fig. 4.23** : Visual colour change (red to purple) in MAP conjugated gold nanoparticles on addition of PPRV.



# *Discussion*



In the present study, our prime aim was to give a proof of concept that phage display technology can be used to identify phage clones and subsequently peptides, which bind specifically to a target molecule. This may in turn help in development of synthetic diagnostic reagents, which can simplify the process of diagnosis by alleviating the need of isolation of nucleic material of pathogen and need of sophisticated lab infrastructure. This is desirable in order to save the time and to take prompt action, if required.

Phage display (PhD) derived high affinity peptide ligand molecules have been used in wide ranging applications from non-invasive molecular imaging of cancer to different therapeutic and diagnostic methods (Deutscher, 2010; Alban *et al.*, 2014). In the present study, we have used PhD technology to identify specific peptide ligands against viral pathogen of small ruminants/PPRV. The identified peptides were chemically synthesized to form a part of clean platform and subsequently analysed as a potential virus detection reagents. As recently reported, PhD derived peptides represent paratopes (antigen binding site of immunoglobulins) and are being considered viable alternative to antibodies, hence can be used to develop better diagnostic applications (Huang *et al.* 2012; Alban *et al.*, 2014).

Previously, phage display method has been used to identify specific peptides for large number of pathogenic viruses including west Nile virus (Bai *et al.* 2007), hepatitis C virus (Hong *et al.* 2010) and HIV (Welch *et al.* 2010). The purpose of the present study was to use PhD to identify specific ligands against PPRV. The Sungri strain of PPR virus was propagated in Vero cells and culture supernatant was collected, cellular debris was removed by low speed

centrifugation followed by ultra-centrifugation. The purified concentrated whole PPRV was used as target molecule in phage selection steps. Earlier, Wu *et al* (2011) similarly utilized culture purified whole influenza virus while identifying specific phages for diagnostic applications.

The process of selection and amplification of phage to enrich the phage pool displaying desired peptide is called biopanning (Mullaney and Pallavicini, 2001). Three rounds of panning were performed following same protocol, only difference was that the tween-20 concentration was increased to increase the stringency of selection. There were chances of some of the Vero cell components that remained in the centrifuged PPRV suspension. Therefore in order to remove phage clones which would be binding to Vero cell components instead of PPRV, negative panning was performed. For this, at the time of 4th round of panning unamplified eluate of 3rd round of panning was incubated with Vero cell supernatant coated wells. Here, supernatant (unbound phages) was collected instead of elution of bound phage and subjected to 5th round of panning. This subtractive panning step is essential to remove any non-specific phages that may falsely be included as virus binding clones. Wu and co-workers also included the step of subtractive panning in their protocol while performing phage display against H5N1 strain of Influenza virus to decrease the reaction background (Wu *et al.*, 2011).

Subsequently, 5th round of panning was done using PPRV as target by following standard protocol. The results of the phage titre determined from first round panning to fifth round of panning indicated a gradual increase. Unamplified eluate of 5th round of panning was used for titration. Randomly, 40 colonies were picked up and amplified separately. The DNA of phage clones were isolated, PCR amplified and sequencing was done. The translation of 40 phage clones DNA insert presenting the random sequence identified 12 unique peptide sequences. Each unique peptide sequence or phage clone appeared in different number of times (frequencies). The phage clones bearing peptide sequence VHWDFRQWWQPS and CIWCVGELAEPF repeated 10 and 8 times respectively. These results indicated the presence of few types of specific phage types with high binding affinity to the PPRV.

All these 12 phage clones were then amplified and subjected to phage ELISA. In phage ELISA, BSA was taken as negative control and bluetongue virus (BTV) was taken as

virus control as it affects the same host species (Sheep and Goat). Our results indicated that only phage number 4, 8, 9 and 12 showed specific reactivity to the coated virus, whereas rest of the phage clones showed nonspecific reactivity by binding to BSA and BTV coated wells. The presence of nonspecific phage clones may be due to the fact that BSA was used as blocking agent during biopanning protocols and there may be chances that phage clones having affinity to BSA were also got selected. Similarly in the virus control wells coated with BTV, BSA was used for blocking which could be responsible for increased reactivity shown by some of the nonspecific phage clones.

The sequence analysis of specific reactive phage clones identified in Phage ELISA indicated the presence of putative motifs in their peptide sequence. The conserved peptide motif L\_YW\_\_R. was observed among the three reactive phage clones. The specifically positioned amino acids may have role in binding to the viral proteins. The function of these residues in binding to the virus needs to be investigated.

The phage ELISA was compared with the direct antibody mediated ELISA for detection of PPRV (at different concentrations of PPRV). At 1µg/well concentration, phage clones 4, 8 and 9 showed higher P/N ratio than that of polyclonal sera against PPRV collected from a strong positive case. The phage clone 12 was having lower P/N ratio than that of polyclonal sera. At 0.5µg/well concentration, phage 9 and 8 showed same level whereas phage 4 and 12 showed lower level of P/N as compared to that of the polyclonal sera. At lower concentrations the ratio became equal for all 4 phage clones with polyclonal sera.

All 12 peptides were synthesised in linear format and subjected to ELISA to observe whether the same pattern of affinity is seen in virus capture ELISA as that of phage-ELISA. The results indicated that none of the peptides (including 4, 8, 9 or 12) showed significant reactivity with PPRV. It may be due to loss of conformation or improper orientation of linear peptide during coating as a result of binding to the plate surface, which may result in their reduced affinity towards PPRV.

As the peptide sequences are expressed in pentavalent form in phage, it is possible that single linear sequence of peptide is not able to bind to the target virus with that much

strength, resulting into decrease in its reactivity. To overcome this difference in valency, 4 armed-MAP format of selected peptide sequences (phage clones: 4, 8, 9 & 12) were synthesised and subjected to virus capture ELISA. Here we observed high reactivity of the MAP peptides with PPRV. This may be due to increased valency (avidity) in a single molecule. The high reactivity of multivalent branched peptides to the PPRV may be due to the presence of lysine residue in the MAP-core which binds to the plate surface via its hydrophobic domain. This enhances the projection of linked peptide sequences and maintains the conformation and orientation of peptide sequences even after coating. Peptide captured PPRV was further confirmed by RT-PCR.

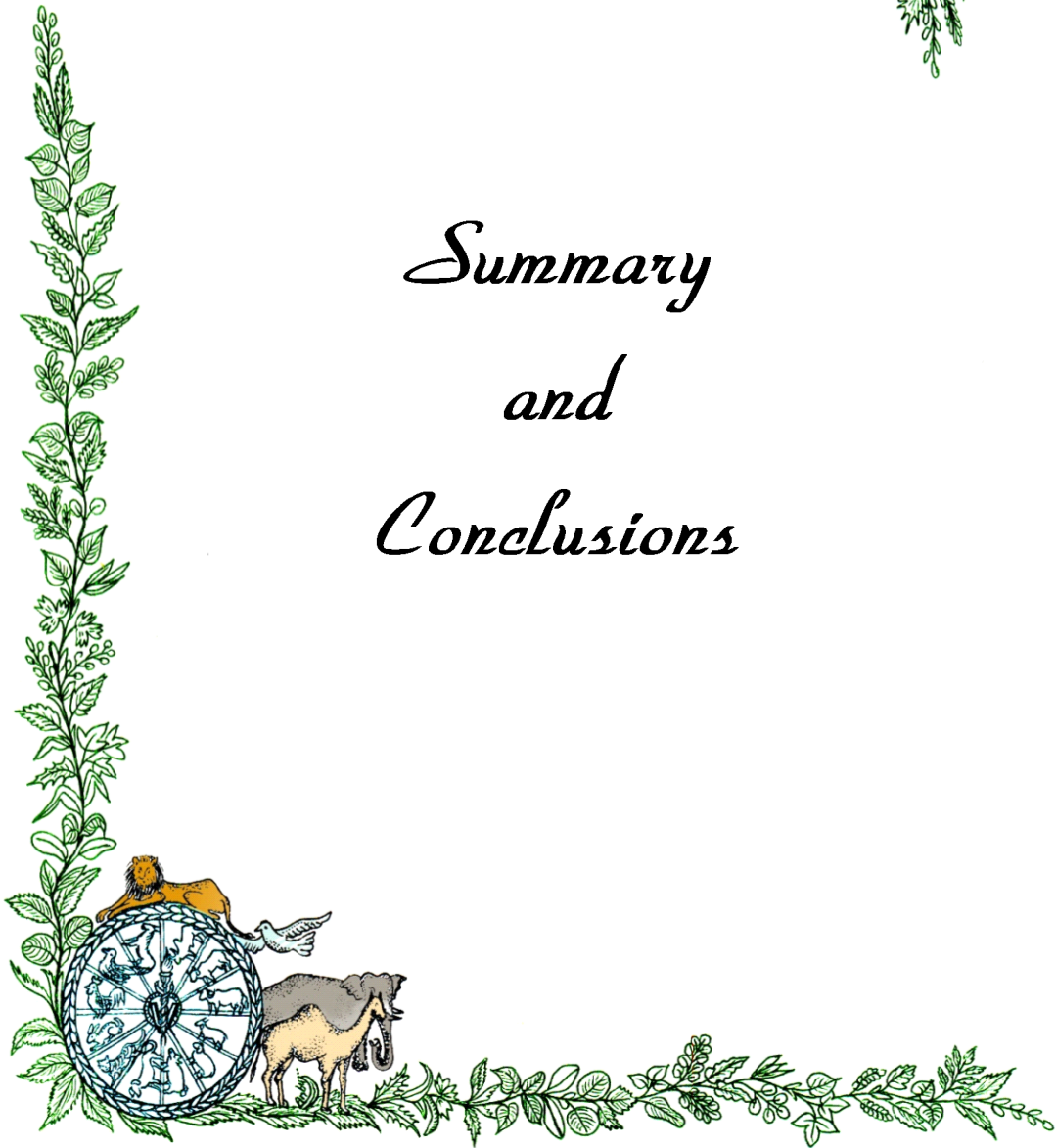
The secondary structures of all linear peptides and MAP format of peptide 4, 8, 9 & 12 of peptides were determined by circular dichroism study using polar and apolar solvents. C.D. results showed that all the peptides contain high percentage of beta structures. As beta structures are found to be involved in epitope-paratope binding, it supports our hypothesis that selected peptides are supposed to mimic the paratopes of PPRV.

The gold nanoparticles (20nm size) were activated with MAP peptides. The conjugation was confirmed by UV-Vis spectrophotometry where a red shift of  $\lambda_{\max}$  was observed. On addition of PPRV there was visual plasmon change due to networking of MAP conjugated AuNPs and virus particles, leading to change in the colour of AuNPs suspension (red to purple). Thus these peptides can be used to develop novel rapid visual tests for detection of any target. These MAP conjugated AuNPs can be used for quantification of PPRV, as it has also been observed earlier in case of NDV (Sajjanar B., 2015).





*Summary  
and  
Conclusions*



The purpose of current study was to give a proof of concept that synthetic peptides derived from the phage display technology can be used to develop novel diagnostic reagents. For this we took PPRV as our model of study. Sungri strain of PPRV was propagated in Vero cells and the virus was purified by sucrose gradient ultra-centrifugation and resuspended in PBS. The concentration of resuspended PPRV was determined by Bradford assay.

The PPR virus was used as an immobilized target in a biopanning process using a 12-mer phage display random peptide library. After five rounds of panning, which also involved one step of subtractive panning; forty phage colonies were picked and amplified. The DNA was isolated and PCR amplified followed by sequencing. The random amino acid sequences which were being expressed on the surface of phage clones were deduced by DNA star Lasergene software. A total of 12 different sequences were retrieved from the 40 phage DNA sequenced.

Phage-ELISA was performed using 12 phage clones in order to select those phage clones which were showing specific affinity to PPRV. Results indicated that four phage (4, 8, 9 & 12) were having specific reactivity for PPRV, while rest of the phage clones were showing non-specific binding with BSA as well. This could be due to the fact, that BSA was used for blocking in biopanning steps and there may be chances that phages having affinity to BSA also got selected in successive rounds of panning. Only PPRV specific phage clones (i.e, No. 4, 8, 9 & 12) were used for further study as they were again subjected to phage-ELISA to be compared with direct antibody mediated ELISA. Results indicated that at 1 µg/well concentration phage 4, 8 and 9 and at 0.5 µg/well concentration phage 8 & 9 had had P/N ratio more than

that of polyclonal sera whereas, at lower concentrations, it tend to be equal to that of the polyclonal sera.

All the random peptide sequences expressed by the 12 clones were synthesised in monovalent linear format using solid phase peptide synthesis protocols using F-moc chemistry. These peptides were cleaved and purified using semi-preparatory RP-HPLC. All the peptides were hydrophobic in nature and so eluted at higher percentage of non-polar solvent i.e, 80-90%ACN in water. The purity of peptides were then analysed in analytical RP-HPLC in an isocratic manner using 80% ACN in water as solvent. The peaks were collected from the analytical RP-HPLC and their (P4, P8, P9 & P12) respective molecular weights were confirmed by MALDI-TOF. Peptide ELISA results indicated no significant affinity of monovalent linear peptides with PPRV, which may be attributed to the poor coating efficiency of the linear peptides or change in their conformation while binding to ELISA-plate surface or lower valency as compared to that of pentavalent binding sites of phage.

4 armed-MAP format of random peptides expressed by selected phage clones i.e, phage clone number 4, 8, 9 and 12 were synthesized in order to mimic the pentavalent binding site of phage using solid phage peptide synthesis. MAP-core was having cysteine residue at C-terminal end and lysine residues which provided it the hydrophobic mosaic. In MAP-ELISA, MAP-peptides show high reactivity with PPRV. This may be due to the increased valency and/or proper projection of peptides. The virus captured by MAP peptides was confirmed by RT-PCR.

The MAP peptides were also conjugated with AuNPs and the conjugation was confirmed by red shift in  $\lambda_{\max}$  in UV-Vis spectrophotometry. The colour of MAP-conjugated AuNPs turned wine red to purple on addition of PPRV, which may be due to the binding of MAPs to virus particles leading to change in surface plasmon.

The secondary structure analysis of all the linear peptides and selected (4, 8, 9 and 12) MAP peptides were performed by circular dichroism. All the peptides were having  $\beta$ -structures in high percentage. Generally beta structures are involved in epitope-paratope binding. It indicated that these  $\beta$ -structures may be responsible for binding of our peptides to PPRV.

This study concludes that, phage display technology can be used to identify phage clones and subsequently peptide sequences that are capable of binding to a specific target. This approach may be helpful in development of novel simple diagnostic reagents, which would lack inter- as well as intra-assay variations and would not require tedious steps like nucleic acid isolation of pathogen for diagnosis.





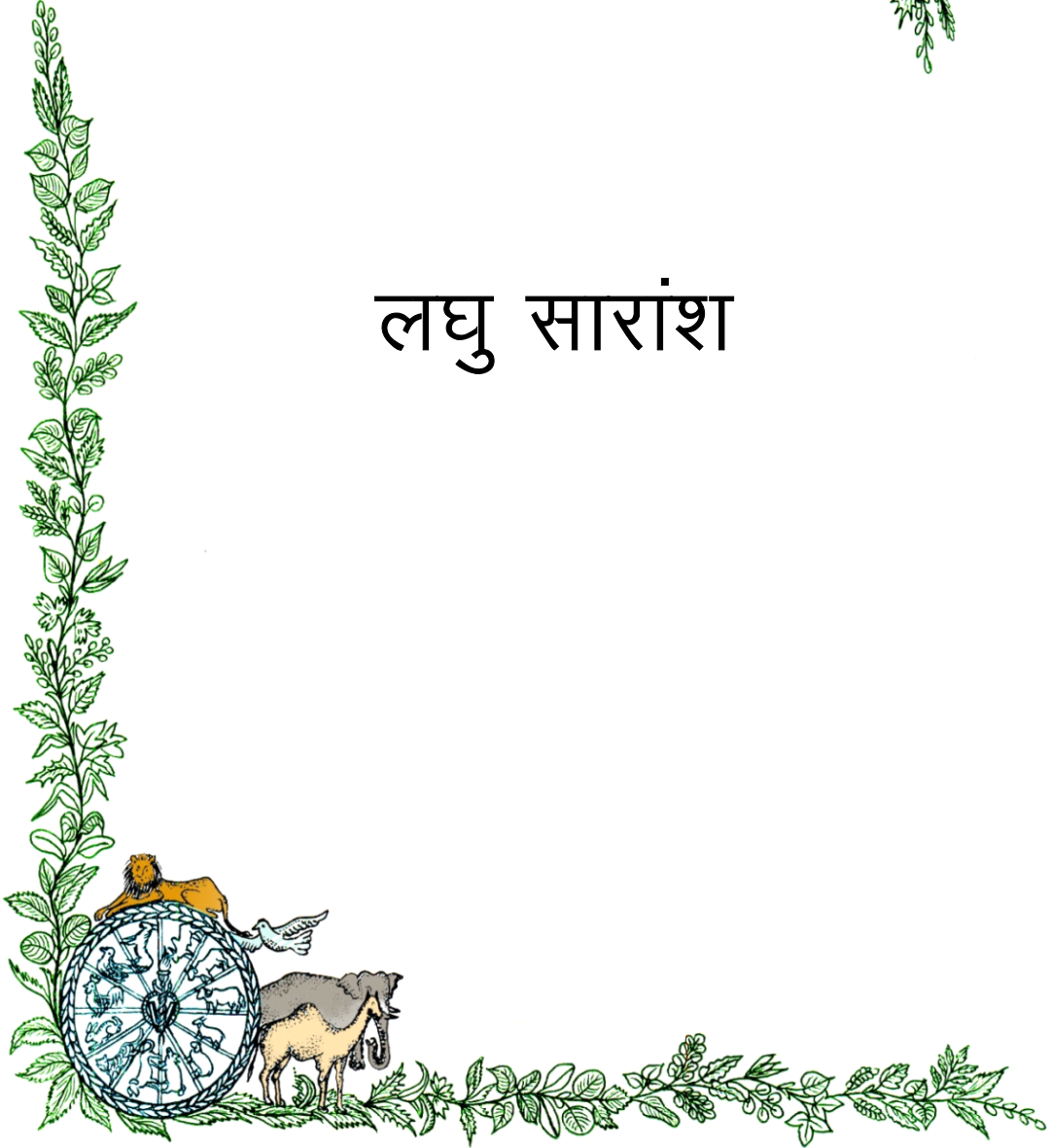
*Mini Abstract*



Phage display is a powerful tool for selecting novel peptides and antibodies that can bind with a wide range of targets, involving whole cells, protein as well as lipid targets. Using this technology many small peptide ligands and antibodies have been identified, which have tendency to bind with targeted receptors for a wide range of applications. In the present study, using phage display technology we identified and characterised the peptides that bind with PPR virus. PPR virus had been taken as the model of our study because this disease is widely prevalent in India and small ruminant rearing practice faces a very serious hurdle due to challenges posed by frequent incidences of PPR. The PPR virus was used as an immobilized target in a biopanning process using a 12-mer phage display random peptide library. After five rounds of panning, forty colonies were picked and amplified followed by DNA isolation and amplification for sequencing. Sequencing suggested 12 different clones expressing different peptide sequence Phage-ELISA was performed using all 12 phage clones. Results indicated that four phage clones i.e, P4, P8, P9 and P12 had a specific binding activity to PPR virus. The ratio of O.D. value at 450 nm of positive wells with respect to negative control wells was depicted by P/N ratio. At 0.5 µg/well concentration, P/N ratio for phage 8 and 9 was more but at lower concentrations, it gradually decreased and become equal to that of polyclonal sera of PPRV. Linear peptides (P4, P8, P9 and P12) were synthesized using solid phase peptide synthesis and subjected to virus capture ELISA. No significant binding of the peptides with PPRV was evident which may be attributed to poor coating efficiency of monovalent linear peptides. When MAP-formats of same peptides were used in virus capture ELISA, the results indicated binding of PPRV to the MAP formats of same peptide sequence. It may be due to increased valency of peptide sequence in 4-armed MAP or due to proper projection of peptides in MAP-format while coating. The captured PPRV was confirmed by RT-PCR. MAP-peptides were also conjugated on AuNPs. When in these MAP-conjugated AuNPs, PPRV was added, their colour changed from wine red to purple. This colour change may be due to networking of PPRV with MAP-conjugated AuNPs resulting in visual Plasmon change. All these results support the hypothesis that peptides identified through Phage display technology are capable of binding to a specific target and by doing some minor modifications in them they may be used to develop novel and simple diagnostic reagents.



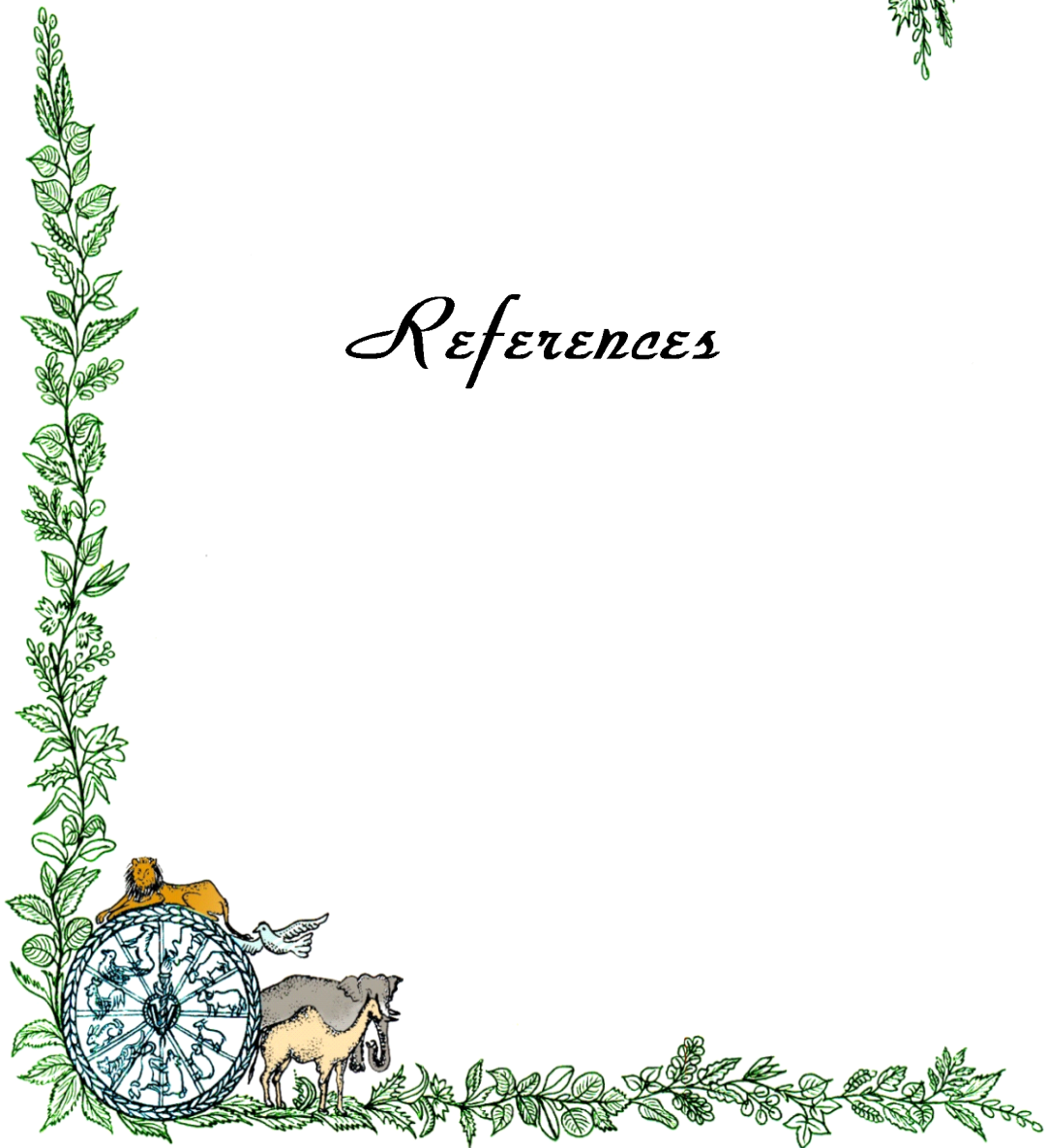
# लघु सारांश



फेज डिसप्ले किसी भी लक्ष्य विशेष से अभिरुचि रखने वाले पेप्टाइड्स व एन्टीबॉडी के चयन के लिए एक शक्तिशाली उपकरण है। इसके लक्ष्यों की विस्तृत श्रृंखला में कोशिका, प्रोटीन तथा वसा कण शामिल किए जा सकते हैं। इस तकनीक के उपयोग द्वारा कई नवीन लीगेन्ड तथा एन्टीबॉडीज की पहचान की गई है, जो किसी लक्ष्य रिसेप्टर से बंधकर विभिन्न कार्यों को सम्पूर्ण कराते है। प्रस्तुत कार्य में, इस तकनीक का उपयोग कर हमने पीपीआर वायरस के प्रति रुचि रखने वाले पेप्टाइड्स की पहचान व जाँच की। यहाँ पर पीपीआर वायरस का नमूना लिया गया है। क्योंकि यह रोग भारत में व्यापक रूप से पाया जाता है तथा इससे उत्पन्न चुनौतियां छोटे जुगाली पशु पालने वाले किसानों के लिए गम्भीर बाधा उत्पन्न करती हैं। पीपीआर वायरस को स्थिर लक्ष्य बनाकर उसके साथ 12-मर फेज लाइब्रेरी से बायोपैनिंग की गई। 5 बार बायोपैनिंग दोहराने के बाद चालीस कॉलोनी उठाई गई तथा डीएनए निकालकर सीक्वेन्सिंग कराई गई। इससे हमे भिन्न पेप्टाइड्स को प्रकट करने वाले 12 फेज क्लोन्स के बारे में सूचना प्राप्त हुई। इन 12 फेज क्लोन्स को लेकर ऐलीसा लगाया गया, जिसके परिणाम में इंगित किया कि चार फेज क्लोन्स अर्थात् **P4, P8, P9** तथा **P12** विशेष रूप से पीपीआर वायरस से बंधने की संक्रियता रखते हैं। पोजिटिव वेल तथा निगेटिव वेल की 450nm पर ओडी के अनुपात को **P/N** रेशियों के द्वारा दर्शाया गया। 0.5  $\mu\text{g/well}$  सांद्रता पर फेज क्लोन्स 8 व 9 के लिए **P/N** रेशियों पोलिक्लोनल सीरा की तुलना में अधिक था। परन्तु सांद्रता के कम करने पर यह कम होता गया तथा पोलिक्लोनल सीरा के बराबर हो गया। सोलिड फेज पेपटाइड सिन्थैसिस द्वारा रैखिक (लीनियर) पेप्टाइड्स **P4, P8, P9** व **P12** बनाये गये तथा इन्हें वायरस कैप्सर एलीसा में उपयोग किया गया। किसी भी प्रकार की बाइंडिंग के प्रमाण नहीं मिले। इसका कारण रैखिक पेप्टाइड्स की खराब कोटिंग क्षमता हो सकता है। जब इन्हीं पेप्टाइड्स के मैप प्रारूप को वायरस कैप्सर एलीसा में उपयोग में लाया गया तो परिणामों ने पीपीआर वायरस तथा मैप की बाइंडिंग को दर्शाया। इसका कारण पेप्टाइड की 4 भुजीय मैप में बड़ी हुई संयोजकता अथवा उचित प्रकट होना हो सकता है। कैप्सरड वायरस का आरटी-पीसीआर द्वारा पुष्टिकरण किया गया। मैप पेप्टाइड्स को स्वर्ण नैनों कण में संयुग्मित किया गया। जब इन मैप संयुग्मित स्वर्ण नैनों कण में पीपीआर वायरस संकलित किया गया तो विलियन का रंग लाल से बैंगनी हो गया। इसका कारण पीपीआर वायरस तथा मैप संयुग्मित स्वर्ण नैनों कण के बीच नेटवर्किंग होना तथा फलस्वरूप विजुअल प्लाजमोन्चेन्ज होना हो सकता है। ये सभी परिणाम इस परिकल्पना को आधार प्रदान करते हैं कि फेस डिसप्ले तकनीक से पहचाने गए पेप्टाइड्स किसी विशेष लक्ष्य से बाइंड होने की क्षमता रखते हैं तथा कुछ सूक्ष्म परिवर्तन करने पर नवीन व सरल नैदानिक अभिकर्मकों के निर्माण में सहायक हो सकता है।



# *References*



- Abu Elzein, E. M. E., M. M. Hassanien, A. I. Alafaleq, M. A. Abdel Hadi, and F. M. T. Housawi, 1990. Isolation of PPR virus from goats in Saudi Arabia. *Vet Rec*, **127**: 309-310.
- Alban S.M., de Moura J.F., Soccol V.T., Sékula S.B, Alvarenga L.M., Mira M.T., Olortegui C, Minozzo J.C. 2014. Phage Display and Synthetic Peptides as Promising Biotechnological Tools for the Serological Diagnosis of Leprosy. *Plos one*, **9**(8): e106222.
- Anderson J., Mckay J. A. 1994. The detection of antibodies against peste des petits ruminants virus in cattle, sheep and goats and the possible implications to rinderpest control programmes. *Epidemiol Infect*, **112**(1): 225-31.
- Arap W., Haedicke W., Bernasconi M., Kain R., Rajotte D., Krajewski S., Ellerby HM., Bredesen D.E., Pasqualini R and Ruoslahti E. 2002. Targeting the prostate for destruction through a vascular address. *Proc Natl Acad Sci USA*, **99**: 1527-1531.
- Augustine-Rauch K.A., Zhang Q.J., Leonard J.L., Chadderton A., Welsh M.J., Rami H.K., Thompson M., Gaster L and Wier P.J. 2004. Evidence for a molecular mechanism of teratogenicity of SB-236057, a 5-HT1B receptor inverse agonist that alters axial formation. *Birth Defects Res. A Clin Mol Teratol*, **70**: 789-807.
- Bai Fengwei, Town Terrence , Pradhan Deepti , Cox Jonathan, Ashish, Ledizet Michel , Anderson J.F. , Flavell R.A. , Krueger J.K. , Koski R.A. and Fikrig Erol. 2007. Antiviral Peptides Targeting the West Nile Virus Envelope Protein. *J Virol*, **81**(4): 2047-2055.

- Bailey D., Banyard A., Dash P., Ozkul A. and Barrett T. 2005. Full genome sequence of peste des petits ruminants virus, a member of the Morbillivirus genus. *Virus Research*, **110**: 119-124.
- Balamurugan V., Sen A., Venkatesan G., Yadav V., Bhanot V., Riyesh T., Bhanuprakash V. and Singh R.K. 2010. Sequence and phylogenetic analyses of the structural genes of virulent isolates and vaccine strains of peste des petits ruminants virus from India. *Transbound Emerg Dis*, **57**: 352-364.
- Balamurugan V., Sen A., Venkatesan G., Bhanot V., Yadav V., Bhanuprakash V. and Singh R.K. 2012. Peste des petits ruminants virus detected in tissues from an Asiatic lion (*Panthera leo persica*) belongs to Asian lineage IV. *J Vet Sci*, **13**: 203-206.
- Bandyopadhyay S.K. 2002. The economic appraisal of PPR control in India. In: 14th Annual Conference and National Seminar on Management of Viral Diseases with Emphasis on Global Trade and WTO Regime. Indian Virological Society, New Delhi, India.
- Banyard A.C., Parida S., Batten C., Oura C., Kwiatek O. and Libeau G. 2010. Global distribution of peste des petits ruminants virus and prospects for improved diagnosis and control. *J Gen Virol*, **91**: 2885-2897.
- Basha S., Rai P., Poon V., Saraph A., Gujraty K., Go MY., Sadacharan S., Frost M., Mogridge J and Kane RS. 2006. Polyvalent inhibitors of anthrax toxin that target host receptors. *Proc Natl Acad Sci USA*, **103**: 13509-13.
- Baron M.D., Parida S. and Oura C.A. 2011. Peste des petits ruminants: a suitable candidate for eradication? *Veterinary Record*, **169**: 16-21.
- Barrett T, Banyard A.C., Diallo A. 2006. Molecular biology of the morbilliviruses. In: Thomas B, Paul-Pierre P, William PT, editors. *Rinderpest and Peste des Petits Ruminants*. Oxford: Academic Press. 31-67.
- Bazarghani T.T., Charkhkar S., Doroudi J. and Bani Hassan E. 2006. A review on peste des petits ruminants (PPR) with special reference to PPR in Iran. *J Vet Med, Series B* **53** (Suppl 1): 17-18.
- Benhar I. 2001. Biotechnological applications of phage and cell display. *Biotechnol Adv*, **19**: 1-33.
- Berggard T., Linse S., James P. 2007. Methods for the detection and analysis of protein-protein interactions. *Proteomics*, **7**: 2833-42.

- Bonetto S., Carlván I and Baty D. 2005. Isolation and characterization of antagonist and agonist peptides to the human melanocortin 1 receptor. *Peptides*, **26**: 2302-13.
- Boxer E.L., Nanda S.K. and Baron M.D. 2009. The rinderpest virus non-structural C protein blocks the induction of type 1 interferon. *Virology*, **385**: 134-142.
- Bradbury A.R. 2010. The use of phage display in neurobiology. *Curr. Protoc. Neurosci.* Chapter **5**: Unit 5.12.
- Bratkovic T. 2010. Progress in phage display: evolution of the technique and its applications. *Cell Mol Life Sci*, **67**:749-67.
- Bundza A., Afshar A., Dukes T.W., Myers D.J., Dulac G.C. and Becker S.A. 1988. Experimental peste des petits ruminants (goat plague) in goats and sheep. *Canad J Vet Res*, **52**: 46-52.
- Cardinale A and Biocca S. 2008. The potential of intracellular antibodies for therapeutic targeting of protein-misfolding diseases. *Trends Mol Med*, **14**:373-80.
- Carnazza S, Foti C, Gioffre G, Felici F, Guglielmino S. 2008. Specific and selective probes for *Pseudomonas aeruginosa* from phage-displayed random peptide libraries. *Biosens Bioelectron*, **23**: 1137-1144.
- Das S.C., Baron M.D. and Barrett T. 2000. Recovery and characterization of a chimeric rinderpest virus with the glycoproteins of peste des petits ruminants virus: homologous F and H proteins are required for virus viability. *J Virol*, **74**: 9039-9047.
- Deutscher Susan L. 2010. Phage Display in Molecular Imaging and Diagnosis of Cancer. *Chem Rev*, **110**(5): 3196-3211.
- Dhar P., Sreenivasa B.P., Barrett T., Corteyn M., Singh R.P. and Bandyopadhyay S.K. 2002. Recent epidemiology of peste des petits ruminants virus (PPRV). *Vet Microbiol*, **88**: 153-159.
- Diallo A., Barrett T., Barbron M., Meyer G and Lefevre P. C. 1994. Cloning of the nucleocapsid protein gene of peste des petits ruminants virus: relationship to other morbilliviruses. *J Gen Virol*, **75**: 233-237.
- Diallo A., Barrett T., Lefevre P.C. and Taylor W.P. 1987. Comparison of proteins induced in cells infected with rinderpest and peste des petits ruminants viruses. *J Gen Virol*, **68**: 2033-2038.

- Diallo A., Minet C., Le Goff C., Berhe G., Albina E., Libeau G. and Barrett T. 2007. The threat of peste des petits ruminants: progress in vaccine development for disease control. *Vaccine*, **25**: 5591-5597.
- Diamond SL. 2007. Methods for mapping protease specificity. *Curr Opin Chem Biol*, **11**: 46-51.
- Dighe V. 2014. Identification and characterization of brain and testes homing peptides using phage display library. Thesis, PhD. Deemed University, Indian Veterinary Research Institute, Izatnagar, India. 169 p.
- Durojaiye O.A., Taylor W.P. and Smale C. 1985. The ultrastructure of peste des petits ruminants virus. *Zentralblatt Fur Veterinarmedizin Reihe, B* **32**: 460-465.
- Efimov V.P., Nepluev I.V., Mesyanzhinov V.V. 1995. Bacteriophage T4 as a surface display vector. *Virus genes*, **10**: 173-177.
- Evans E.R., Sutton J.M., Gravett A and Shone C.C. 2005. Analysis of the substrate recognition domain determinants of botulinum type B toxin using phage display. *Toxicon*, **46**: 446-53.
- Ezeokoli C.D., Umoh J.U., Chineme C.N., Isitor G.N. and Gyang E.O. 1986. Clinical and epidemiological features of peste des petits ruminants in Sokoto Red goats. *Revue d'élevage et de médecine vétérinaire des pays tropicaux*, **39**: 269-273.
- Fack F., Hügle-Dörr B., Song D., Queitsch I., Petersen G and Bautz E.K. 1997. Epitope mapping by phage display: random versus gene-fragment libraries. *J Immunol Methods*, **206**: 43-52.
- Flanagan E.B., Ball L.A. and Wertz G.W. 2000. Moving the glycoprotein gene of vesicular stomatitis virus to promoter-proximal positions accelerates and enhances the protective immune response. *J Virol*, **74**: 7895-7902.
- Förster-Waldl E., Riemer A.B., Dehof A.K., Neumann D., Brämwig K., Boltz-Nitulescu G., Pehamberger H., Zielinski C.C., Scheiner O., Pollak A., Lode H and Jensen-Jarolim E. 2005. Isolation and structural analysis of peptide mimotopes for the disialoganglioside GD2, a neuroblastoma tumor antigen. *Mol Immunol*, **42**(3): 319-25.
- Fuh G., Pisabarro M.T., Li Y., Quan C., Lasky L.A. and Sidhu S.S. 2000. Analysis of PDZ domain-ligand interactions using carboxyl-terminal phage display. *J Biol Chem*, **275**: 21486-91.

- Gargadennec L. and Lalanne A. 1942. La Peste des petits ruminants. Bulletin des services zootechniques et des epizooties de l' Afrique Occidentale Francaise, **5**: 15-21.
- Gilbert Y. and Monnier J. 1962. Adaptation du virus de la peste des petits ruminants aux cultures cellulaires. Revue d'élevage et de médecine vétérinaire des pays tropicaux, **15**: 321.
- Greenwood J., Hunter GJ and Perham R.N. 1991. Regulation of filamentous bacteriophage length by modification of electrostatic interactions between coat protein and DNA. J Mol Biol, **217**: 223-227.
- Gujraty K., Sadacharan S., Frost M., Poon V., Kane R.S. and Mogridge J. 2005. Functional characterization of peptide-based anthrax toxin inhibitors. Mol Pharm, **2**: 367-72.
- Hall P.R., Hjelle B., Brown D.C., Ye C., Bondu-Hawkins V., Kilpatrick K.A., Larson R.S. 2008. Multivalent presentation of antihantavirus peptides on nanoparticles enhances infection blockade. Antimicrob Agents Chemother, **52**(6): 2079-88.
- Hall P.R., Hjelle B., Njus H., Ye C., Bondu-Hawkins V., Brown D.C., Kilpatrick K.A., Larson R.S. 2009. Phage display selection of cyclic peptides that inhibit Andes virus infection. J Virol, **83**(17): 8965-8969.
- Hamdy F.M., Dardiri A.H., Nduaka O., Breese S.R.J. and Ihemelandu E.C. 1976. Etiology of the stomatitis pneumocentritis complex in Nigerian dwarf goats. Canad J Comp Med, **40**: 276-284.
- Hegde R., Gomes A. R., Gowda S. M. B., Santhosh A. K and Renukprasad C. 2009. Cytopathic effect of PPR vaccine virus strains in Vero cells. Vet World, **2**(3): 93-94.
- Hong H.W., Lee S.W., Myung H. 2010. Selection of peptides binding to HCV e2 and inhibiting viral infectivity. J Microbiol Biotechnol, **20**(12): 1769-1771.
- Hoogenboom H. 2005. Selecting and screening recombinant antibody libraries. Nature Biotechnology, **23**: 1105-1116.
- Huang J.X., Bishop-Hurley S.L., Cooper M.A. 2012. Development of anti-infectives using phage display: biological agents against bacteria, viruses, and parasites. Antimicrob Agents Chemother, **56**(9): 4569-82.
- Huang W., Zhang Z, Palzkill T. 2000. Design of potent beta-lactamase inhibitors by phage display of beta-lactamase inhibitory protein. J Biol Chem, **275**: 14964 -14968.

- James K.J., Hancock M.A., Gagnon J.N. and Coulton J.W. 2009. TonB Interacts with BtuF, the *Escherichia coli* periplasmic binding protein for cyanocobalamin. *Biochemistry*, **48**: 9212-20.
- Janka Bábířková, Ľubomíra Tóthová, Peter Boor, Peter Celec. 2013. In vivo phage display- A discovery tool in molecular biomedicine. *Biotechnology Advances* **31**: 1247-1259.
- Johansson K., Bourhis J.M., Campanacci V., Cambillau C., Canard B. and Longhi S. 2003. Crystal structure of the measles virus phosphoprotein domain responsible for the induced folding of the C-terminal domain of the nucleoprotein. *J Biol Chem*, **278**, **44**: 567-573.
- Ke Liu., Xiuli Feng., Zhiyong Ma, Chao Luo, Bin Zhou, Ruibing Cao, Li Huang, Denian Miao, Ran Pang, Danni He, Xue Lian, Puyan Chen. 2012. Antiviral activity of phage display selected peptides against Porcine reproductive and respiratory syndrome virus in vitro. *Virology*, **432**: 73-80.
- Kehoe J.W. and Kay B.K. 2005. Filamentous phage display in the new millennium. *Chem Rev*, **105**: 4056-72.
- Knittelfelder R., Riemer A.B. and Jensen-Jarolim E. 2009. Mimotope vaccination-from allergy to cancer. *Expert Opin Biol Ther*, **9**: 493-506.
- Koivunen E., Arap W., Valtanen H., Rainisalo A., Medina O.P., Heikkilä P., Kantor C., Gahmberg C.G., Salo T., Konttinen Y.T., Sorsa T., Ruoslahti E. and Pasqualini R. 1999. Tumor targeting with a selective gelatinase inhibitor. *Nat. Biotechnol*, **17**: 768-774.
- Kolonin, M.G., Pasqualini R and Arap W. 2002. Teratogenicity induced by targeting a placental immunoglobulin transporter. *Proc Natl Acad Sci USA*, **90**: 13055-13060
- Kolonin M.G., Saha P.K., Chan L., Pasqualini R and Arap W. 2004. Reversal of obesity by targeted ablation of adipose tissue. *Nat Med*, **10**: 625-632.
- Koolpe M., Burgess R., Dail M. and Pasquale E.B. 2005. EphB receptor-binding peptides identified by phage display enable design of an antagonist with ephrin-like affinity. *J Biol Chem*, **280**: 17301-11.
- Kumar N., Maherchandani S., Kashyap S.K., Singh S.V., Sharma S., Chaubey K.K., Hinh Ly. 2014. Peste des petits ruminants Virus Infection of Small Ruminants: A Comprehensive Review. *Viruses*, **6**:2287-2327.

- Kwiatek O., Minet C., Grillet C., Hurard C., Carlsson E., Karimov B., Albina E., Diallo, A. and Libeau, G. 2007. Peste des petits ruminants (PPR) outbreak in Tajikistan. *J Comp Pathol*, **136**: 111-119.
- Kwiatek O., Ali Y.H., Saeed, I.K., Khalafalla, A.I., Mohamed, O.I., Obeida, A.A., Abdelrahman, M.B., Osman, H.M., Taha, K.M., Abbas, Z., El Harrak, M., Lhor, Y., Diallo, A., Lancelot, R., Albina, E. and Libeau, G. 2011. Asian lineage of peste des petits ruminants virus, Africa. *Emerg Infec Dis*, **17**: 1223-1231.
- Lefevre P.C. and Diallo, A. 1990. Peste des petits ruminants. *Revue Scientifique et Technique*, **9**: 935-981.
- Lefevre P. C.; Diallo A., Schenkel F., Hussein S. and Staak G. 1991. Serological evidence of peste des petits ruminants in Jordan. *Vet Rec*. **128**: 110.
- Li W, Jin H, Sui X, Zhao Z, Yang C, Wang W., Li J, Li G. 2014. Self-Assembly and Release of Peste des Petits Ruminants Virus-Like Particles in an Insect Cell-Baculovirus System and Their Immunogenicity in Mice and Goats. *PLoS ONE* **9**(8): e10479.
- Libeau G., Diallo, A., Colas F. and Guerre, L. 1994. Rapid differential diagnosis of rinderpest and peste des petits ruminants using an immunocapture ELISA. *Veterinary Record*, **134**: 300-304.
- Libeau G., Prehaud C., Lancelot R., Colas F., Guerre L., Bishop D.H. and Diallo A. 1995. Development of a competitive ELISA for detecting antibodies to the peste des petits ruminants virus using a recombinant nucleoprotein. *Res Vet Sci*, **58**: 50-55.
- Mahapatra M., Parida S., Egziabher B.G., Diallo A. and Barrett T. 2003. Sequence analysis of the phosphoprotein gene of peste des petits ruminants (PPR) virus: editing of the gene transcript. *Virus Research*, **96**: 85-98.
- Matthews D.J. and Wells J.A. 1993. Substrate phage: selection of protease substrates by monovalent phage display. *Science*, **260**: 1113-7.
- Mayrose I., Shlomi T., Rubinstein N.D., Gershoni JM., Ruppin E., Sharan R., and Pupko T, 2007. Epitope mapping using combinatorial phage-display libraries: a graph-based algorithm. *Nucleic Acids Res*, **35**: 69-78.
- Merrifield R.B. 1963. Solid phase peptide synthesis. Synthesis of a tetrapeptide. *J Am Chem Soc*, **85**: 2149-2154.

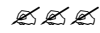
- Meyer G. and Diallo A. 1995. The nucleotide sequence of the fusion protein gene of the peste des petits ruminants virus: the long untranslated region in the 5'-end of the F-protein gene of morbilliviruses seems to be specific to each virus. *Virus Research*, **37**: 23-35.
- Mielke A., Roubíček T. 2003. A Rate-Independent Model for Inelastic Behavior of Shape-Memory Alloys. *Multiscale Model Simul*, **1**(4): 571-597.
- Molinkova D., Skladal P and Celer V. 2008. In vitro neutralization of equid herpesvirus 1 mediated by recombinant antibodies. *J Immunol Methods*, **333**: 186-91.
- Mullaney B.P., Pallavicini M.G., Marks J.D. 2001. Epitope mapping of neutralizing botulinum neurotoxin A antibodies by phage display. *Infect Immun.*, **69**(10):6511-4.
- Munir M., Abubakar M., Zohari S. and Berg M. 2012. Serodiagnosis of Peste des Petits Ruminants Virus. In: Al-Moslih, M. (ed.) *Serological Diagnosis of Certain Human, Animal and Plant Diseases*. InTech, Croatia, pp. 37-58.
- Munir M., Zohari S. and Berg M. 2013. Current advances in molecular diagnosis and vaccines for peste des petits ruminants. In: Munir, M., Zohari, S. and Berg, M. (eds) *Molecular Biology and Pathogenesis of Peste des Petits Ruminants Virus*. Springer, Berlin, Germany, pp. **105**-133.
- Muthuchelvan D., Sanyal A., Singh R.P., Hemadri D., Sen A., Sreenivasa B.P., Singh R.K. and Bandyopadhyay S.K. 2005. Comparative sequence analysis of the large polymerase protein (L) gene of peste-des-petits ruminants (PPR) vaccine virus of Indian origin. *Archive of Virology*, **150**: 2467-2481.
- Nanda Y.P., Chatterjee A., Purohit A.K., Diallo A., Innui K., Sharma R.N., Libeau G., Thevasagayam J.A., Bruning A., Kitching R.P., Anderson J., Barrett T. and Taylor W.P. 1996. The isolation of peste des petits ruminants virus from northern India. *Vet Microbiol*, **51**: 207-216.
- Naz R.K. Status of contraceptive vaccines. *Am J Reprod Immunol*, 2009; 61: 11-18.
- Ozawa Makoto, Ohashi Kazuhiko and Onuma Misao 2005. Identification and Characterization of peptides binding to Newcastle disease virus by phage display. *J. Vet. Med. Sci.*, **67**(12): 1237-1241.
- Pasqualini R and Ruoslahti E. 1996. Organ targeting in vivo using phage display peptide libraries. *Nature*, **380**: 364-366.

- Philibert P., Stoessel A., Wang W., Sibling AP., Bec N., Larroque C., Saven J.G., Courtete J., Weiss E and Martineau PA. 2007. focused antibody library for selecting scFvs expressed at high levels in the cytoplasm. *BMC Biotechnol*, **7**: 81.
- Renukaradhya G.J., Sinnathamby G., Seth S., Rajasekhar M. and Shaila M.S. 2002. Mapping of B-cell epitopic sites and delineation of functional domains on the hemagglutinin-neuraminidase protein of peste des petits ruminants virus. *Virus Research*, **90**: 171-185.
- Russel M. 1991. Filamentous phage assembly. *Mol Microbiol*, **5**: 1607-1613.
- Sajjanar B., Kakodia B., Bisht D., Saxena S., Singh A.K., Tiwari A.K., Kumar S. 2015. Peptide activated gold nanoparticles for selective visual sensing of virus. *J Nanopart Res*, **17**: 234.
- Saliki J.T., G Libeau J.A. House C.A. Mebus and E.J. Dubovi. 1993. Monoclonal antibody based blocking ELISA for specific detection and titration of PPR virus antibody in caprine and ovine sera. *J. Clin. Microb*, **31**(5): 1075- 1082.
- Saliki J.T., House J.A., Mebus C.A. and Dubovi E.J. 1994. Comparison of monoclonal antibody-based sandwich enzyme-linked immunosorbent assay and virus isolation for detection of peste des petits ruminants virus in goat tissues and secretions. *J Clin Microbiol*, **32**: 1349-1353.
- Scott J.K. and Smith GP. 1990. Searching for peptide ligands with an epitope library. *Science*, **249**: 386-390.
- Servan De Almeida, R., Keita, D., Libeau, G. and Albina, E. 2007. Control of ruminant morbillivirus replication by small interfering RNA. *J Gen Virol*, **88**: 2307-2311.
- Seth S. and Shaila M.S. 2001. The hemagglutinin-neuraminidase protein of peste des petits ruminants virus is biologically active when transiently expressed in mammalian cells. *Virus Research*, **75**: 169-177.
- Shaila M.S., Shamaki D., Forsyth M.A., Diallo A., Goatley L., Kitching R.P. and Barrett T. 1996. Geographic distribution and epidemiology of peste des petits ruminants virus. *Virus Research*, **43**: 149-153.
- Shaila M.S., Puroshottam V., Venugopal K and Venkatasan R.A. 1989. PPR of sheep in India. *Veterinary Record*, **125**: 602.

- Sidhu S.S., Bader G.D., Boone C. 2000. Functional genomics of intracellular peptide recognition domains with combinatorial biology methods. *Curr Opin Biotechnol*, **11**: 610-616.
- Sidhu S.S.; Fair brother W.J.; Deshayes K. 2003. Exploring protein-protein interactions with phage display. *Chembiochemistry*, **4**: 14-25.
- Singh R.P., Sreenivasa B.P., Dhar P., Shah L.C. and Bandopadhyay S.K. 2004. Development of monoclonal antibody based cELISA for detection and titration of antibodies to PPR virus. *Vet. Microbiol*, **98**:3-15.
- Smith G.P. 1985. Filamentous fusion phage: novel expression vectors that display cloned antigens on the virion surface. *Science*, **228**(4705): 1315-7.
- Smith G.P., Scott J.K. 1993. Libraries of peptides and proteins displayed on filamentous phage. *Methods Enzymol*, **217**: 228-57.
- Smith G.P. and Petrenko V.A. 1997. Phage Display. *Chem Rev*, **97**: 391-410.
- Sternberg N and Hoess RH. 1995. Display of peptides and proteins on the surface of bacteriophage lambda. *Proc Natl Acad Sci. U.S.A.*, **92**: 1609-1613.
- Taylor W.P. 1979. Protection of goats against peste-des-petits-ruminants with attenuated rinderpest virus. *Research in Veterinary Science*, **27**: 321-324.
- Taylor W.P. and Abegunde A. 1979. The isolation of peste des petits ruminants virus from Nigerian sheep and goats. *Research in Veterinary Science*, **26**: 94-96.
- Thombare N.N. and Sinha M.K. 2009. Economic implications of Peste des petits ruminants (PPR) disease in sheep and goats: a sample analysis of district Pune, Maharashtra. *Agri Economics Res Rev*, **22**: 319-322.
- Tober C., Seufert M., Schneider H., Billeter M.A., Johnston I.C., Niewiesk S., Ter Meulen V. and Schneider-Schaulie S., 1998. Expression of measles virus protein is associated with pathogenicity and control of viral RNA synthesis. *J Virol*, **72**: 8124-8132.
- Turnbough C.L., Jr. 2003. Discovery of phage display peptide ligands for species-specific detection of Bacillus spores. *J Microbiol Methods*, **53**: 263-271.
- Van Houten N.E., Zwick M.B., Menendez A. and Scott J.K. 2006. Filamentous phage as an immunogenic carrier to elicit focused antibody responses against a synthetic peptide. *Vaccine*, **24**: 4188-4200.

- Varsanyi T.M., Utter G. and Norrby E. 1984. Purification, morphology and antigenic characterization of measles virus envelope components. *J Gen Virol*, **65**: 355-366.
- Verhaert R.M., Beekwilder J., Olsthoorn R., Duin J and Quax W.J. 2002. Phage display selects for amylases with improved low pH starch-binding. *J Biotechnol*, **96**: 103-18.
- Welch B.D., Francis J.N., Redman J.S., Paul S., Weinstock M.T., Reeves J.D., Lie Y.S., Whitby F.G., Eckert D.M., Hill C.P., Root M.J., Kay M.S. 2010. Design of a potent D-peptide HIV-1 entry inhibitor with a strong barrier to resistance. *J Virol*, **84**(21): 11235-44.
- Woo P.C., Lau S.K., Wong B.H., Fan R.Y., Wong A.Y., Zhang A.J., Wu Y., Choi G.K., Li K.S., Hui J., Wang M., Zheng B.J., Chan K.H. and Yuen K.Y. 2012. Feline morbillivirus, a previously undescribed paramyxovirus associated with tubulointerstitial nephritis in domestic cats. *Proceedings of the National Academy of Sciences of the USA*, **109**: 5435-5440.
- Wu Dan, Li G., Qin C., Ren X. 2011. Phage Displayed Peptides to Avian H5N1 Virus Distinguished the Virus from Other Viruses. *PLoS ONE*, **6**(8): e23058.
- Yoneda M., Bandyopadhyay S.K., Shiotani M., Fujita K., Nuntaprasert A., Miura R., Baron M.D., Barrett T. and Kai C. 2002. Rinderpest virus H protein: role in determining host range in rabbits. *J Gen Virol*, **83**: 1457-1463.
- Yoneda M., Miura R., Barrett T., Tsukiyama-Kohara K. and Kai C. 2004. Rinderpest virus phosphoprotein gene is a major determinant of species-specific pathogenicity. *J Virol*, **78**: 6676-6681.
- Yu L.; Yu P.S.; Yee Yen Mui E.; McKelvie, J.C. Pham, T.P. Yap, Y.W. Wong, W.Q., Wu J., Deng W., Orner B.P. 2009. Phage display screening against a set of targets to establish peptide-based sugar mimetics and molecular docking to predict binding site. *Bioorg. Med. Chem.*, **17**: 4825-4832.
- Yunus M. and Shaila M.S. 2012. Establishment of an in vitro transcription system for peste des petits ruminant virus. *Virology Journal*, **9**: 302.
- Zhang MY and Dimitrov DS. 2009. Sequential antigen panning for selection of broadly crossreactive HIV-1-neutralizing human monoclonal antibodies. *Methods Mol Biol*, **562**: 143-54.

- Zhikui L., Changcun G., Yongzhan N., Fengtian H., Xingling R., Shujun L., Zheyi H., Ying H., Xin W and Daiming F. 2010. Screening and identification of recombinant anti-idiotypic antibodies against gastric cancer and colon cancer monoclonal antibodies by a phage-displayed single-chain variable fragment library. *J Biomol Screen*, **15**: 308-13.
- Zhou Y and Marks JD. 2009. Identification of target and function specific antibodies for effective drug delivery. *Methods Mol Biol*, **525**: 145-60.





*Appendix*



# APPENDIX

---

## Buffers and reagents

### Buffers and reagents for phage titration, biopanning and amplification isolation:

#### LB Medium:

Components	For 1000ml
Bacto-Tryptone	10 g
Yeast extract	5 g
NaCl.	5 g

Autoclave and store at room temperature.

#### IPTG/Xgal Stock:

Components for	10 ml
IPTG (isopropyl- $\beta$ -D-thiogalactoside)	500mg
Xgal (5-Bromo-4-chloro-3-indolyl- $\beta$ -D-galactoside)	200mg
DMF	10 ml

Mix well, make aliquots of 1 ml and store at  $-20^{\circ}\text{C}$ .

#### LB/IPTG/Xgal Plates:

Components	1000 ml
LB medium	1000ml
Agar	15gm

Autoclaved and allowed to cool  $45-50^{\circ}\text{C}$ .

Then 1 ml IPTG/Xgal Stock per liter i.e. 100  $\mu\text{l}$  in 100ml was added, mixed and approx. 20 ml was poured in sterile petridishes in laminar hood, allowed to solidify the plates and stored at  $4^{\circ}\text{C}$  in dark until use.

#### Top Agar:

Components	100 ml
LB medium	100 ml
Agarose	700 mg

Autoclaved and stored at room temperature. Melted in microwave when required.

#### Tetracycline (suspension):

Stock solution 20 mg/ml in 1:1 Ethanol:Water.

Working solution: 20 µg/ml i.e. 20ng/µl

200 µl stock in 100ml ethanol: water (1:1) or 20 µl in 9.98 ml ethanol: water (1:1)

Stored at -20°C. Vortexed before use.

#### **LB+Tet Plates:**

Components	For 500ml
LB medium	500 ml
Agar	750mg

Autoclaved and cooled to 45-50°C. Then tetracycline was added @ 40 ng/ml of medium and approx. 20 ml LB medium poured into plate. Plates were stored at 4°C in dark.

#### **TBS:**

Components
50 mM Tris-HCl (pH 7.5)
150 mM NaCl

Autoclaved, stored at room temperature.

#### **PEG/NaCl:**

Components
20% (w/v) polyethylene glycol-8000
150 mM NaCl

Autoclave, mix well to combine separated layers while still warm.

Store at room temperature.

#### **10X PBS (Calcium and Magnesium free, 100ml)**

NaCl	8.00g
KCl	0.20g
Na <sub>2</sub> HPO <sub>4</sub>	1.15g
KH <sub>2</sub> PO <sub>4</sub>	0.24g

Total volume was made upto 80 ml with MilliQ water. pH was adjusted to 7.4 with HCl and finally was adjusted to 100 ml and autoclaved. Solution was stored at room temperature.

#### **Buffers and reagents for DNA isolation:**

##### **Tris EDTA buffer (TE)- 10:1 TE buffer of pH 8.0**

Tris (1 M, pH 8.0)	1ml
EDTA (0.5 M, pH 8.0)	200 µl

Volume was made to 100 ml with water and autoclaved before use.

### **Tris saturated phenol**

100 ml phenol was melted at 68°C for 10-15 min and 8-hydroxyl Quinoline was added to a final concentration of 0.1%. Equal volume (100ml) of 1 M Tris pH 8 was added to saturate phenol. It was left on magnetic stirrer for around 30 minutes and was allowed to settle at RT. Then remove the upper layer and 0.1 M Tris pH 8 was added until pH of phenol reaches to greater than 7.8. Phenol was now stored with the layer of 0.1 M Tris (pH 8.0) containing 0.2% β-ME in a brown bottle at 4°C to prevent pH changes and photo oxidation.

### **3 M sodium acetate**

246 g sodium acetate was dissolved in distilled water; pH was adjusted to 5.2 with glacial acetic acid. Volume was made to 1000 ml with water. This solution was stored in sterilized polypropylene bottles at room temperature.

### **Proteinase K (10 mg/ml)**

100 mg proteinase k (Sigma) was dissolved in 10 ml of TE buffer at room temperature, solubilization took around 30 min. proteinase k solution was aliquoted in small volumes in 0.5 ml eppendorf tubes and stored around -20°C.

### **Phenol: Chloroform: Isoamyl alcohol (25:24:1)**

25 ml (Tris saturated), 24 ml chloroform and 1 ml isoamyl alcohol were mixed in a tube and gently shaken before use.

## **REAGENT USED IN CELL CULTURE**

### **HBSS**

HBSS powder 9.8 gm (without sodium carbonate)

Distilled water 1000 ml

pH was adjusted to 7.4 using sodium carbonate. Sterilized by filtration.

### **DMEM (Gibco)**

DMEM powder 13.4 gm

Distilled water 1000 ml

Dissolved in 950 ml of distilled water and mixed. To this, 3.7 gm of NaHCO<sub>3</sub> per litre of medium was added and the final volume was made up to 1000 ml. The pH was Adjusted to 7.2-7.3 below desired working pH. Sterilized by filtration.

### **Growth medium**

DMEM 90 ml

NBCS (Gibco) 10 ml

**Trypsin Versene solution (2.5%)**

Trypsin	2.5 gm
Versene	1.4 gm

1 X PBS was added to make the volume up to 1000 ml.

**Phosphate Buffer Saline (PBS pH 7.4)**

Sodium chloride (NaCl)	8.00gm
Pottasium dihydrogen phoshphate ( $\text{KH}_2\text{PO}_4$ )	0.20gm
Disodium hydrogen phosphate ( $\text{Na}_2\text{HPO}_4, 2\text{H}_2\text{O}$ )	1.16gm
Pottassium chloride (KCl)	0.20gm
Distilled water upto	1000ml

Prepared PBS was autoclaved at 121°C, 15lb pressure for 20 min and stored at 4°C for further use.

# VITAE

---

---

**Name** : **Dr. Deepika Bisht**  
**Date of Birth** : 04.10.1990  
**Father's Name** : Mr. Gyan Singh Bisht  
**Mother's Name** : Mrs. Basanti Bisht  
**Nationality** : Indian  
**Language known** : Hindi, English  
**Permanent Address** : Govindpur garwar,  
P.O.-Kamaluaganja, Haldwani,  
Nainital (Uttarakhand)-263139  
**Email Address** : dpbisht4n@gmail.com

## **Educational Qualifications:**

---

<b>Degree</b>	<b>University/ College</b>	<b>Year</b>	<b>% / O.G.P.A.</b>
Highschool	Uttarakhand Board	2005	74.67%
Intermediate	Uttarakhand Board	2007	70.2%
B.V.Sc. & A.H.	G.B.P.U.A.T. Pantnagar	2013	7.73/10
M.V.Sc.	ICAR-IVRI	2015	8.607/10

---

## **Awards/ Membership**

1. Awarded Junior Research Fellowship by I.C.A.R. during M.V.Sc. programme.

This document was created with Win2PDF available at <http://www.win2pdf.com>.  
The unregistered version of Win2PDF is for evaluation or non-commercial use only.  
This page will not be added after purchasing Win2PDF.